PAVEMENT RESEARCH
at the
WASHINGTON STATE UNIVERSITY
TEST TRACK

VOLUME THREE

EXPERIMENTAL RING NO. 3: A STUDY OF UNTREATED, EMULSION TREATED, AND ASPHALTIC-CEMENT TREATED BASES

Research Project Y-993

Highway Research Section
College of Engineering Research Division
Washington State University
Pullman, Washington

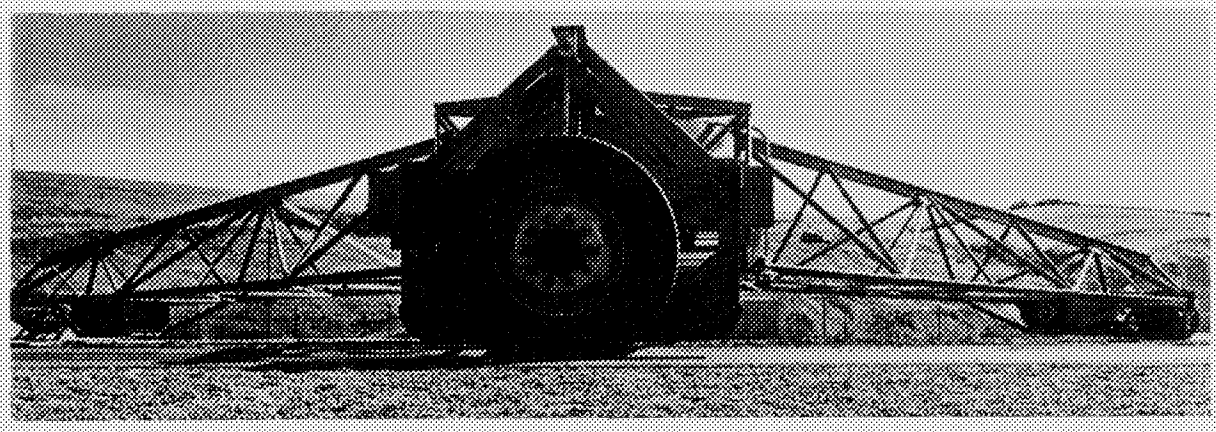

A Federal Aid Research Project in Cooperation
with the Department of Transportation
Federal Highway Administration
Bureau of Public Roads
The Washington Department of Highways
and
The Asphalt Institute
1969

PAVEMENT RESEARCH
at the
WASHINGTON STATE UNIVERSITY
TEST TRACK

VOLUME THREE

EXPERIMENTAL RING NO. 3: A STUDY OF UNTREATED, EMULSION TREATED, AND ASPHALTIC-CEMENT TREATED BASES

Report to the Washington State Department of Highways
on Research Project Y-993

by

Milan Krukar and John C. Cook

Highway Research Section
College of Engineering Research Division
Washington State University
Pullman, Washington
July, 1969

In Cooperation with
U. S. Department of Transportation
Federal Highway Administration
Bureau of Public Roads

Washington Department of Highways
and
The Asphalt Institute

(Highway Research Section Publication H-30)

ACKNOWLEDGMENTS

The Highway Research Staff wishes to thank the Washington State Highway Department for their financial and technical support. There were many Highway Department staff personnel from Olympia who helped, but we want to single out the following: Carl E. Minor, Assistant Director for Planning and Research; Roger V. LeClerc, Materials Engineer; Mrs. Willa Mylroie, Special Assignments and Research Engineer; and Tom R. Marshall, Special Assignments Engineer. Art Sinclair, Materials Engineer from District 6, Spokane, was also involved in the project. Both Tom R. Marshall and Art Sinclair were the Highway Department's field representatives on the projects and their interest and advice helped immeasurably.

Continual financial and technical support was given the project by The Asphalt Institute, College Park, Maryland. Particular acknowledgment and thanks are given to the following individuals of that organization: J. E. Buchanan, President; John M. Griffith, Director of Research and Development; and R. Ian Kingham, Staff Engineer. Provision of funds and expert technical knowledge from men such as these has helped immensely.

Appreciation is recorded to Ron Trolle, Sales Engineer, and Lloyd D. Coyne, Engineer, Western Laboratory with the Chevron Asphalt Company for their continued help, interest and advice on the project, especially with the emulsion treated bases.

Thanks go to the secretary, Judy Benes, who helped in typing and editing the rough drafts. The following Washington State University students contributed to the preparation of this report by helping with the tabulation and evaluation of the data and with drafting: Ted Rees, John Harrison, Al Badal, Dale Barr, Don Averill and Chuck Cooper.

Last but not least, a word of appreciation to Jack E. Schaefer, Leadman, who ran the test track and was responsible for construction inspection, maintenance and data accumulation, and to Bob Bureau and John Hunter of the Electrical Engineering Section who helped with instrumentation.

TABLE OF CONTENTS

LIST OF TABLES

LIST OF FIGURES

ABSTRACT

Three different kinds of base material of varying base thicknesses were tested at the Washington State University Test Track on Ring #3 during the fall of 1967 and the spring of 1968. Twelve 18-foot test sections consisting of 4.5, 7.0, 9.5 and 12 inches of untreated crushed rock surfacing top course base; 3.0, 5.0, 7.0 and 9.0 inches of emulsion treated crushed surfacing top course base; and 0.0, 2.0, 3.5 and 5.0 inches of special non-fractured screened aggregate asphalt treated base, covered by a uniform 3.0-inch thick Class "B" asphalt concrete wearing course were tested during this period. The pavement structure was built on a clay-silt subgrade soil.

Instrumentation consisted of moisture tensiometers, strain gages, pressure cells, LVDT gages and thermocouples for measuring moisture, strain, stress, dynamic deflections and temperatures. Benkelman beam readings were taken.

The testing period revealed that the fall failure modes were different from the spring failures. The fall failure pattern started from transverse cracks in the thin sections which developed into alligator cracking patterns. These cracks appeared after a period of cold weather and heavy rains followed by a warming trend. It seems that thermal and mechanical loads were responsible for the fall failures on the thin sections. The spring failures were very rapid and sudden and were due to environmental factors which led to saturated subgrade, thus resulting in poor bearing capacity. Punching shear was the failure mode. The thickest sections survived without cracks but

developed severe rutting. Examination revealed that these ruts extended into the subgrade and that fatigue cracking was developing on the bottom of the bases.

Comparison of the results with those obtained from Ring #2, which was similar in base materials and thickness, show that they were similar in many respects. This indicates that the test track is capable of replicating results and is a reliable research instrument.

Equivalencies were developed for the different materials. On this basis the special aggregate asphalt treated base was superior to the emulsion treated and untreated crushed rock bases in that order. These results were comparable to those obtained from test Ring #2.

Maximum values for static and dynamic deflections, strains and stresses for different times and temperatures were developed. The lateral position of the dual tires with respect to the gage severely affected the strain, stress and deflection values. Temperature also caused variations in the measurements.

Spring instrument readings for static and dynamic deflections, strain and stress show increased values by as much as 2 to 4 times of those obtained in the fall. Spring subgrade conditions probably are responsible for these differences.

Ring #3 series operational time was twice that of Ring #2 and sustained four times the wheel load applications. Construction and testing environmental conditions were superior to those for Ring #2 and hence contributed to the longer test period. This points out that environmental factors are very important in pavement life.

EXPERIMENTAL PAVEMENT RING NO. 3

INTRODUCTION

Experimental pavement Ring No. 3 was the second of three rings built and tested in a continuing pavement experiment designed to test bases constructed from different materials varying in thicknesses in order to study their strengths and determine their relative equivalencies. This ring was the first of two rings built under contract Y-993, which is a continuation of contract Y-651.

Each ring consists of 12 sections constructed from three different base materials, which are subdivided into four sections of varying base thickness. Crushed rock base is used as the standard control for comparison purposes.

The three rings, under contracts Y-651 and Y-993, were to be constructed during the summer and tested under different environmental conditions. Rings #2, #3 and #4 were constructed during the summers of 1966, 1967 and 1968 respectively. Ring #2 was tested the fall of 1966 and spring of 1967, Ring #3 the fall of 1967 and spring of 1968, and Ring #4 the fall of 1968 and the spring of 1969. The results from Ring #2 were published as Highway Research Publication H-29 (1)*. The following results from Ring #3 are tentative and subject to modification upon evaluation of results from all the rings.

The construction, testing and experimental results are described in this report. The data obtained from this ring will be used along with data from other rings to obtain an overall evaluation of test track testing and for theoretical analysis of the results, which hopefully will lead to a better understanding of pavement systems and materials.

---

*Figures in parenthesis refer to specific reports in the References.

This project was conceived and initiated by the Highway Research Section, College of Engineering Research Division, Washington State University. Financing is a joint undertaking among the University, the Washington Highway Department, the Bureau of Public Roads of the Federal Highway Administration, Department of Transportation, as a HRP federal aid research project, and The Asphalt Institute, which provided professional guidance in design planning and in evaluation of results.

EXPERIMENTAL DESIGN

The success of Ring #2 showed that it was possible to use twelve 18-foot test sections separated by 3.7-foot transition zones within the 260-foot centerline circumference test track limits with a minimum of boundary conditions. This division permits testing of three base types of four thickness levels in any one-ring experiment. The inclusion of several thicknesses of each base type was considered necessary for proper evaluation of the performance of several base types. The degree of thickness was chosen to provide estimated pavement lives from several hundred up to two million wheel load applications of 10,000 pounds. The actual load per set of duals is 10,600 pounds.

The subgrade, surfacing and other variables were kept constant, while base types and thicknesses were varied. A subbase was not used so as to keep the pavement layers at a minimum and to simplify the analysis of the theoretical system.

Although a random distribution of base types of varying thicknesses might have been preferable (2), sections of the base type were grouped to facilitate construction with standard construction equipment.

The materials and bases in Ring #3 were similar to those in Ring #2; the two changes being 1) that section bases were rotated 120 degrees to try to eliminate the effects of boundary conditions and any subgrade differences, and 2) the thickest section of the special aggregate asphalt treated base was eliminated and replaced with one of zero thickness. This was done to achieve failures in all sections. Ring #3 had the same materials and bases as Ring #2 which was a change from original plans and was due to the fact that the behavior of the emulsion treated bases and some of the other bases in the fall in Ring #2 were unexpected, hence it was decided with the sponsors to duplicate Ring #2 in Ring #3 and see if the results would change.

The location and dimensions of the pavement sections of Ring #3 are shown in Figure 1. Table 1 lists the base types, sections and thicknesses. The thicknesses of the sections and transition zones are shown schematically in Figure 2. Figure 3 shows the typical cross section of pavement structure. The subgrade soil, Type A-6 (10), was common to all sections.

Materials

Subgrade

The subgrade soil, a clay-silt A-6 (10) known as Palouse silt, was the same type as used in Rings #1 and #2 and is described in detail in the first part of these reports (3,1). Soil moisture-density curves are shown in Figure 4 and Table 2. Characteristics and classifications are shown in Table 3. Further results of tests done by The Asphalt Institute are in Table 4 (4), and show that test results obtained by WSU and The Asphalt Institute are similar. Some of the soil came from the contractor's local pit and the curve is also shown in Figure 3. The slight difference in density

PLAN VIEW

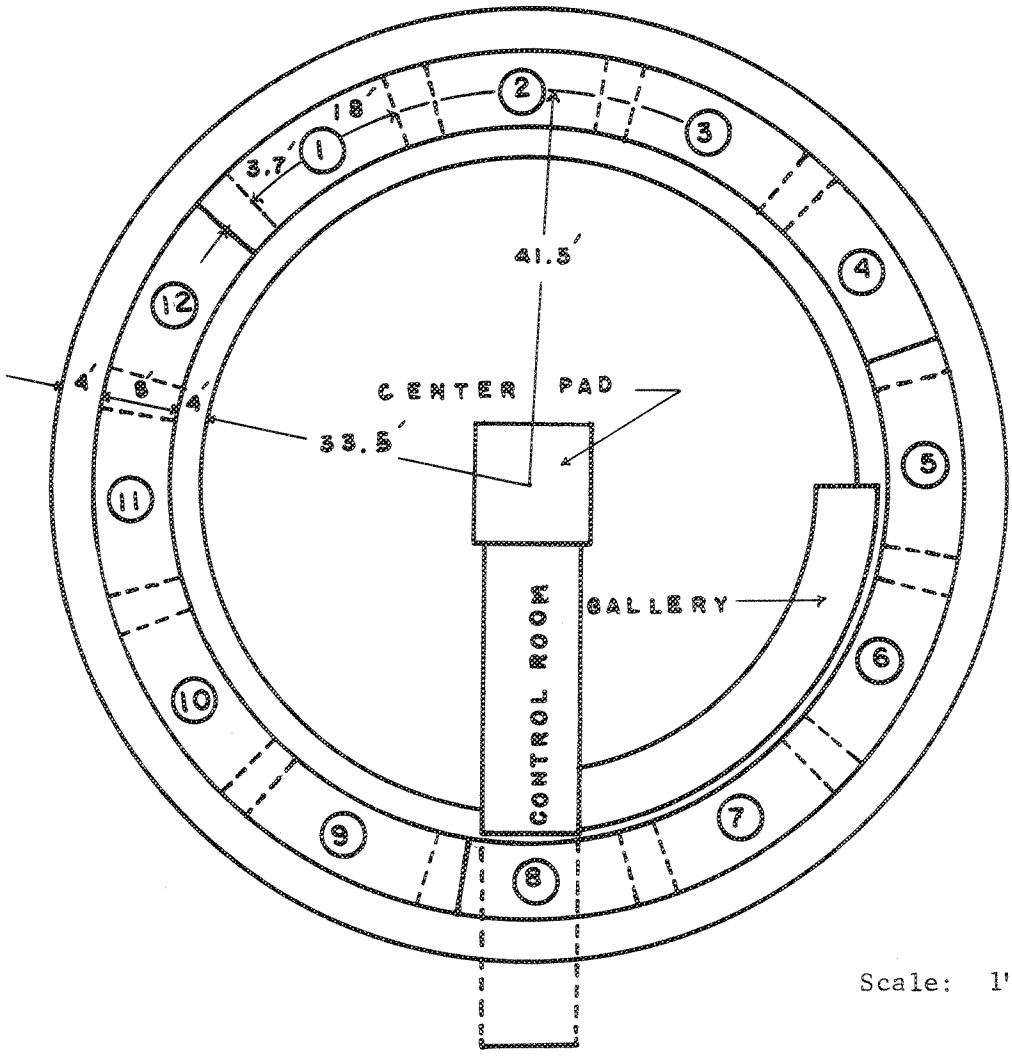

Scale: 1" = 20'

FIGURE 1. PERMANENT STRUCTURES AND PAVEMENT SECTIONS
TEST RING NO. 3

TABLE 1: TYPES, SECTIONS AND THICKNESSES OF RING #3

Type of Base	Sections	Thickness Levels--Inches			
		A	B	C	D
Crushed Surfacing Top Course	5 - 8	4.5	7.0	9.5	12.0
Emulsion-Treated Top Course	9 - 12	3.0	5.0	7.0	9.0
Special Aggregate Asphalt Treated	1 - 4	0.0	2.0	3.5	5.0
Wearing Course-- Class "B" Asphalt	All Sections	3.0			

Highway Research Section
Washington State University
May 1969

FIGURE 2. SCHEMATIC PROFILE FOR RING #3

Sections 1-4 - Special Aggregate Asphalt Treated Base (A.T.B.)
Sections 5-8 - Untreated Crushed Surfacing Top Course Base (U.T.B.)
Sections 9-12 - Emulsion Treated Crushed Surfacing Top Course Base (E.T.B.)

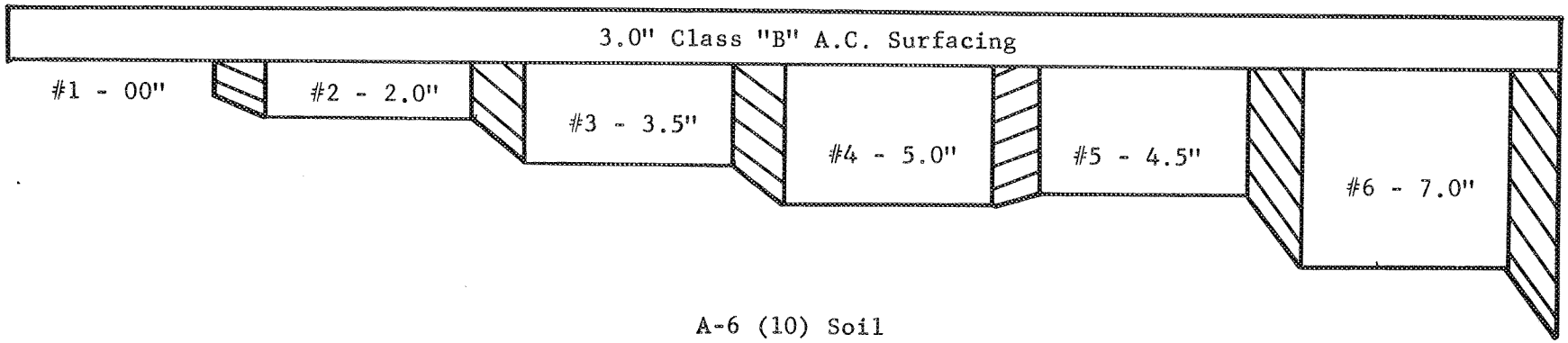

A-6 (10) Soil

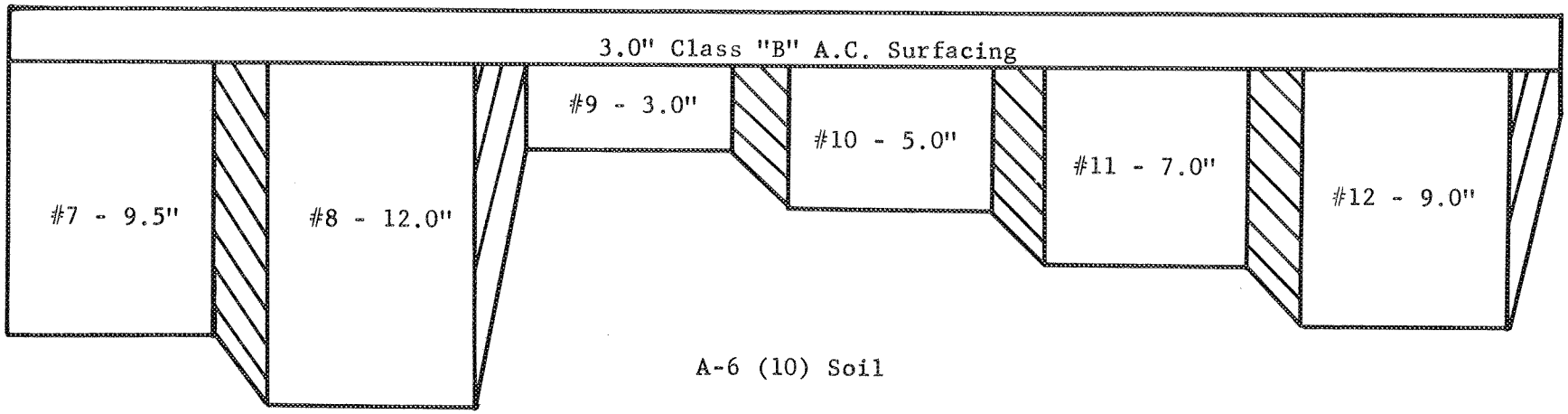

A-6 (10) Soil

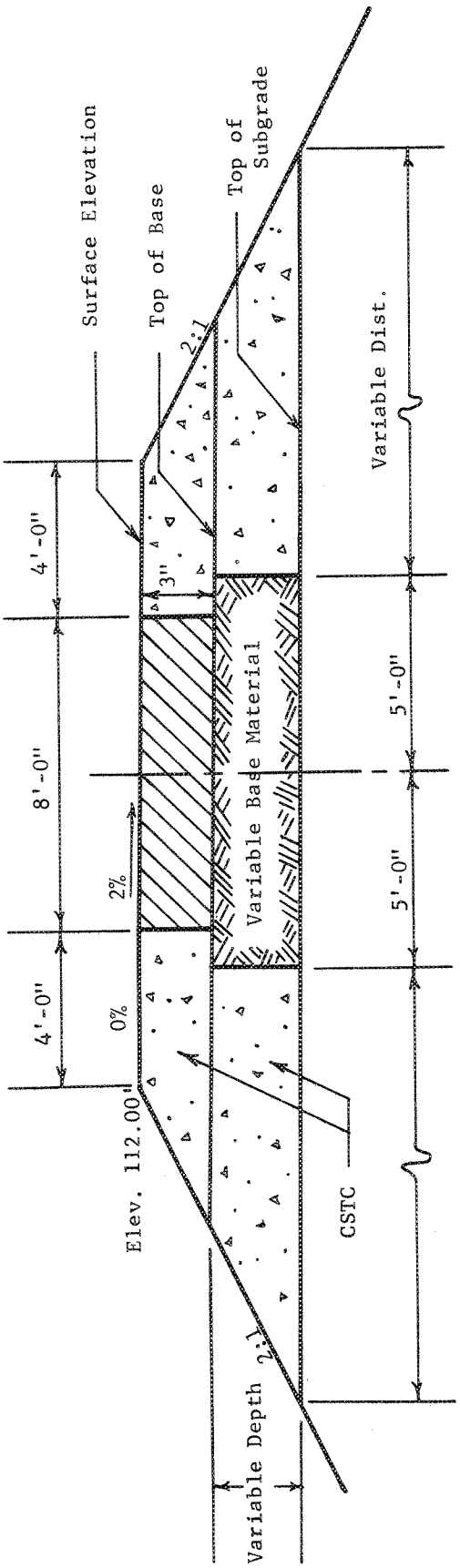

FIGURE 3. TYPICAL CROSS-SECTION OF PAVEMENT STRUCTURE

Rings 2, 3 and 4

FIGURE 4. DENSITY - MOISTURE CURVES
(Subgrade Soil Characteristics)

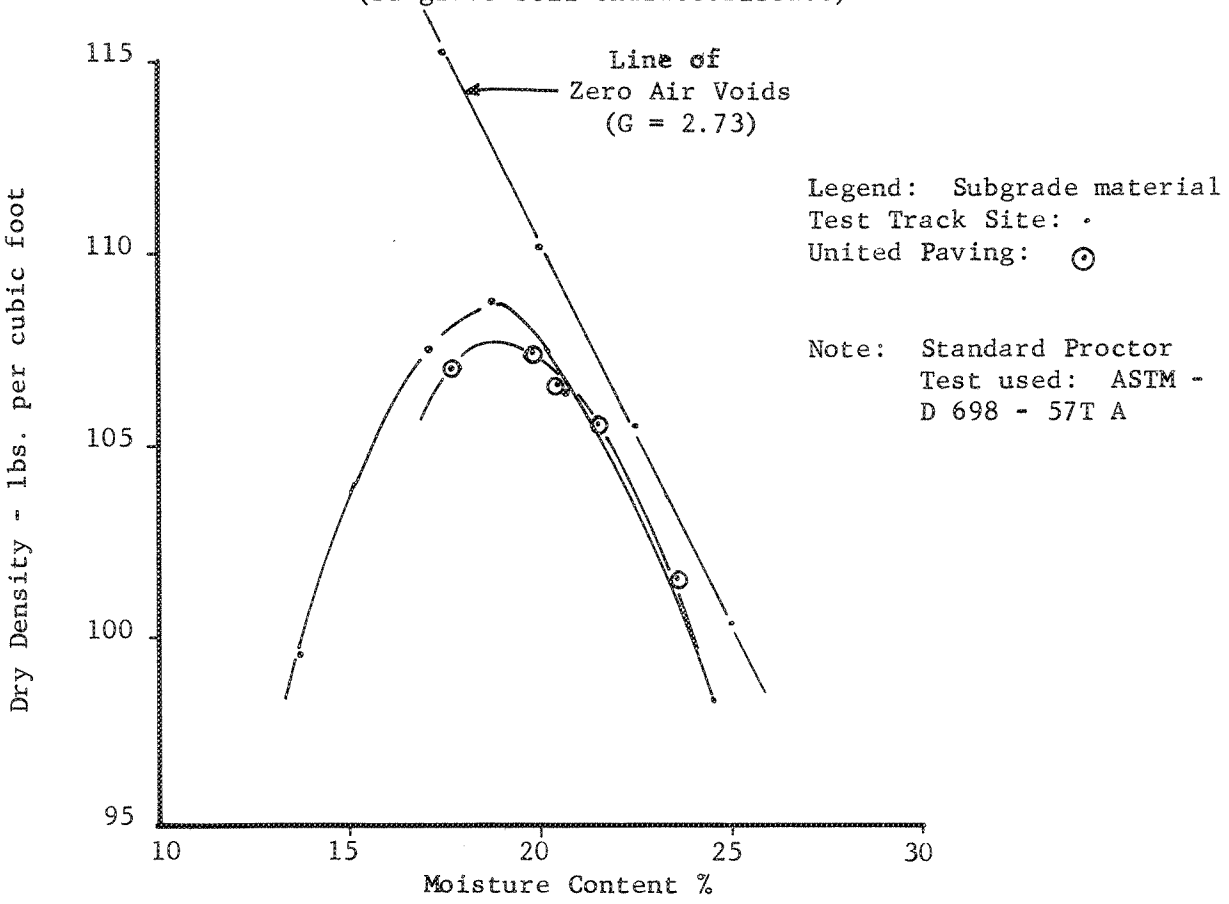

TABLE 2: OPTIMUM DENSITY AND MOISTURE
FOR SUBGRADE MATERIAL

Source	Max. Optimum Dry Density	Optimum Moisture
Test Track	108.8	18.8
United Paving	107.8	18.8

TABLE 3: SOIL CHARACTERISTICS AND CLASSIFICATION

Soil	Specific Gravity S.G.	Liquid Limit L.L.	Plastic Limit P.L.	Plasticity Index P.I.	Highway Res., Board Class.	Airfield Classification
Clay-silt	2.73	34.9	20.2	14.7	A - 6 (10)	CL

Stabilometer "R" Value = 16
pH Factor = 6.1

FIGURE 5. COMBINED GRADATION CURVE FOR CRUSHED SURFACING TOP COURSE UNTREATED SECTIONS 5-8 AND EMULSION TREATED SECTIONS 9-12

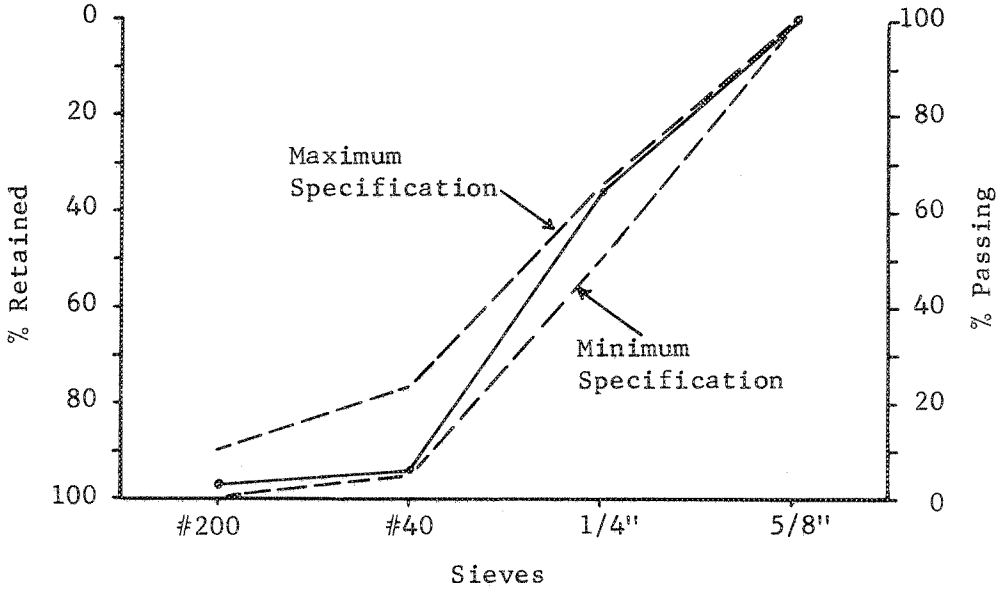

FIGURE 6. MAXIMUM DENSITY CURVE
CRUSHED SURFACING TOP COURSE

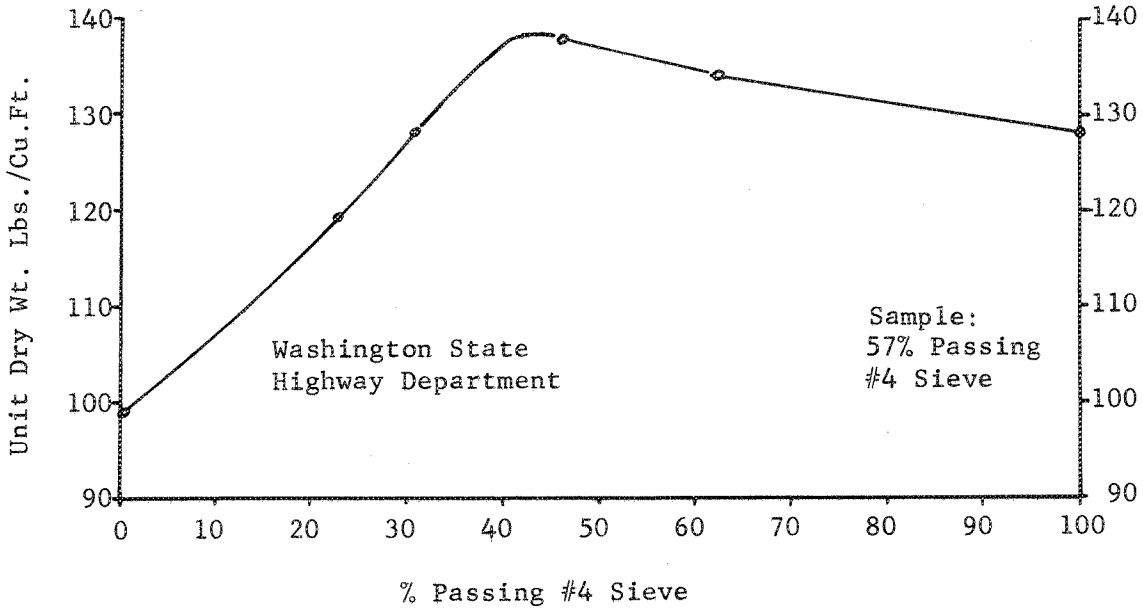

TABLE 4: CALIFORNIA BEARING RATIO (CBR) TEST ON PALOUSE SILT SUBGRADE SOIL

Water Content (%)	Dry Density (lb./cu.ft.)	CBR (%)	Swell (%)	Water Content After Soaking (%)
		SERIES 1		
13.0	105.1	4.6	2.4	20.2
16.4	108.0	9.2	0.8	18.9
19.3	105.8	2.8	0.3	19.9
		SERIES 2		
13.0	114.0	13.5	1.5	16.4
16.4	112.5	7.5	0.5	17.3
19.3	106.6	2.2	0.4	19.6

NOTE: Specimens soaked 4 days, 10 lb. surcharge weight.

Series 1 compaction: 10 lb. hammer, 18 in. drop, 5 layers, 12 blows per layer (12,200 ft.-lb./ft.^{3}).

Series 2 compaction: 10 lb. hammer, 18 in. drop, 5 layers, 29 blows per layer (26,400 ft.-lb./ft.^{3}).

(After Kallas)

may be attributed to a difference in the clay contents of the two silts or to testing variance.

Crushed Surfacing Top Course

The basaltic aggregate, hauled from United Paving's Geiger Pit in Spokane, where it was stockpiled from the previous year, just met Washington State Highway specifications (5) for crushed surfacing top course. Sampling was difficult due to segregation in the stockpile in Spokane. This rock was used for the untreated bases in sections 5 to 8 as standard control and for the emulsion treated base aggregate in sections 9 through 12. Figure 5 shows the gradation curve for this aggregate. Figure 6 represents the maximum density curve which can be obtained with this aggregate.

Special Screened Non-Fractured Aggregate

This aggregate was specially blended at the Fort Wright site of Central Pre-Mix of Spokane under the supervision of Washington State Highway personnel. The coarse aggregate came from the Fort Wright gravel pit and the fine aggregate from their Mead sand pit. This blended aggregate was trucked to Pullman in the summer of 1966 and stockpiled at the test track site for use with asphalt cement for the special asphalt treated bases in Ring #2, sections 9 through 12 (1), and Ring #3, sections 1 through 4 (6).

It is a river-run gravel and contains less than 5% freshly fractured surfaces. Figure 7 shows the gradation curve for this aggregate. Figure 9 (photo) shows its appearance and size. Although this type of aggregate is scarce in Eastern Washington, it is prevalent on the west side of the state. Since good aggregate is becoming scarce in the populated western areas of the state, the highway department wants to make use of more readily available glacial gravels--and therefore, has included them for study as base aggregates.

FIGURE 7. GRADATION DESIGN CURVE
SPECIAL ASPHALT TREATED BASE

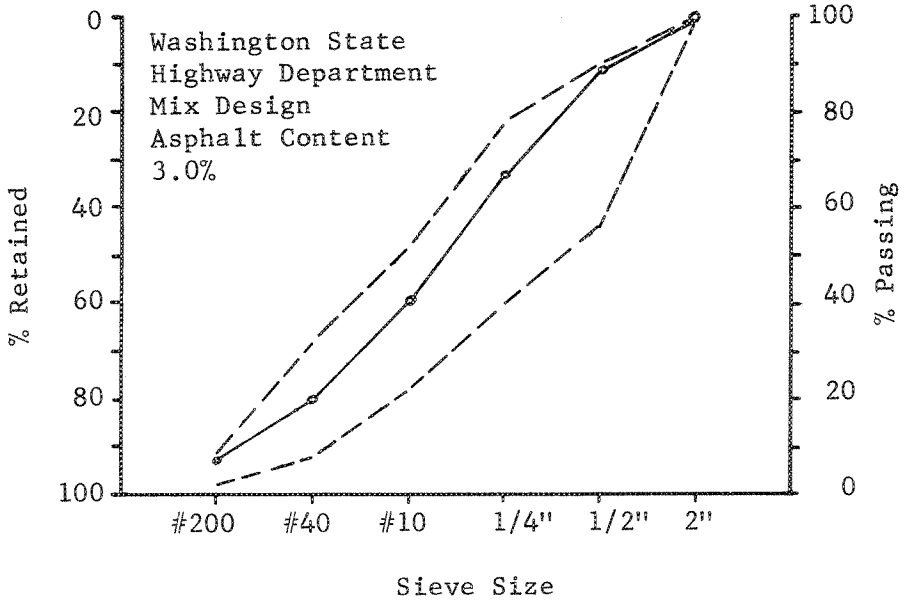

FIGURE 8. COMBINED GRADATION CURVE
FOR CLASS "B" ASPHALT CONCRETE - ALL SECTIONS

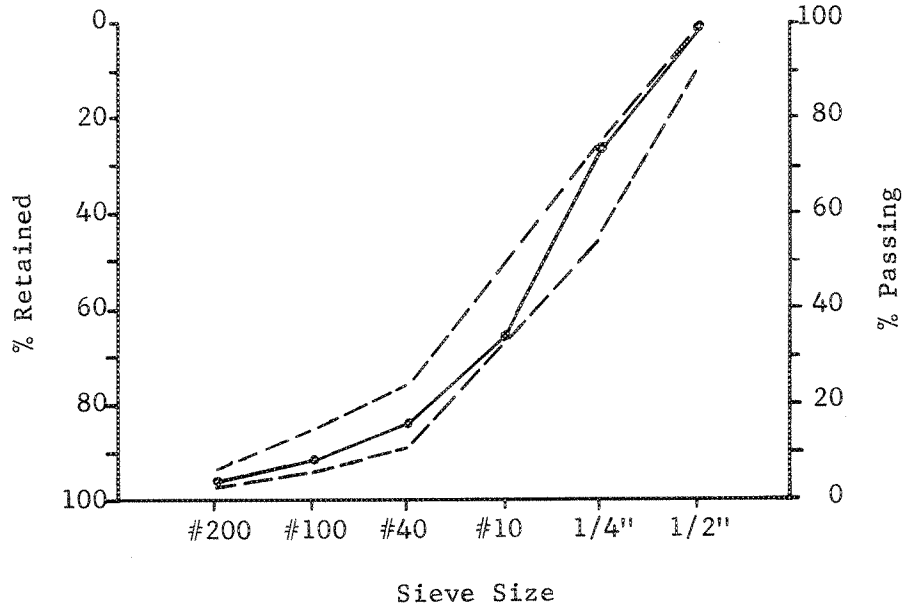

FIGURE 9. THE APPEARANCE OF THE SPECIAL SCREENED NON-FRACTURED AGGREGATE AT THE TEST TRACK STOCKPILE.

FIGURE 10. THIS SHOWS THE APPEARANCE OF THE SUBGRADE AFTER RING #2 PAVEMENT WAS REMOVED. NOTE THE TIRE TRACKS INDICATING THE SATURATED CONDITION OF THE PALOUSE SILT.

Asphalt Concrete Class "B" Aggregate

This aggregate came from United Paving's Pullman pit and was blended to meet Washington State Highway specifications (5). It is a basalt rock similar to the crushed surfacing top course. The combined gradation curve is shown in Figure 8 and in Table 8.

Construction

Pre-Conditioning

When the old test pavements of Ring #2 were removed, the subgrade was found to be non-uniformly wet. Moisture contents varied from section to section as shown in Table 5. The moisture content was found to be above optimum in most sections, and some were at a saturated level. The contractor, United Paving, Inc., excavated the subgrade to the 110-foot elevation and tried to dry it so that specified compaction and moisture levels could be reached. This proved to be unsuccessful. Figure 10 shows the appearance of wet subgrade. Other methods, such as scarification, were tried to obtain compaction and uniform moisture without success.

A work order arrangement was agreed upon with contractor which called for excavation of the subgrade to elevation 108 feet and where needed, to further excavate the non-uniform subgrade areas. The subgrade was excavated to the 108-foot elevation. Non-uniform spots were found in sections 10-11, 1-2-3, and 5-6 and were excavated to 106-,105- and 107-foot elevations respectively. At these elevations, the subgrade was found to be uniform in moisture. New silt material was used to build up the subgrade to the 108-foot elevation. A 10-ton, 9-pneumatic rubber-tired roller was used for compaction, which was checked by nuclear density equipment. This work order cost $3,802.07 and caused a delay of over a month.

TABLE 5: SUBGRADE MOISTURE CONTENTS DURING PRECONDITIONING

Section	Average Moisture Content %	Remarks
1	20.2	
2	23.2	
3	20.0	
4	20.4	
6	38.36	Just Below Base (Approx. 1" thick layer)
9	21.2	
10	23.8	
11	23.5	
12	22.4	

Subgrade

The subgrade was brought up in 6-inch lifts loose depth, watered when necessary, and compacted with a pneumatic rubber-tired roller and a steel vibratory roller. The moisture contents and densities were checked by nuclear density equipment. The weather during this period was sunny and the temperature was in the high nineties. The silt subgrade was compacted on the dry side rather than at optimum moisture levels because the narrow moisture density range restricted the workable compaction levels. Each section of the subgrade was brought up to rough final grade, blue tops placed, then each section cut and filled to final grade.

A Huber blade was used for cutting and spreading silt to final grade. Much handwork via shovel and hand screeding was required to bring the sections to the desired elevations. A straight edge and rod and level were used to check final grade and elevation to a rigid $\pm$ ½ inch tolerance. The appearance of subgrade at final grade is shown in Figure 11. Table 6 shows the subgrade density and moisture achieved prior to instrumentation. The subgrade was ready for instrumentation at the end of July.

Crushed Surfacing Top Course Base - Untreated (Sections 5-8)

On the morning of August 4, two 4-inch lifts of crushed surfacing top course were laid with a Blaw-Knox paver starting from the deepest base section 8 and working towards the shallow base section 4 (see Figure 12). The crushed rock source came from United Paving's Geiger pit in Spokane, and was processed at their Pullman plant and hauled to the test track site. The rock contained 8.91% moisture when laid. Each lift was compacted with a steel-faced roller. About 12 complete passes on each lift were needed to obtain the specified density. A third lift was laid in the afternoon and

TABLE 6: DENSITIES OF SILT SUBGRADE AT FINAL GRADE

Section	Dry Density lbs./cu.ft.	Moisture Content %	Per Cent of Maximum Density *	Per Cent of Optimum Moisture Content*
1	109.1	14.3	102.0	75.3
2	101.6	15.0	95.0	78.9
3	109.8	14.5	102.6	76.3
4	103.0	14.3	96.3	75.3
5	106.3	16.5	99.3	86.8
6	104.4	15.2	97.6	80.0
7	105.4	15.2	98.5	80.0
8	104.6	13.7	97.8	72.1
9	101.6	15.0	95.0	78.9
10	106.6	15.0	99.6	78.9
11	105.8	14.0	98.6	73.7
12	107.1	14.9	100.1	78.4
Average	105.4	14.8	98.5	77.9

Maximum Density = 107 lbs./cu.ft. Optimum Moisture Content = 19%

*Standard Proctor Test used: ASTM - D698 - 57TA

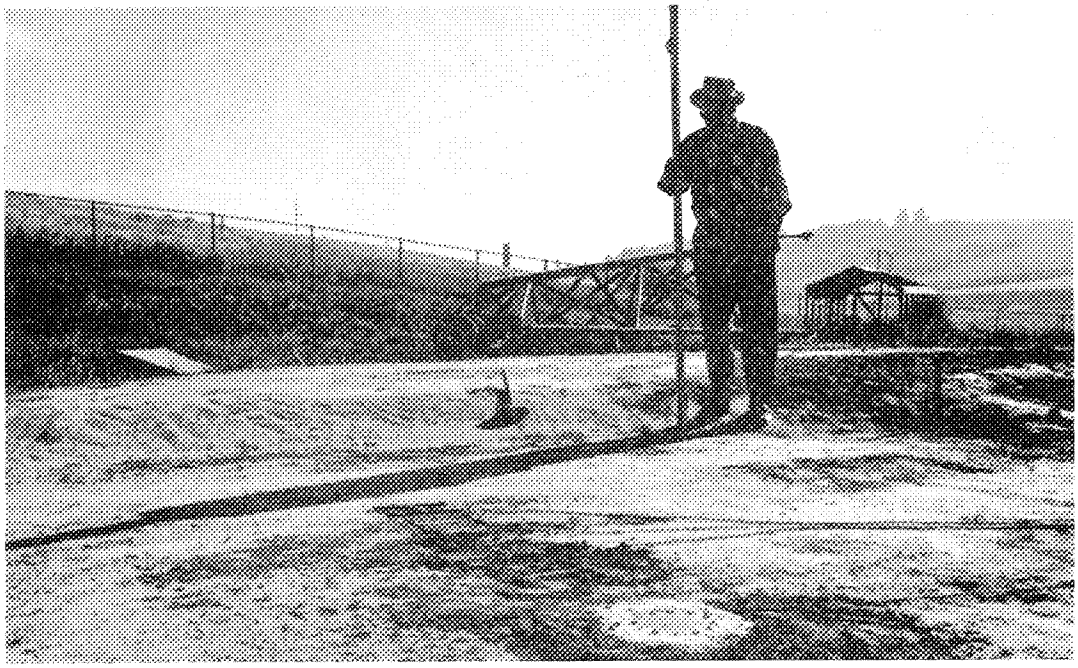

FIGURE 11. THIS SHOWS THE APPEARANCE OF THE PALOUSE SILT SUBGRADE AT FINAL GRADE. NOTE THE TRANSITION ZONE. IN THE FOREGROUND, INSTRUMENTS HAVE BEEN PLACED ON TOP OF THE SUBGRADE PRIOR TO PLACEMENT OF BASE MATERIAL.

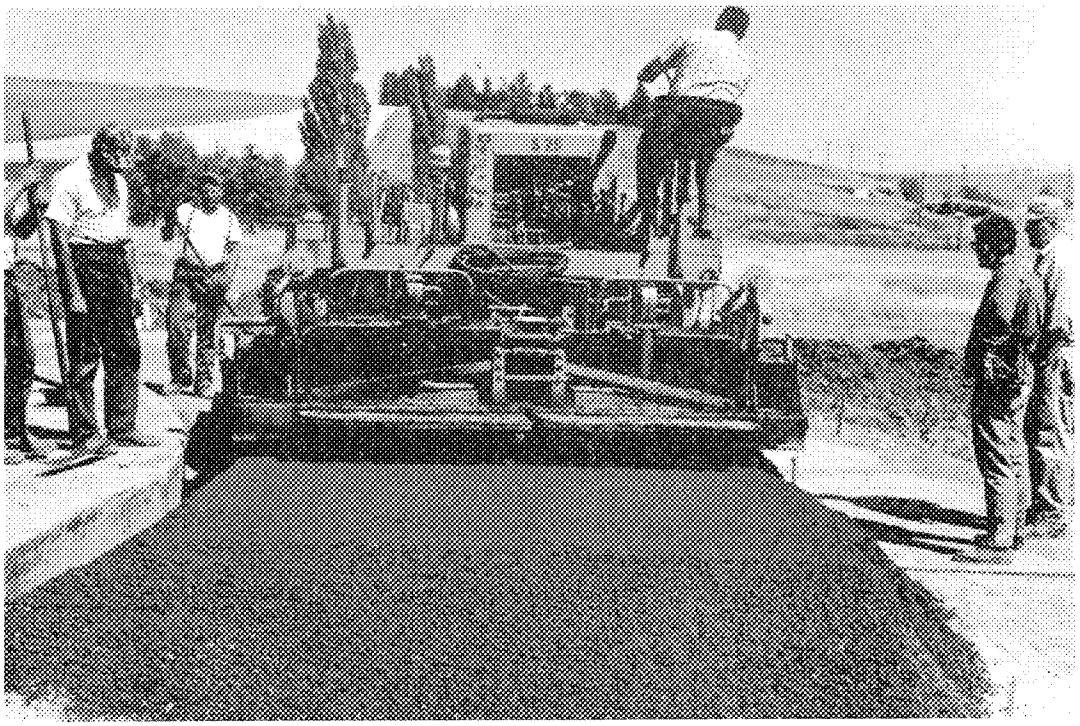

FIGURE 12. THE CRUSHED SURFACING TOP COURSE BASE IN SECTION 8 IS BEING LAID DOWN WITH A BLAW-KNOX PAVING MACHINE.

compacted. These sections were later fine graded with hand labor. An average density of 144.9 lbs./cu. ft. was obtained using nuclear equipment; this density was 106.5% above laboratory densities.

Emulsion Treated Base (Sections 9-12)

The crushed rock used with SS-Kh emulsion was the same material as used in the untreated bases. Construction of the emulsion treated base began on August 4. Checks on the aggregate prior to mixing indicated it had 4.3% moisture. An additional 2.5-3.0% moisture was added during mixing to bring the water content up to that determined as necessary to achieve good coating. The aggregate was brought into the pugmill untreated, and then water and bitumals were added to the mixing pug using calibrated 5-gallon cans. The water was mixed with the aggregate for approximately 30 seconds, followed by the emulsion which was mixed for an additional 45 seconds. It was a dry mix and contained 6.64% water and about 9.0% total fluids. The batch proportions at the contractor's plant are shown in Table 7.

The first lift of 2-3/4" thickness was laid in Section 12. Time was 11:10 a.m., August 4. The mix looked dry. Three complete passes with the pneumatic roller were made within 2 hours as shown in Figure 13. One complete pass covers the whole 10-foot width. The relative dry density was 134 lb./cu. ft. One additional pass increased the relative dry density to 136 lb./cu. ft. No shoving or displacement of the mix was observed--except along the edges due to lack of lateral support. During the placement of the first lift rolling was delayed up to one hour to facilitate removal of excess water. Later lifts were rolled almost immediately with no adverse effects.

A tack coat of 4:1 SS-Kh was broom applied between each lift to insure proper bond due to the roller tracking silt from the subgrade onto the treated

base. The next lift of 2-3/4" thickness was laid down at 2:15 p.m. with the air temperature being 90°F. At 3:50 p.m. the steel roller was used to compact the edges which were unsupported. Afterwards the base was compacted by a pneumatic rubber-tired roller.

On Monday morning, August 7, at 9 a.m., a final 2-3/4" lift was laid on a tacked surface. At 11:48 a.m. this lift was compacted with a pneumatic rubber-tired roller. A total of 5 complete passes was made on the final lift with a final dry density of 140.4 lb./cu. ft.

Special Asphalt Treated Base (Sections 1-4)

This aggregate was the same as that used in sections 9-12, Ring 2, and has less than 5% fractures. Originally this rock came from the Spokane area and was stockpiled at the test track site. The material was hot mixed in the pu mill with 3.0% 60-70 penetration asphalt in 3,000 lb. batches. This was placed in three lifts on August 7. The temperature of the laid mix was 292°F, and at the start of compaction 250°F. A steel roller was used for compaction; this is shown in Figure 14. The relative density obtained by nuclear equipment was 143.5, which is 96.6% of optimum laboratory density.

The contractor's crew had difficulty in obtaining close tolerance of grade and some cutting and scraping was necessary to obtain the proper thickness, thus giving parts of the base surface a rough appearance.

Class "B" Asphalt Concrete Wearing Course (All Sections)

Thermocouples, pressure cells, extensiometer strain gages, and strain gages were placed on the base. Then a tack coat was sprayed.

A change in the specifications was agreed upon; this called for the changing of the asphalt cement penetration grade from 85-100 to 60-70. This was done to prevent contamination of the asphalts in the plant tank. The

TABLE 7: EMULSION TREATED BASE BATCH PROPORTIONS

Description (2000 lb. Wet Weight Batches)	Percentage	Pounds
Bin #1 (-1/4")	60	1200
Bin #2 (1/4"-3/8")	22	440
Bin #3 (3/8"-5/8")	18	360
Amount of SS-Kh	5	100
Water Added	2.5	25

TABLE 8: DENSITIES OBTAINED FROM CORES[1] AND NUCLEAR GAGE

Section	Type	Thickness In.	Density lb/cu.ft.	Nuclear Density	% of Lab Density
4	Total	8.4	149.1	---	--
	Cl B	3.1	152.3	153.5	98.9
	ATB	5.3	143.5	143.2	96.6
8	Cl B	3.1	151.0	151.0	98.0
11	Cl B	3.0	149.1	152.0	96.8
12	Cl B	3.1	149.8	147.5	97.3
6*	Cl B	---	153.1	---	99.4
10*	Cl B	---	153.3	---	99.5

[1]The 4" diameter cores were taken outside the wheel path.

*Core diameters from these sections were 1-1/4" drilled for LVDT gages. The other core diameters are 4". Both were drilled by Pittsburg Testing Lab of Spokane.

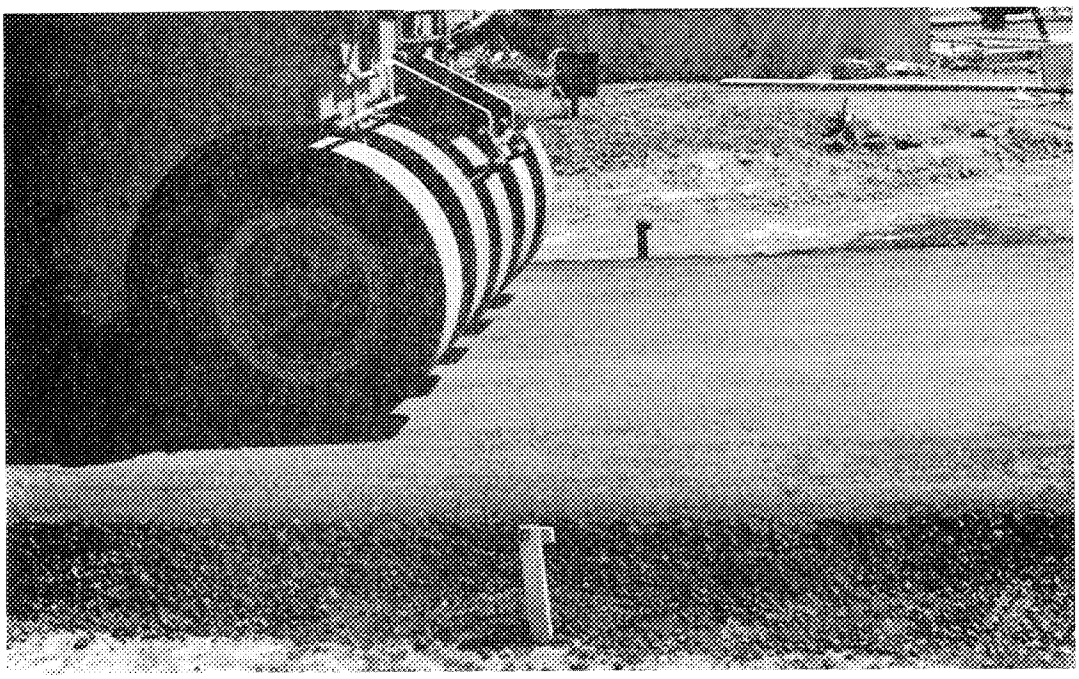

FIGURE 13. THE EMULSION TREATED BASE IS BEING COMPACTED WITH A PNEUMATIC RUBBER-TIRED ROLLER. NOTE THE SURFACE HAS A TIGHT COMPACTED APPEARANCE.

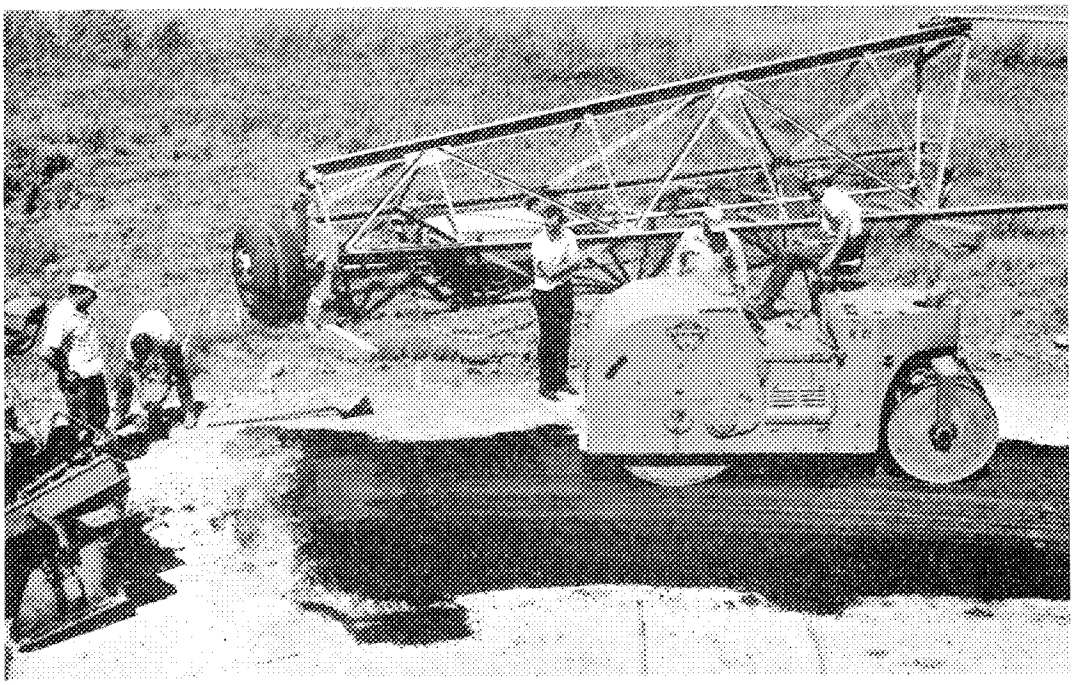

FIGURE 14. THE SPECIAL ASPHALT TREATED BASE IN SECTION 2 IS BEING COMPACTED WITH A STEEL ROLLER. NOTE THE TRANSITION ZONE FEATHERING INTO SECTION 1.

TABLE 9: MIX DESIGN REQUIREMENTS

Sieves-% Passing	Emulsion Treated Base (C.S.T.C.)		Special Asphalt Treated Base (Non-Fractured)		Cl. "B" A.C. Wearing Course	
	Specified	From * Extraction	Specified	From * Extraction	Specified	From * Extraction
2" Square			100	100		
1" Square				100		
5/8" Square	100	100		95	100	100
1/2" Square		99	56-90	89	90-100	100
1/4" Square	50-65	83	40-78	67	55-75	73
U.S. No. 10		59	22-52	41	32-48	42
U.S. No. 40	8-23	25	8-32	20	11-24	23
U.S. No. 80		15		11	6-15	14
U.S. No. 200	10 max.	9.2	2-9	7.6	3-7	9
Sand Equivalent % Min.	40		35			
% Fractures			5% max.	3%	75% min.	
Penetration Grade A.C.	SS-Kh		60-70	60-70	85-100	60-70
Amount of A.C. %	5.0 Emulsion	2.9 Residue	2.8	3.0	5.3	5.7
Wt. Per Cu. Ft. of Mix	140.4	133.5	148.5	143.2	152.0	149.4
Voids-Volume in Mix		17.0				1.2
Rice Density		2.579				2.580

*Extracted and tested by the Washington Highway Department, Materials Laboratory at Olympia, Washington.

Samples submitted at the end of testing of Ring 3.

aggregate used came from the United Paving's Pullman pit, hence requiring the use of a higher asphalt content. Extraction of samples showed the average asphalt content to be 6.1%.

The hot mix was laid on August 14 in two lifts with a tack coat between each lift. The wearing course was compacted by a steel and pneumatic-tired roller. Densities were checked by nuclear methods as shown in Figure 15. Cores were taken and Table 8 shows the densities and thicknesses achieved.

Shoulders

Shoulders of crushed surfacing top course aggregate were put in place after all instrumentation was put in. The shoulders were compacted to specifications and then a water proofing tack coat was sprayed on the inside shoulders and ditch.

Comments

The contractor encountered problems in scheduling of his equipment and men resulting in delays in the finishing of the subgrade, laying of bases, wearing course and shoulders. The weather during August was continually hot and dry. During the period from July 17 to the end of September, rain fell only once and that only for a short interval.

Instrumentation

Instruments to measure stresses, strains, temperatures, dynamic deflection, and moisture were installed in the different layers of the pavement structure in similar positions used in Ring #2 and the San Diego County Experimental Base Project (7). Figure 16 shows the depth and location of some of the instruments in one section; Table 10 shows the type of instrumentation installed and their location in various sections.

TABLE 10: LOCATION OF INSTRUMENTS ALONG CENTER LINE

Type of Instrument	Subgrade		Base	Surface
	Below	On Top	On Top	On Top
	Sections	Sections	Sections	Sections
Moisture Probes	2,3[a],4,6[a], 7,9,10[a],11	--	--	--
WSU Cell	--	6,8	--	--
S.G.Pressure Cell	--	3,6,8,10, 12	--	--
Thermocouples	1-12	1-12	1-12	1-12
Strain Gages[b]	--	3,6,8,10, 12	3,4,6,8, 10,12	1-12
LVDT[c]	--	--	--	3,6,10,12

[a] In sections 3, 6 and 10 three moisture probes were installed.

[b] The strain gages were installed in pairs; one longitudinal to the direction of travel and the other transverse. Spares were also installed except on the surface.

[c] One shallow and one deep LVDT was installed in these sections.

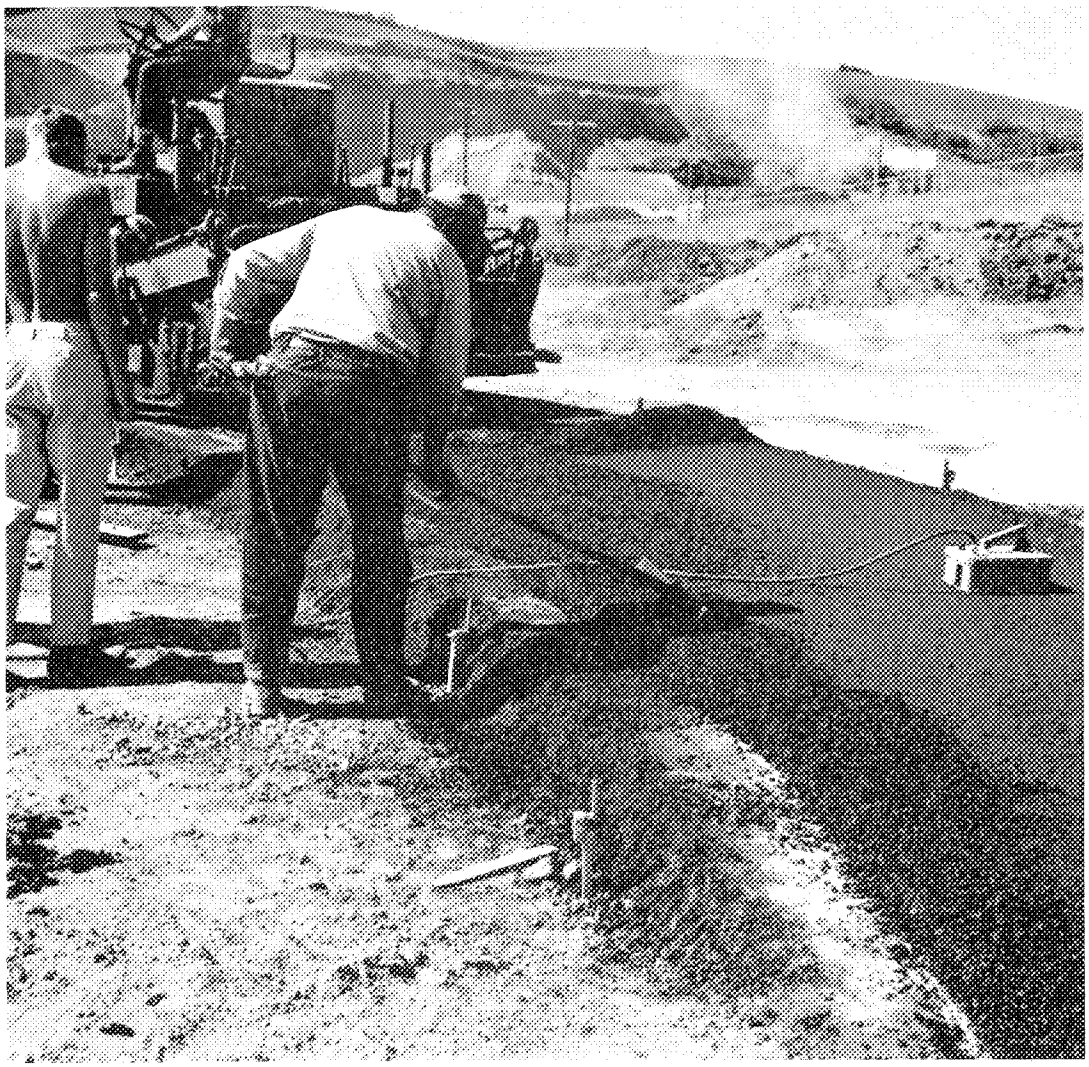

FIGURE 15. THIS SHOWS THE MEASURING OF DENSITY OF THE FIRST LIFT OF CLASS "B" ASPHALT CONCRETE WEARING COURSE IN SECTION 1. THE EDGES HAVE TO BE HAND TRIMMED DURING ROLLING TO PREVENT EDGE BREAKDOWN.

All the instruments, with the exception of the thermocouples, moisture probes, and the WSU pressure cells, were wired into an amplifier, manual switching panel and recorder. The other instrument readings were taken visually and recorded manually. Rebound deflection measurements were measured with a Soiltest Benkelman beam.

Measurement of Moisture

Nuclear methods were used to measure subgrade moisture during construction. To monitor the quantity and direction of movement of water in the subgrade, 14 moisture tensiometer probes were installed. The principle behind the tensiometer is that there is moisture tension between soil particles which causes soil suction. The tensiometer consists of porous ceramic cups which are filled with water and are attached by long capillary-like copper tubing to a Bourdon dial gage. As the surrounding soil dries out, tension within the water film draws the water from a porous cup, thus creating a suction which registers in centibars on the Bourdon gage. A dry soil is indicated by high gage readings and vice versa.

Laboratory calibrations and work by other researchers on the use of this soil moisture probe indicate that these probes have a hysteresis effect (8); one curve for the drying cycle and another for the wetting cycle. In the field this becomes a problem of using the correct curve. The test track subgrade was on a wetting cycle as the subgrade was on the dry side during construction.

Prior to installation, the ceramic cups were saturated for 24 hours with de-aired distilled water. Then the ceramic probes were installed in a vertical position in pre-wetted vertical auger-bored holes so as to make filling and removal of air bubbles easier. The probes were filled and purged.

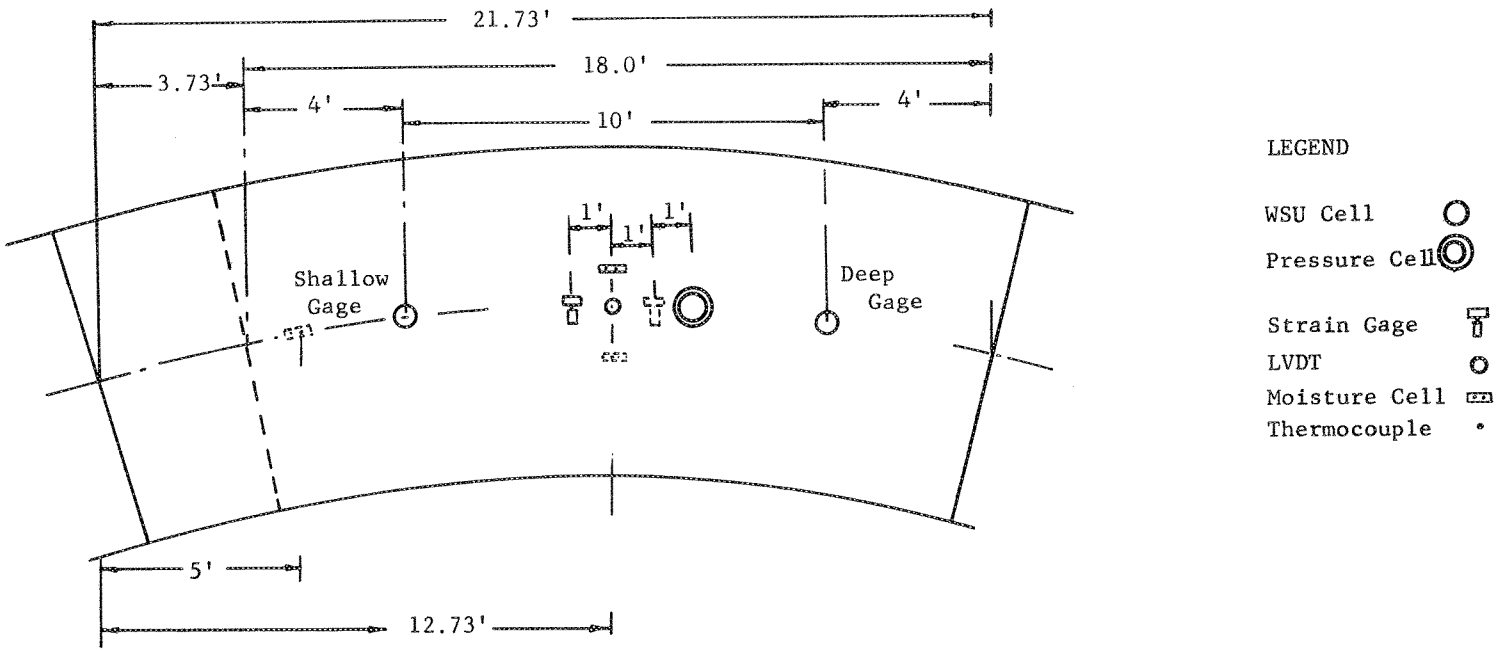

FIGURE 16. INSTRUMENTATION FOR SECTION 3

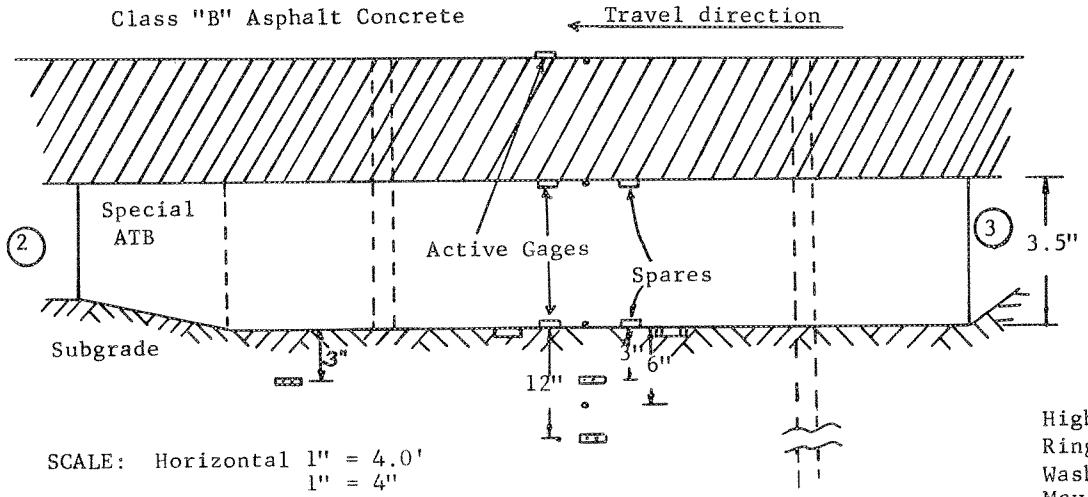

SCALE: Horizontal 1" = 4.0'
1" = 4"

Highway Research Section
Ring No. 3 Y-993
Washington State University
May 25, 1970 M. Krukar

The copper leads were laid on top of the subgrade to the outside shoulders of the track for ease of reading. Special holders were made for the 14 gages.

Readings were obtained from 12 out of the 14 gages. After the first frost, none of the dial gages registered readings.

Temperature Measurements

Iron-constantan thermocouples: Forty-eight Pall Trinity Micro iron-constantan thermocouples type 20-J-TF were installed in four different positions in each section: top of wearing course, top of base, bottom of base, and 6 inches below subgrade. Each conductor was insulated with extruded Teflon with an overall insulation of extruded Teflon. The ends were bared, sanded clean, crimped together, fused and then dipped in a casing full of epoxy for waterproofing. The thermocouples were then hooked up to a manual switch box, which was connected to a direct-reading Leeds and Northrup potentiometer. No problems developed with this system.

Stress Measurements

WSU pressure cells: These cells were similar to those used in Rings #1 and #2. These cells were calibrated in an air pressure chamber. These cells were placed in sections 6 and 8 on top of the subgrade. A hole was dug in the compacted subgrade, leveled with fine silica sand. The cell was then put in flush with the subgrade elevation and then it was covered with a layer of fine silica sand to protect the bed from pressure points (see Figure 17). The system was connected to a manometer board in the tunnel.

WSU strain gage pressure cells: Seven pressure cells with strain gages were installed in sections 3, 6, 8, 10 and 12. These pressure cells are similar to other types of strain gage cells; their diameter is 7 inches and 3/4 inch thick. Five were working and recording after installation.

Calibration was done in an air pressure chamber. Installation procedure was similar to that used for the WSU pressure cells. These cells were connected to a Bruel and Kjar switching panel, a Brush amplifier and recorder. One of these cells was placed on top of the base in section 12. It was installed flush with the top of the base. A hole was cut in the base to fit the cell. Silica sand was used to level the bottom (see Figure 17).

Strain Measurements

Shinkoh polyester SR-4 P#20 strain gages were used for the measurement of strain. Strain gages in longitudinal and transverse positions were installed on the surface, bases, and subgrades as shown in Table 10 and Figure 6.

Strain gages (subgrade): Extensiometers, shown in Figures 17 and 18 were used for installing strain gages in loose material, such as the subgrade and crushed rock. They were installed in sections 3, 6, 10 and 12. The extensiometer design is basically the same as those used in Ring #2. More care was taken in the waterproofing and protection of the leads. They were placed in a strained position and longitudinal and transverse position in the subgrade and covered with a thin layer of asphalt concrete.

Strain gages (bases and surfaces): Extensiometers were used in placement of strain gages on top of the untreated base, section 6, and emulsion treated bases, sections 10 and 12. For mounting on the asphalt and emulsion bases, the surface was prepared by filling it with a silicone seal to level the surface and give consistency of strain to the gage. After curing, the surface was sanded where necessary and the gage and mounting blocks were epoxied, then connected with Belden strain gage wire. A tack coat of SS-1 emulsified asphalt and covered with fine asphalt concrete mix.

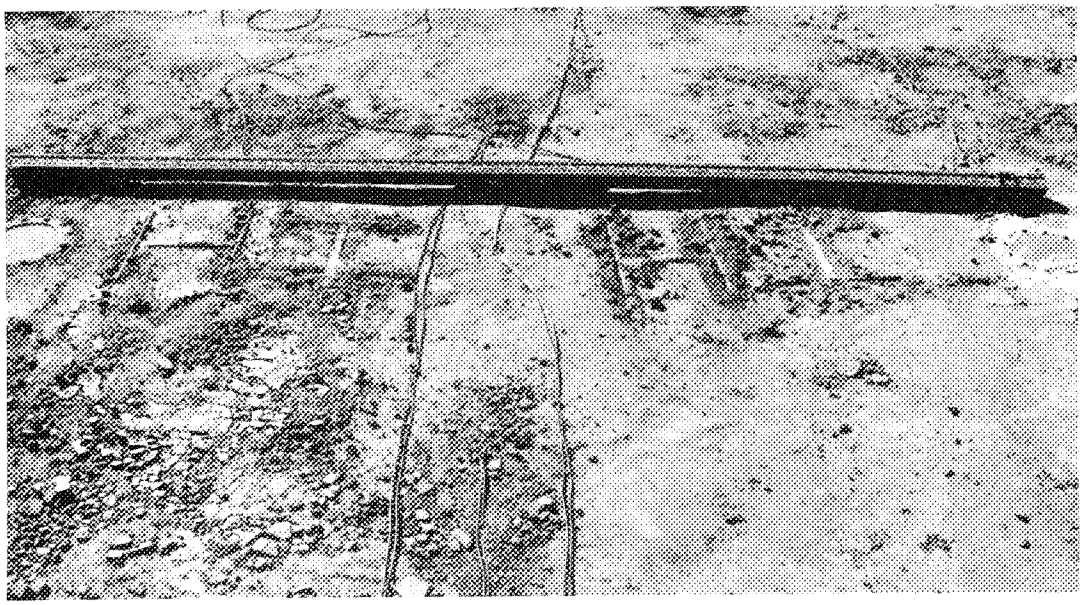

FIGURE 17. THIS PHOTOGRAPH SHOWS THE POSITION AND LOCATION OF TWO TYPES OF PRESSURE CELLS, STRAIN GAGE EXTENSIOMETERS, MOISTURE TENSIOMETERS, AND THERMOCOUPLES ON THE SUB-GRADE IN SECTION 6, 7.0 INCHES OF UTB.

FIGURE 18. LOCATION AND POSITIONING OF THE STRAIN GAGE EXTENSIOMETERS AND THERMOCOUPLES IS SHOWN HERE ON TOP OF THE 9.0 INCHES OF ETB IN SECTION 12.

Strain gages were installed on all sections on the surface. Grooves using dowels were made in the C1 "B" A.C. wearing course during compaction. Some problems were encountered in the installation of surface gages due to the extreme high daily temperatures, frequently above 95°F. The wearing course was soft and seemed to "walk" in the heat. This problem was circumvented by working early in the mornings before the temperatures had a chance to rise. The asphalt surface was ground down and sanded ; the gages were epoxied under pressure with standard strain gage epoxy. A rubberized paint was used for waterproofing and protecting the strain gages. The problem was that once the testing started, the effect was so great on the strain gages that they had to be frequently replaced.

Deflection Measurements

Dynamic deflection measurements: Four short 585 DT-100 and four long 585 DT-500 Sanborn Linear Variable Differential Transformers (LVDT) gages were installed. The short LVDT's measured deflection of the wearing course and base with respect to the subgrade, while the long gages measured the dynamic displacement of the total pavement system. Holders for the gages were constructed at the Research Division's machine shop.

Four deep and four shallow holes were diamond drilled through the asphalt wearing course and bases to the final depth placement of the gages and holders (see Table 11). The gages, which were calibrated before and after installation to insure proper readings, were then connected to the switching panel and recorder.

Rebound deflection measurements: These were measured with a Soiltest Benkelman beam at 5 fixed locations per section, (Fig. 53) longitudinally spaced 2-1/2 feet apart (lettered from A to E) to obtain an average deflection value.

TABLE 11: DEPTH OF LVDT HOLES

Section	Short Holes Inches	Deep Holes Feet
3	6.5	14.6
6	10.0	16.7
10	8.0	16.3
12	12.0	15.4

Read-Out Equipment

A Brush amplifier with input boxes for strains and LVDT gages was utilized. Several manual switching panels were made by the Electrical Engineering Section, WSU, to work with the B & K switcher. The system was manually operated and each strain gage, pressure cell and LVDT was individually switched into the system. The strain gages had to be balanced before read-out.

The thermocouples were switched in manually and readings were taken from the direct reading potentiometer.

PERFORMANCE OF TEST RING #3

Testing Periods

Full time testing began September 13, 1967, after several trial runs to test the reliability of the instruments. Testing was suspended on December 4, 1967, due to the advent of winter and after 735,573 wheel loads and 245,191 revolutions had been applied. Testing was done on a 7-day, 24-hour basis whenever possible.

Signs of distress appeared in all the untreated base sections 5-8 and sections 1 and 2 of the special aggregate asphalt treated bases, but no signs of distress except for some rutting in section 9 were visible in the emulsion treated base sections 9-12. Sections 1, 5, 6, and 7 containing zero inches of base, 4.5, 7.0 and 9.5 inches of untreated base respectively were declared to have failed.

A constant speed of 20 mph was maintained up to 597,943 wheel loads, then was reduced to 15 mph, and then to 10 mph as the pavements became progressively rougher.

Full time testing was resumed on May 10, 1968, after several of the failed sections had been replaced and weather conditions improved. All testing was stopped on July 25 after 870,606 wheel loads and 290,202 revolutions. At this time, all sections showed various degrees of distress and all sections with the exception of sections 5, 11 and 12 having 5.0 inches of asphalt treated base, 7.0 and 9.0 inches of emulsion treated base respectively had some cracks. The above sections were badly rutted.

Testing Conditions

Design Thickness

Special care was taken during construction to insure that the proper specific base and wearing course thicknesses would be achieved. The subgrade was brought to the desired elevation and grade, the former being checked by rod and level and the latter by grade screed board. The achievement of proper thicknesses still was difficult. The contractor found it necessary to scrape off some of the excess thickness in some of the base sections. Thicknesses and densities were checked from cores drilled before and after testing (see Table 12). Densities of the cores were also measured and compared to laboratory and nuclear densities. Complete cores from the emulsion treated bases were impossible to obtain.

Speed

Attempts were made to keep as many of the variables as constant as possible during the testing periods. The speed of the apparatus was kept constant at 20 mph up to 597,943 wheel loads when pavement sections 1 and 6 became too rough. The speed was reduced to 15 mph until 663,702 wheel loads, after which it was reduced to 10 mph. This speed was maintained until operations were concluded. Figure 19 shows speed versus wheel load applications.

TABLE 12: CORE THICKNESSES AND DENSITIES

Section	Type	Design Thickness (in.)	Core Thickness (in.)	Deviation From Design (in.)	Ave. Nuclear Density lbs./cu.ft.	Core Density lbs./cu.ft.	Laboratory Density lbs./cu.ft.	Deviation From Lab lbs./cu.ft.
4	Total	8.0	8.40	+0.40		149.1		
	C1 B	3.0	3.10	+0.10	153.5	152.3	152.0	+2.3
	ATB	5.0	5.30	+0.30	143.2	143.5	148.5	-5.0
	C1 B[2]	3.0				159.4	152.0	+7.4
8	C1 B	3.0	3.10	+0.10	151.0	151.0	152.0	-1.0
	C1 B[2]	3.0			158.0	158.4	152.0	+6.4
11	C1 B	3.0	3.00	0.00	152.0	149.1	152.0	-2.9
12	C1 B	3.0	3.10	+0.10	147.5	149.8	152.0	-2.2
	C1 B[2]	3.0			152.5	149.7	152.0	-2.3
	ETB[2]	9.0				133.5	140.0	-6.5
	ETB[2]					139.5	140.0	-0.5

[1] Cores were taken prior to start and at end of testing. Core diameters were 5.0".

[2] These were taken at the end of testing--all others prior.

FIGURE 19. SPEED VERSUS TIME (EXPRESSED IN WHEEL LOAD REPETITIONS)

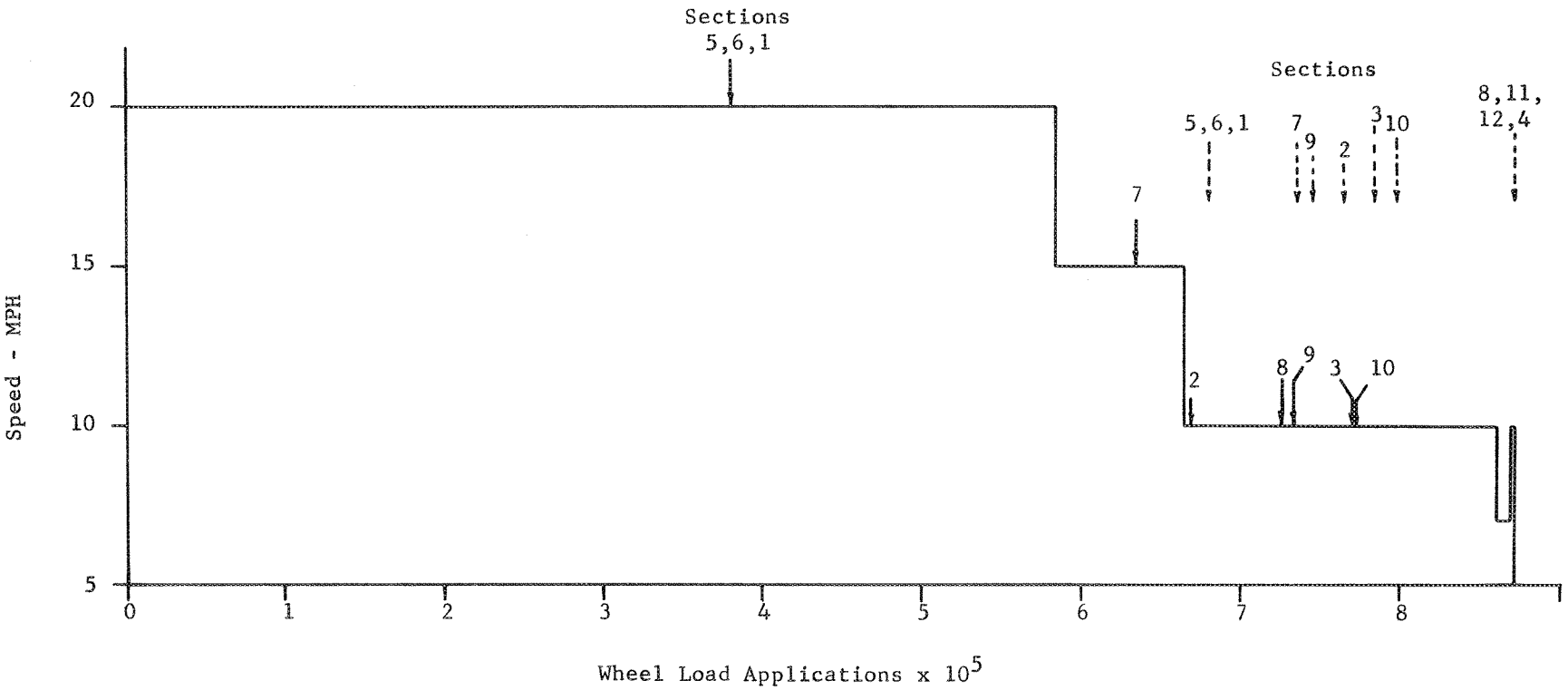

Legend:

Initial Distress ——→

Ultimate Failure - - - →

TABLE 13: WEEKLY WHEEL LOAD APPLICATIONS, RING NO. 3, 1967-68

Month	Week	Applications			
		Revolutions		Wheel Loads	
		Weekly	Accumulated	Weekly	Accumulated
September 1967	10-16[1]	20,037	20,037	60,111	60,111
	17-23	42,407	62,444	127,221	187,332
	24-30	23,793	86,237	71,379	258,811
October 1967	1-7	16,128	102,365	48,384	307,095
	8-14	37,583	139,948	112,749	419,844
	15-21	31,910	171,858	95,730	515,574
	22-28	24,123	195,981	72,369	587,943
	29-31	4,360	200,341	13,080	601,023
November 1967	1-4	10,754	211,095	32,262	633,285
	5-11	15,274	226,369	45,822	679,107
	12-18	1,052	227,421	3,156	682,263
	19-25	11,375	238,796	34,125	716,388
	25-30	6,035	244,831	18,105	734,493
December 1967	1-4[2]	360	245,191	1,080	735,573
May 1968	1-4	15	245,206	45	735,618
	5-11[3]	373	245,579	1,119	736,737
	12-18	2,662	248,241	7,986	744,723
	19-25	--	248,241	--	744,723
	26-31	2,000	250,241	6,000	750,723
June 1968	1-7	1,569	251,810	4,707	755,430
	8-14	2,989	254,799	8,967	764,397
	15-21	2,783	257,582	8,349	772,746
	22-28	3,617	261,199	10,851	783,597
	29-30	--	261,199	--	783,597
July 1968	1-7	1,898	263,097	5,694	789,291
	8-14	8,173	271,270	24,519	813,810
	15-21	13,069	284,339	39,207	853,017
	22-28[4]	5,863	290,202	17,589	870,606

[1] Testing started on September 13, 1967.

[2] Testing ended December 4, 1967.

[3] Testing started on May 10, 1968.

[4] Testing ended July 25, 1968.

The graph illustrates the fact that as the number of wheel loads was increased (thus increasing the pavement roughness), the speed was reduced accordingly. The graph also shows approximately when the first signs of distress occurred in the different sections. Table 13 shows the number of wheel load applications applied during each week.

Environmental Conditions

The pavement research testing facility is open to all the elements of weather, and thus is subject to all the variable effects caused by a changing environment.

All testing was done during a total of some 102 days--65 days in September, October and November of 1967 and 37 days in May, June and July of 1968. Ring #2, which was similar to Ring #3, had only 51 days of testing. The testing period has been divided into two parts--the fall period of September through November 1967 and the spring period of May through July 1968. The fall period was further sub-divided into early and late fall period; the dividing point being mid-October when the temperatures started to drop and precipitation increased (see Table 14).

During the fall period (September-November 1967), large amounts of precipitation were recorded during October, saturating the subgrade. This is shown in Figures 54 and 55.

Testing was resumed in May 1968 because of the late opening of the asphalt concrete plant. At this time the temperatures were starting to rise. The maximum temperature remained at a fairly constant level while the minimum daily temperatures started to rise (see Table 14).

The significance of these temperature differences results in the division of the period into two time and temperature zones. The fall period from September to about the middle of October was relatively dry with a high daily

TABLE 14: WEEKLY AMBIENT TEMPERATURES AND PRECIPITATION, RING NO. 3, 1967-68

Month	Week	Average Ambient Temperatures F°			Total Precipitation Inches
		Maximum	Minimum	Variation	
September 1967	10-16*	73.0	44.0	29.0	0.22
	17-23	82.5	49.0	33.5	0.00
	24-30	78.5	47.5	31.0	0.00
October 1967	1-7	60.0	41.0	19.0	0.39
	8-14	63.5	44.5	19.0	0.31
	15-21	62.5	37.0	25.5	0.24
	22-28	51.0	34.5	16.5	1.71
	29-31	57.5	35.5	22.0	0.00
November 1967	1-4	46.5	29.5	17.0	0.00
	5-11	50.0	34.0	16.0	0.89
	12-18	51.5	36.0	15.5	0.11
	19-25	43.0	30.0	13.0	0.15
	20-30	34.5	20.0	14.5	0.28
May 1968	1-4	64.0	33.0	31.0	0.00
	5-11	63.0	37.0	26.0	0.00
	12-18	67.0	43.0	24.0	0.08
	19-25	64.0	45.0	19.0	1.26
	26-31	66.0	43.0	23.0	0.03
June 1968	1-7	69.0	45.0	24.0	0.27
	8-14	67.0	45.0	22.0	0.28
	15-21	78.0	48.0	30.0	0.03
	22-28	75.0	50.0	25.0	0.18
	29-30	65.0	45.0	20.0	0.00
July 1968	1-7	92.6	42.5	50.1	0.00
	8-14	83.3	52.9	30.4	0.36
	15-21	77.6	44.1	33.5	0.26
	22-28*	88.0	47.0	41.0	0.00

* Testing started on September 13, 1967, and ended on July 25, 1968.

temperature variation as compared to the period of late October to the end of November when the weather was wet and the temperature was dropping with smaller variation in daily temperatures. The spring period can be subdivided into spring and early summer periods; the former being characterized with rising temperatures and wet weather while the latter being high daily temperature and dry weather.

Experimental Results

Section Failures

Fall Period (1967): Several sections started to show signs of distress and ultimately failed during this period. Signs of distress in the form of transverse cracks appeared almost at the same time at 379,047 wheel load repetitions in sections 1, 6 and 5 with zero inches of ATB, 7.0 and 3.5 inches of UTB respectively. Distress occurred in section 7, with 9.5 inches of UTB, at 636,246 wheel loads followed by section 2, with 2.0 inches of ATB, at 669,579 wheel loads, and finally by section 12, with 12 inches of UTB, at 727,161 wheel loads (see Tables 15 and 16).

Testing ceased after 735,573 wheel loads. At this time, sections 1, 5, 6 and 7 had been or were declared failed. These had been or had to be removed prior to resumption of spring testing.

The fall period can be divided into two periods--a period of dry fall weather with fairly high temperatures and a period of wet weather with temperatures falling.

Spring period (1968): Sections continued to develop signs of distress and section failures increased at an accelerated pace. Distress appeared in sections 9, 3 and 10 at 736,737, 770,244 and 772,746 wheel loads respectively.

TABLE 15: SECTION CONDITION PROGRESS REPORT

Base Type	Section	Base Thickness (Inches)	First Appearance of Distress		Section Declared Failed		Condition at 870,606 Wheel Loads
			Wheel Loads	Date	Wheel Loads	Date	
Crushed Surfacing Top Course (CSTC) Untreated (UTB)	5	4.5	379,047	10-12-67	679,107	11-13-67	Replaced
	6	7.0	379,047	10-12-67	679,107	11-13-67	Replaced
	7	9.5	636,246	11-06-67	735,573	12-04-67	Replaced
	8	12.0	727,161	11-29-67	870,606	07-25-68	Transverse cracks and rutting
Emulsion Treated (CSTC) (ETB)	9	3.0	736,737	05-10-68	744,723	05-16-68	Replaced
	10	5.0	772,746	06-22-68	792,538	07-09-68	Overlay, deformation excessive
	11	7.0			870,606	07-25-68	Excessive surface deformation
	12	9.0			870,606	07-25-68	Excessive surface deformation
Special Aggregate Asphalt Treated (ATB)	1	0.0	379,047	10-12-67	679,107	11-13-67	Replaced
	2	2.0	669,579	11-09-67	764,397	06-13-68	Replaced
	3	3.5	770,244	06-21-68	783,597	06-24-68	Replaced
	4	5.0			870,606	07-25-68	Excessive surface deformation

TABLE 16: PAVEMENT PERFORMANCE SUMMARY - FALL & SPRING PERIODS
RING NO. 3

Base Type	Section	Base Thickness Inches	First Appearance of Cracking				Section Failure			
				Wheel Load Applications				Wheel Load Applications		
			Date	Fall	Spring*	Total	Date	Fall	Spring*	Total
Crushed Stone Untreated	5	4.5	10-12-67	379,047	--	379,047	11-13-67	679,107	--	679,107
	6	7.0	10-12-67	379,047	--	379,047	11-13-67	679,107	--	679,107
	7	9.5	11-06-67	636,246	--	636,246	12-04-67	735,573	--	735,573
	8	12.0	11-29-67	727,161	--	727,161	07-25-68	735,573	135,033	870,606
Emulsion Treated	9	3.0	05-10-68	**	1,164	736,737	05-16-68	735,573	9,150	744,723
	10	5.0	06-22-68	**	37,173	772,746	07-09-68	735,573	58,905	794,538
	11	7.0	--	**	***	--	07-25-68	735,573	135,033	870,606
	12	9.0	--	**	***	--	07-25-68	735,573	135,033	870,606
Special Aggregate Asphalt Treated	1	0.0	10-12-67	379,047	--	379,047	11-13-67	679,107	--	679,107
	2	2.0	11-09-67	669,579	--	669,579	06-13-68	735,573	28,824	764,397
	3	3.5	06-21-68	**	34,671	770,244	06-24-68	735,573	48,024	783,597
	4	5.0	--	**	***	--	07-25-68	735,573	135,033	870,606

* To July 25, 1968

** Section did not crack or fail in the time period indicated.

*** These sections did not show any cracking at termination of testing period.

Sections 2, 3, 4, 8, 9, 10 and 12 were declared failed during this testing period as shown in Table 14. At the end only sections 4, 8, 11 and 12 did not have cracks although they are badly rutted. Testing was halted at 870,606 wheel loads.

The spring period can be divided into a spring period characterized by rising temperatures with precipitation and a summer period characterized by high temperatures and dry hot weather.

Failure pattern: The failure patterns of the sections in Rings #2 and #3 for the two periods had enough similarity so that two failure patterns, one for fall and one for spring, could be established.

In the fall, the failure pattern usually followed these steps:

1. Some visible flexing of the pavement section along with some settlement.

2. The appearance of a few transverse cracks of varying lengths and the pumping of mud through them. Since pumping depends upon wetness, cracking and pumping may or may not occur simultaneously, depending upon environmental conditions.

3. The transverse cracks lengthen and increase in frequency with or without pumping.

4. The appearance of a longitudinial crack along the wheel path center, with some noticeable permanent pavement subsidence and pumping. Pumping may or may not increase depending upon the weather.

5. Alligator cracking appearance and more settlement.

6. Longitudinal cracks appear at edge of the wheel path, with extensive subsidence of the traveled part of the pavement. The untraveled part of the pavement may bulge.

7. It becomes necessary to fill in the distressed sections to keep the frame from dragging. At this point the section is declared failed.

In the spring, the failure pattern differed somewhat and usually followed these steps:

1. Ruts became pronounced.

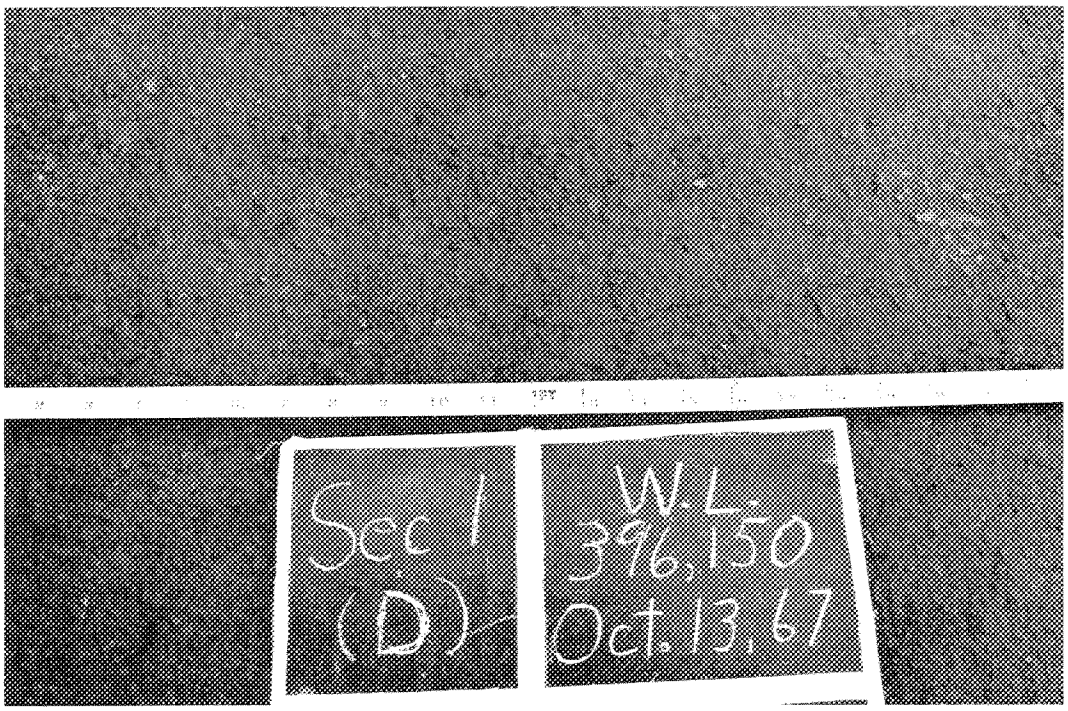

FIGURE 20. THE START OF TRANSVERSE CRACKS IN SECTION 1 (NO BASE) AFTER 396,150 WHEEL LOADS ON LINE D--OCTOBER 13, 1967.

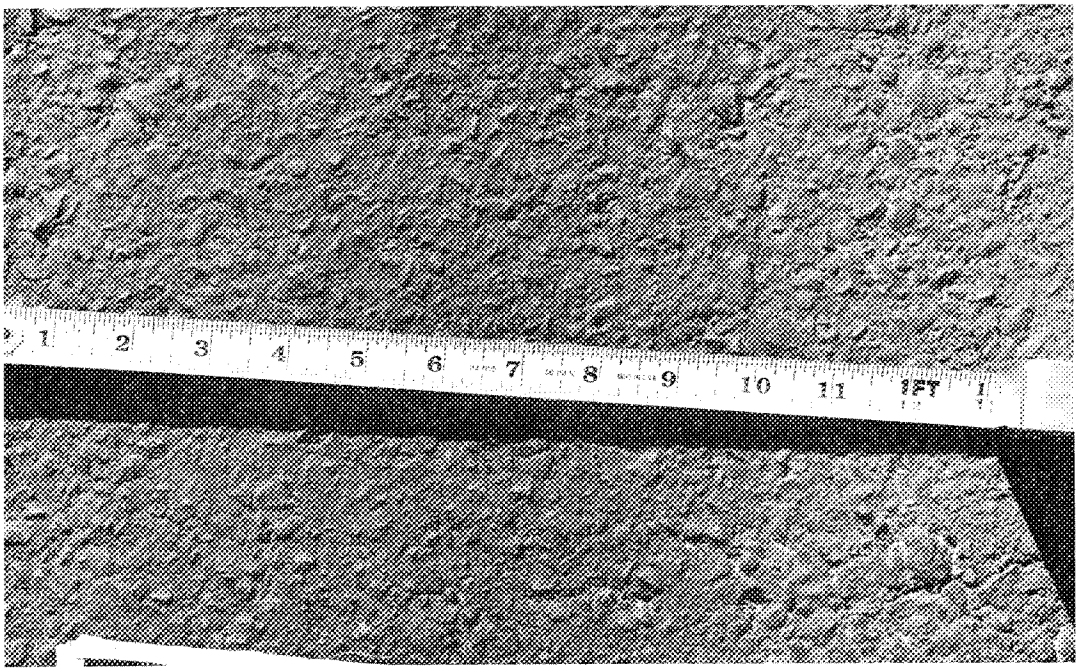

FIGURE 21. APPEARANCE OF SECTION 1 AFTER 562,335 WHEEL LOADS--OCTOBER 26, 1967.

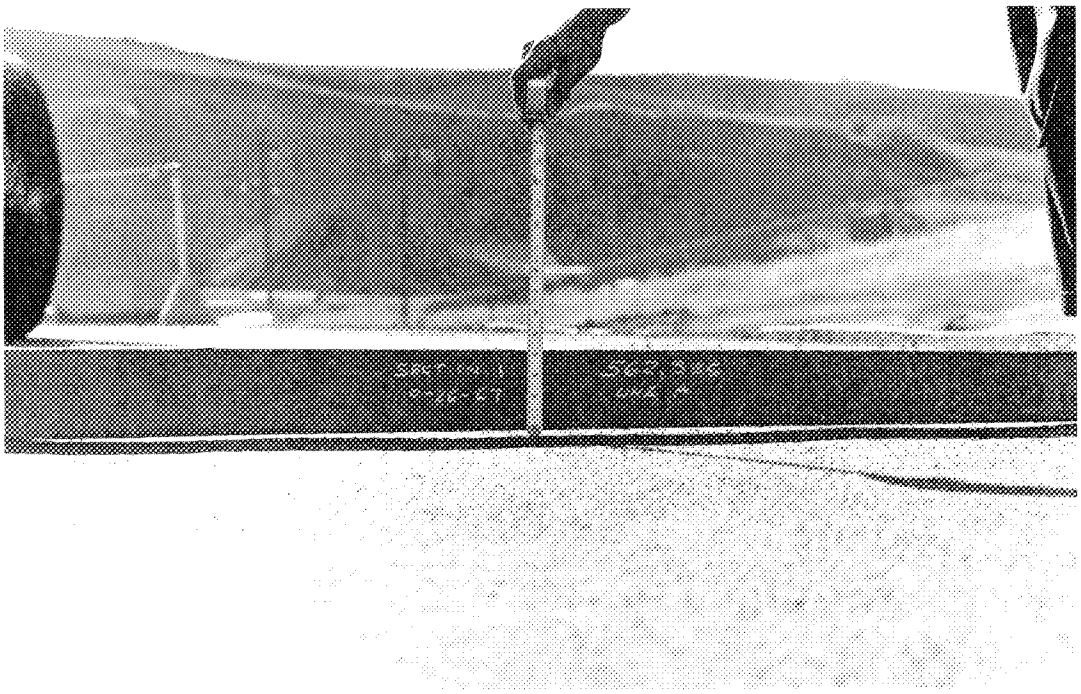

FIGURE 22. PERMANENT SETTLEMENT OF PAVEMENT IN SECTION 1 AFTER 562,335 WHEEL LOAD REPETITIONS ON LINE D-- OCTOBER 26, 1967.

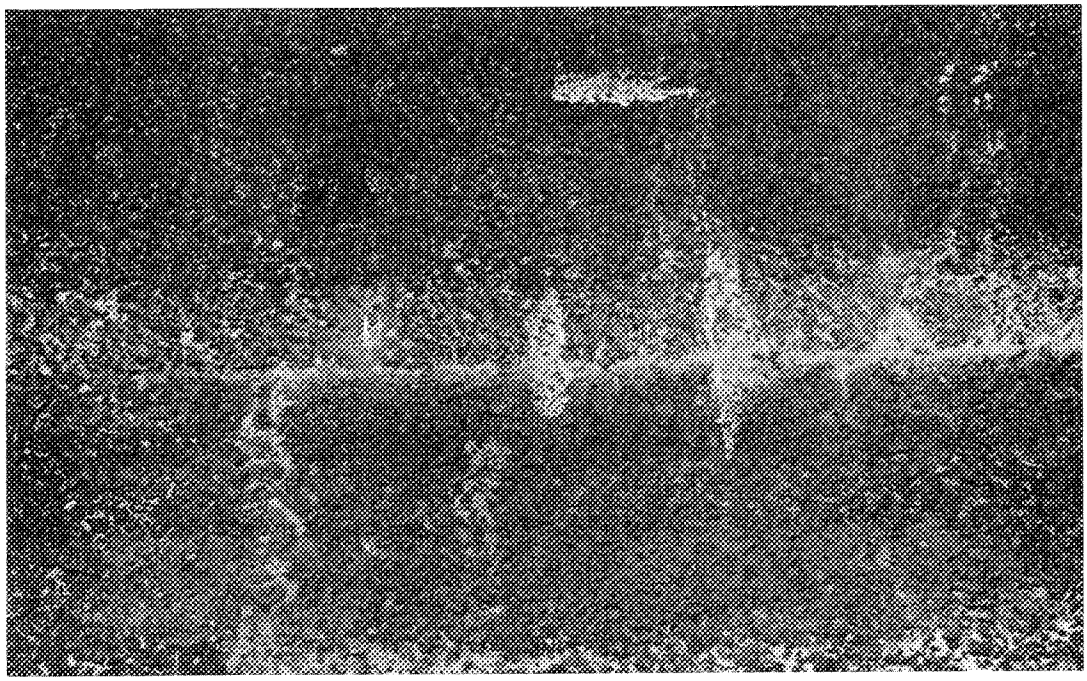

FIGURE 23. CONTINUED DETERIORATION OF SECTION 1 AFTER 588,000 WHEEL LOADS ON OCTOBER 30, 1967. NOTE THE INCREASED FREQUENCY OF TRANSVERSE CRACKS.

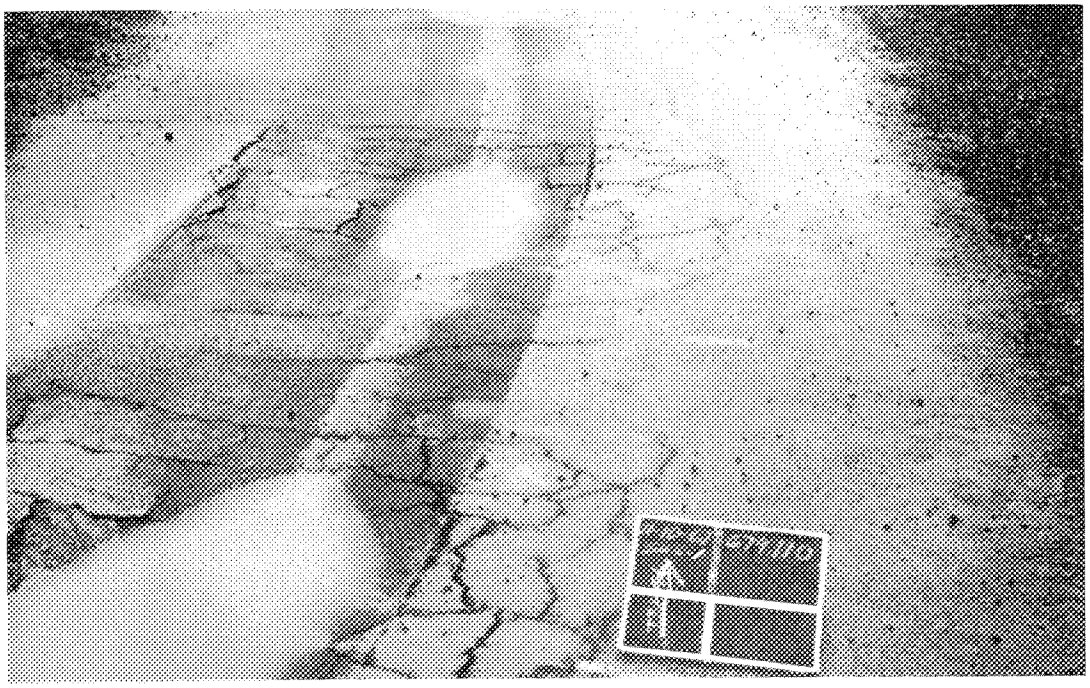

FIGURE 24. APPEARANCE OF SECTION 1 AFTER "ULTIMATE" FAILURE AND 679,107 WHEEL LOAD REPETITIONS ON NOVEMBER 10, 1967. THIS SECTION WAS REMOVED AND REPLACED WITH 8 INCHES OF ASPHALT CONCRETE.

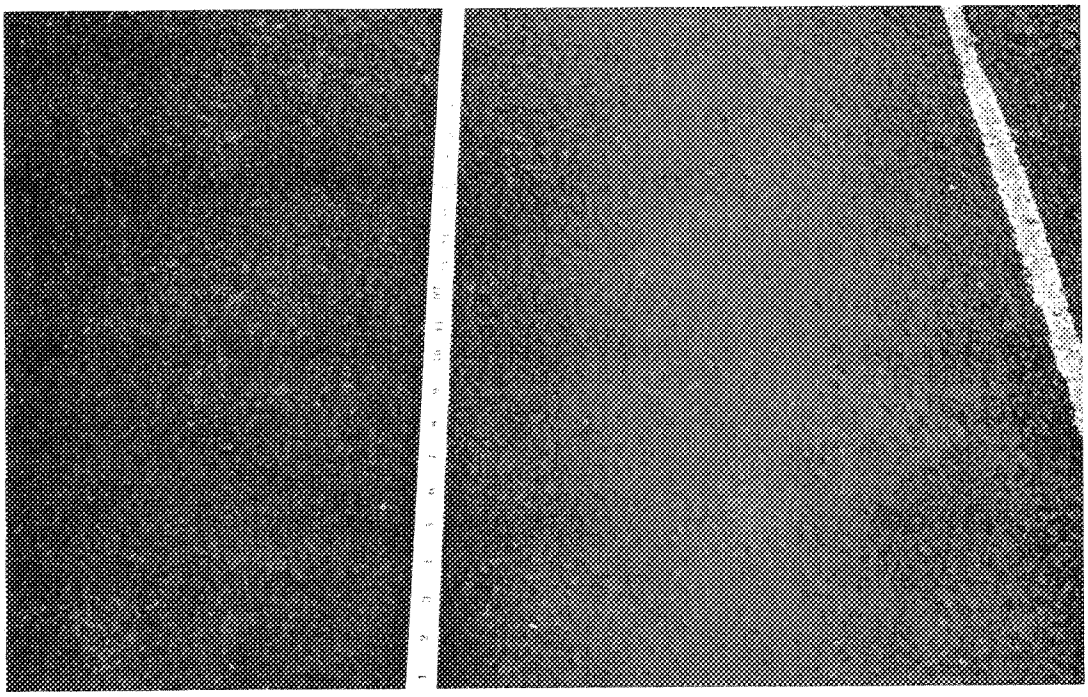

FIGURE 25. THE START OF TRANSVERSE CRACKS IN SECTION 6 (7.0 INCHES OF UNTREATED BASE) AFTER 396,150 WHEEL LOADS ON LINE A, OCTOBER 13, 1967.

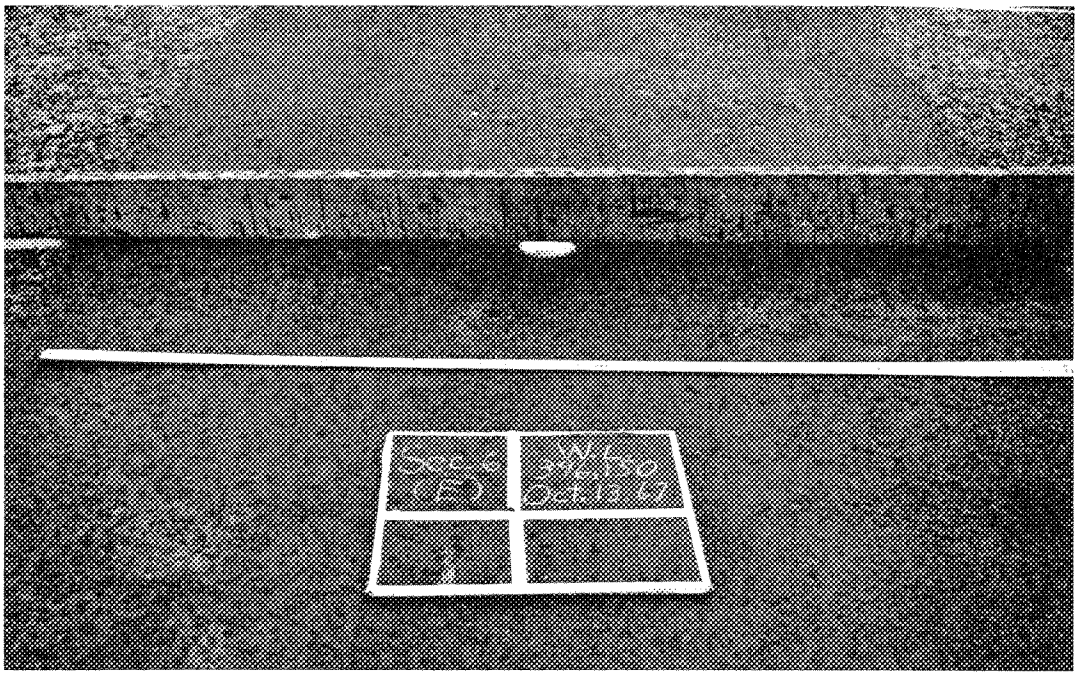

FIGURE 26. PERMANENT SETTLEMENT OF PAVEMENT IN SECTION 6 ON LINE E AFTER 396,150 WHEEL LOAD REPETITIONS.

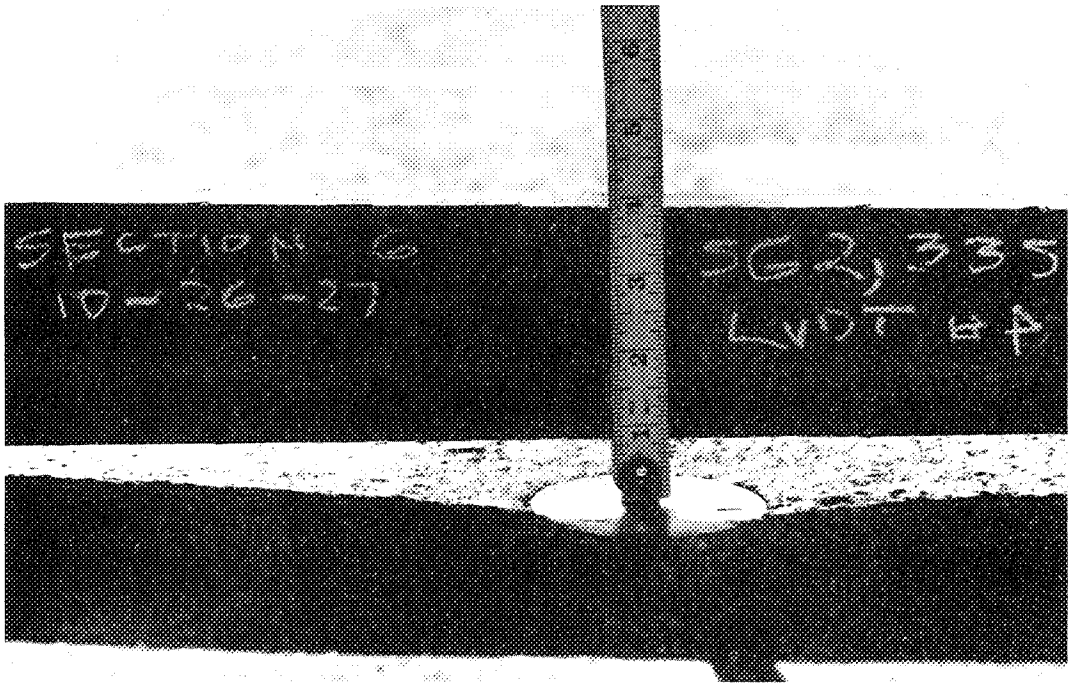

FIGURE 27. PERMANENT SETTLEMENT OF PAVEMENT IN SECTION 6 ON LINE E AFTER 562,335 WHEEL LOAD REPETITIONS, OCTOBER 26, 1967.

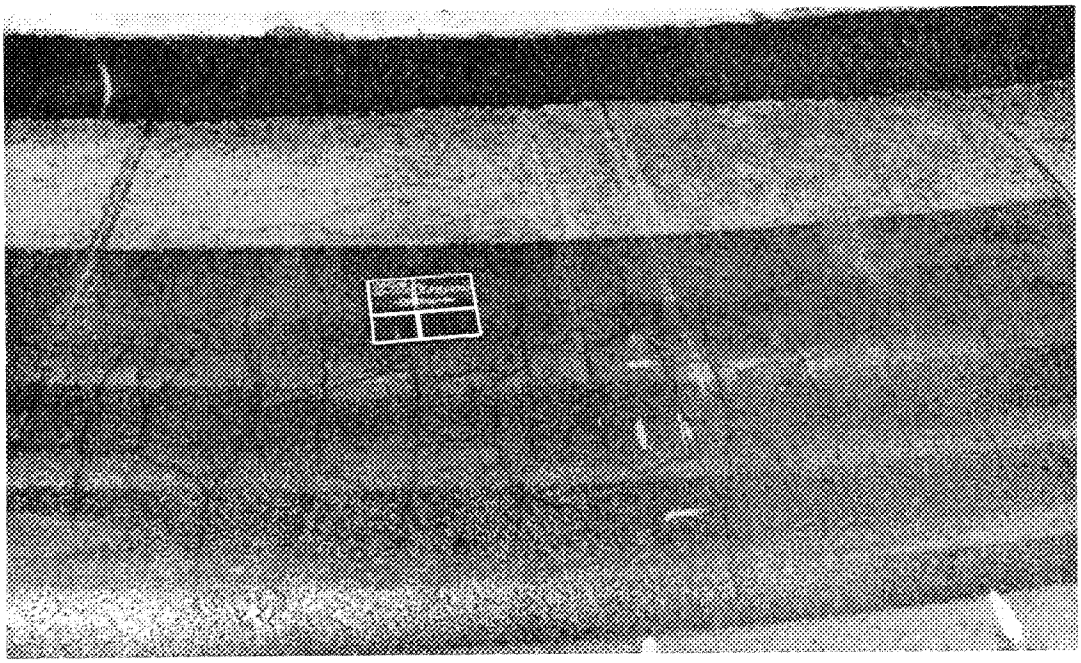

FIGURE 28. CONTINUED DETERIORATION OF SECTION 6 AFTER 588,000 WHEEL LOADS ON OCTOBER 30, 1967. NOTE THE UNIFORM "LARGE" ALLIGATOR CRACKING PATTERN.

FIGURE 29. "ULTIMATE" FAILURE IN SECTION 6 AFTER 679,107 WHEEL LOADS ON NOVEMBER 10, 1967. NOTE LONGITUDINAL CRACKS AT BOTH WHEEL PATH EDGES, THE UNIFORM ALLIGATOR CRACKING PATTERN AND THE WATER IN THE CENTER.

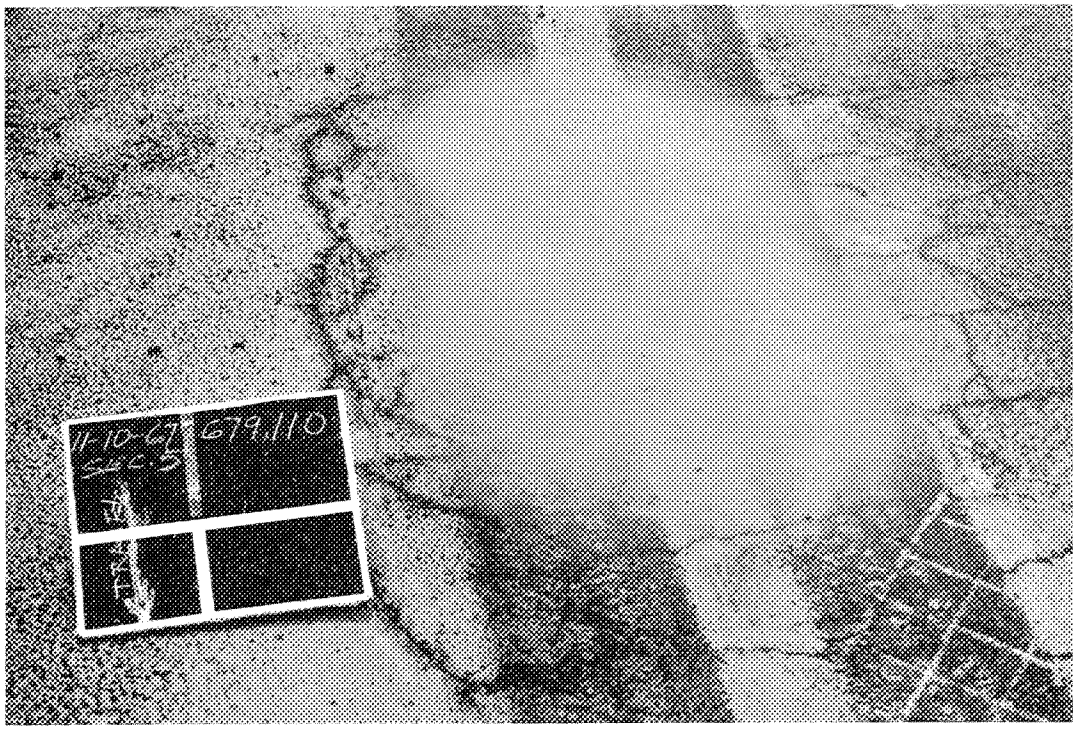

FIGURE 30. THE APPEARANCE OF SECTION 5 (4.5 INCHES OF UNTREATED BASE) AT "ULTIMATE" FAILURE AT 679,107 WHEEL LOAD REPETITIONS. THIS WAS LOCALIZED AROUND LINES E AND D.

FIGURE 31. APPEARANCE AND FAILURE IN THE TRANSITION ZONE BETWEEN SECTIONS 6 AND 7 (9.5 INCHES OF UTB) AFTER 679,107 WHEEL LOAD REPETITIONS. AN ASPHALT OVERLAY WAS PUT OVER THIS AREA.

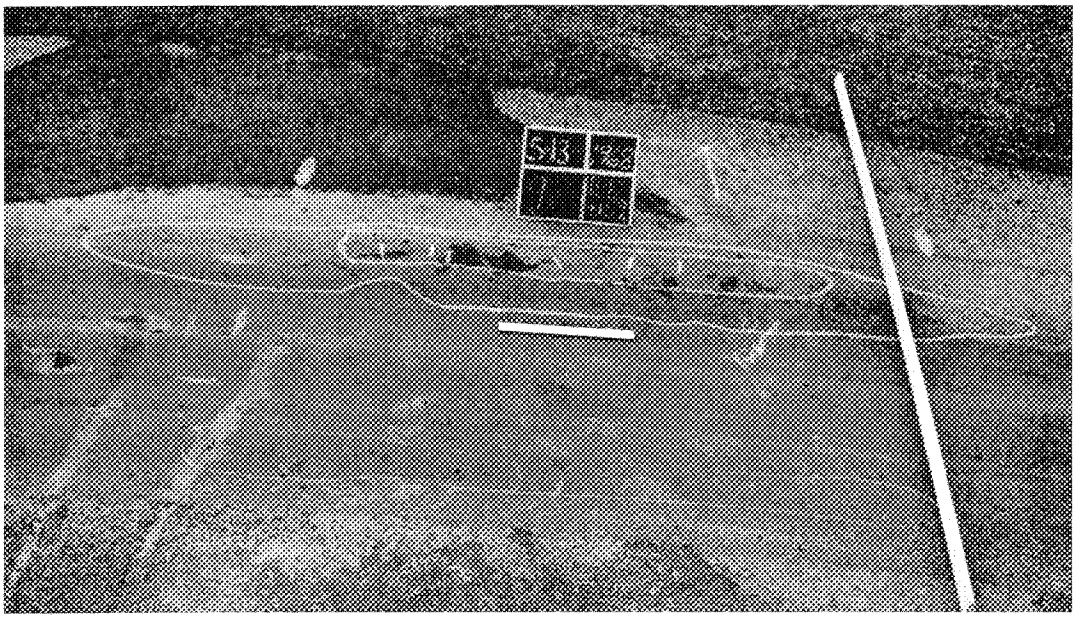

FIGURE 32. THE START OF FAILURE IN SECTION 9 (3.5 INCHES OF ETB) AFTER 736,896 WHEEL LOAD REPETITIONS. NOTE THE START OF LONGITUDINAL SHEAR CRACKS ALONG THE EDGE OF WHEEL PATH. THE INNER CHALK OUTLINED AREA WAS MARKED EARLIER AT 736,737 WHEEL LOADS ON MAY 13, 1968.

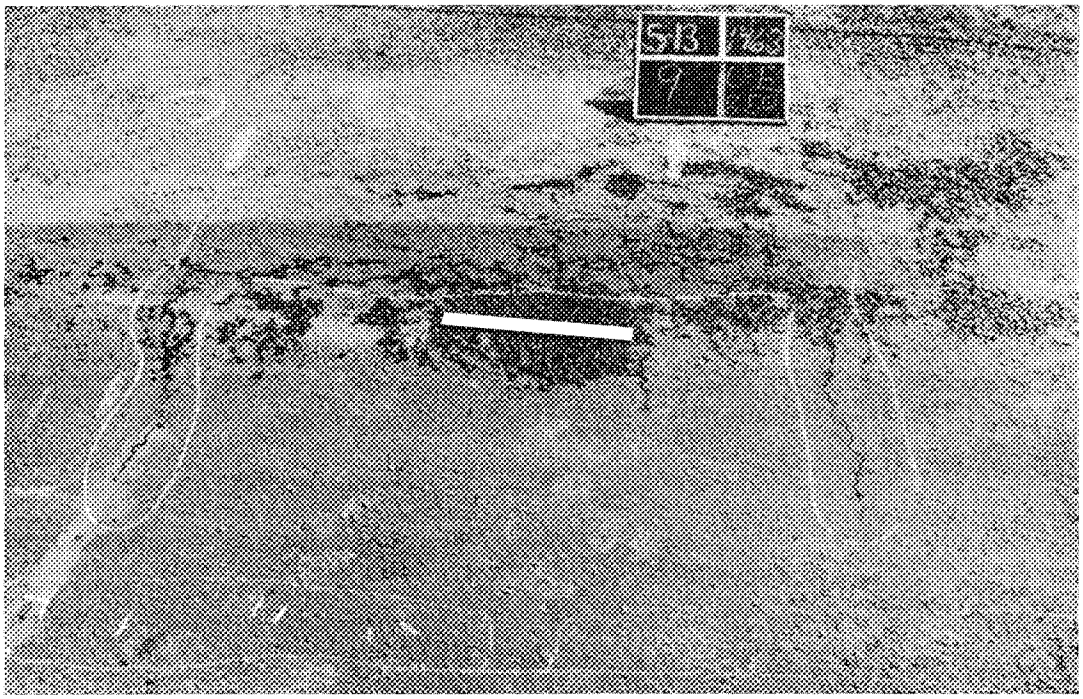

FIGURE 33. APPEARANCE OF SECTION 9 AFTER 737,587 WHEEL LOAD APPLICATIONS. NOTE THE TRANSVERSE CRACKS AND THE PERMANENT SETTLEMENT, MAY 13, 1968.

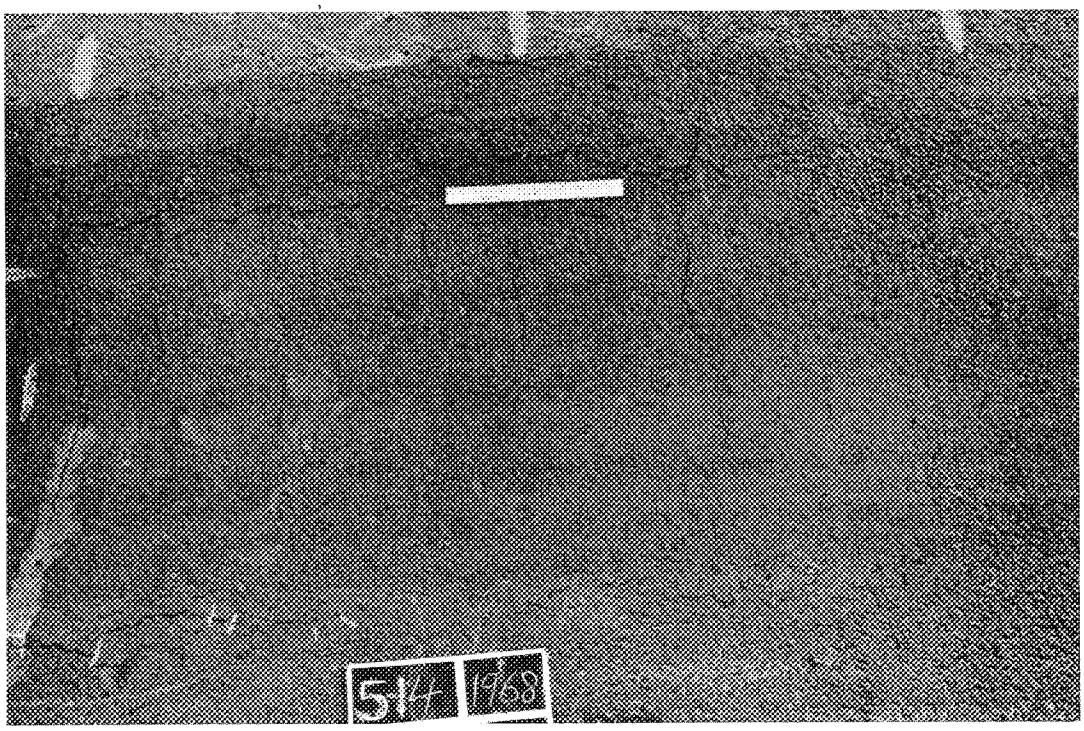

FIGURE 34. CONTINUED DETERIORATION OF SECTION 9 AFTER 740,279 WHEEL LOAD APPLICATIONS ON MAY 14, 1968.

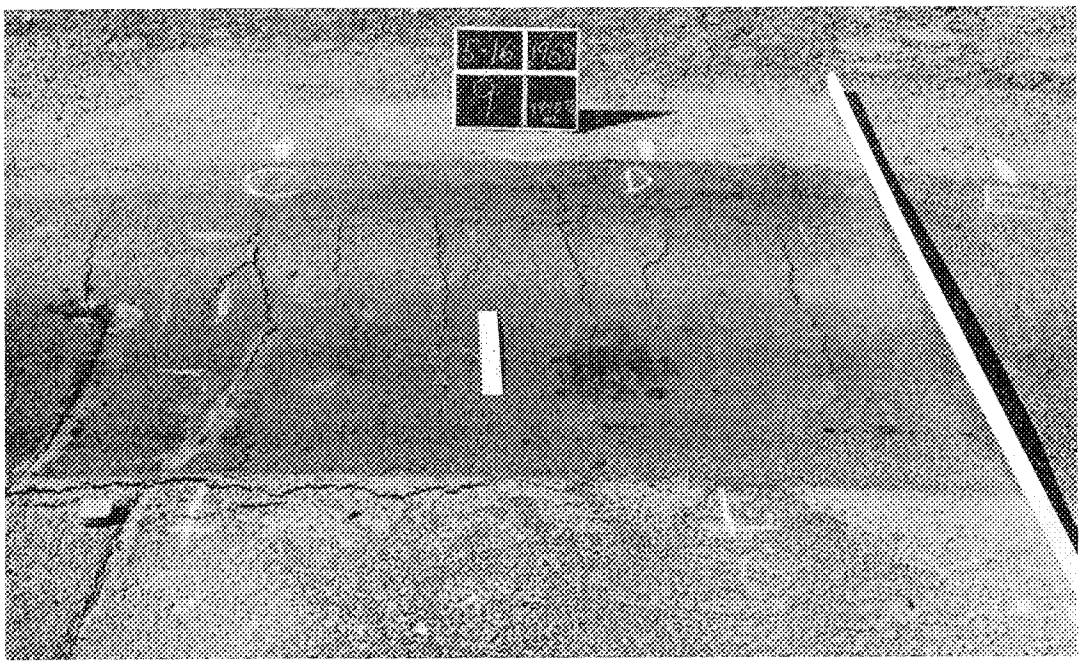

FIGURE 35. CONTINUED DETERIORATION OF SECTION 9 AFTER 744,072 WHEEL LOAD APPLICATIONS, MAY 16, 1968. NOTE THE PERMANENT SETTLEMENT.

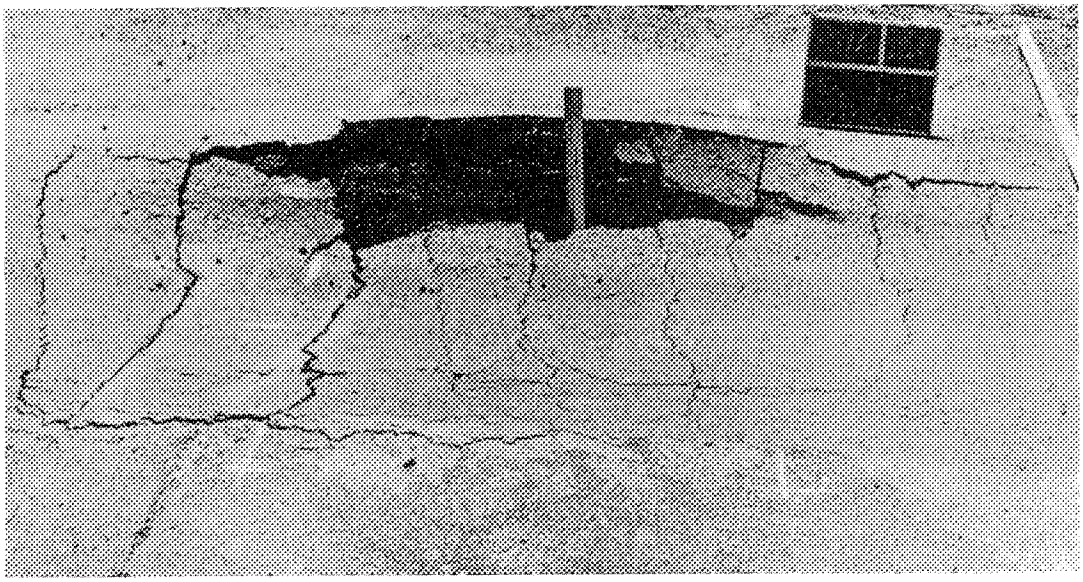

FIGURE 36. "ULTIMATE" FAILURE OF SECTION 9 AFTER 744,723 WHEEL LOAD APPLICATIONS ON MAY 16, 1968.

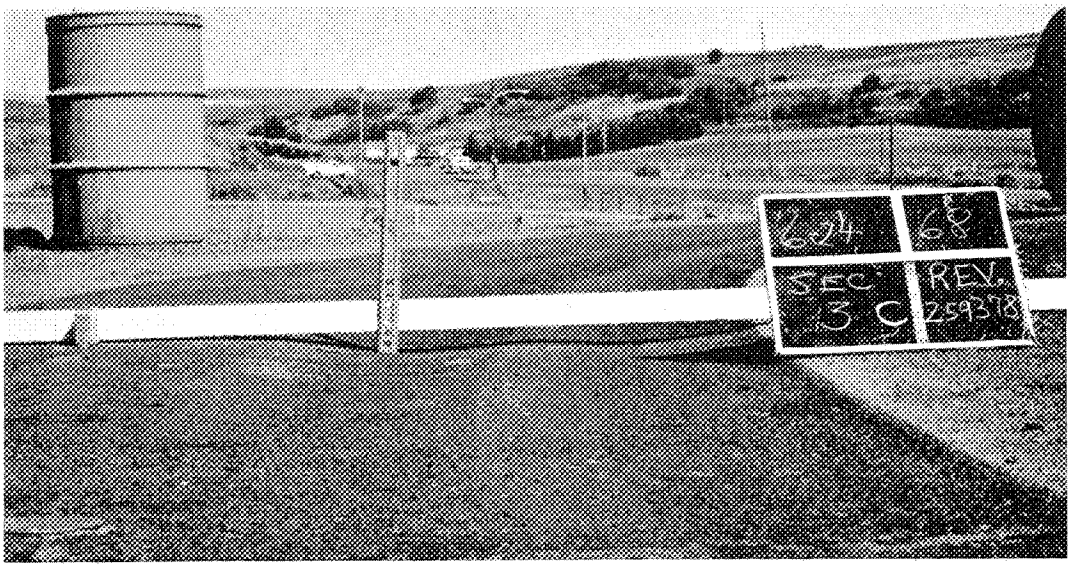

FIGURE 37. PERMANENT SETTLEMENT OF PAVEMENT IN SECTION 3 (3.5 INCHES OF ATB) AFTER 778,134 WHEEL LOAD APPLICATIONS ON JUNE 24, 1968.

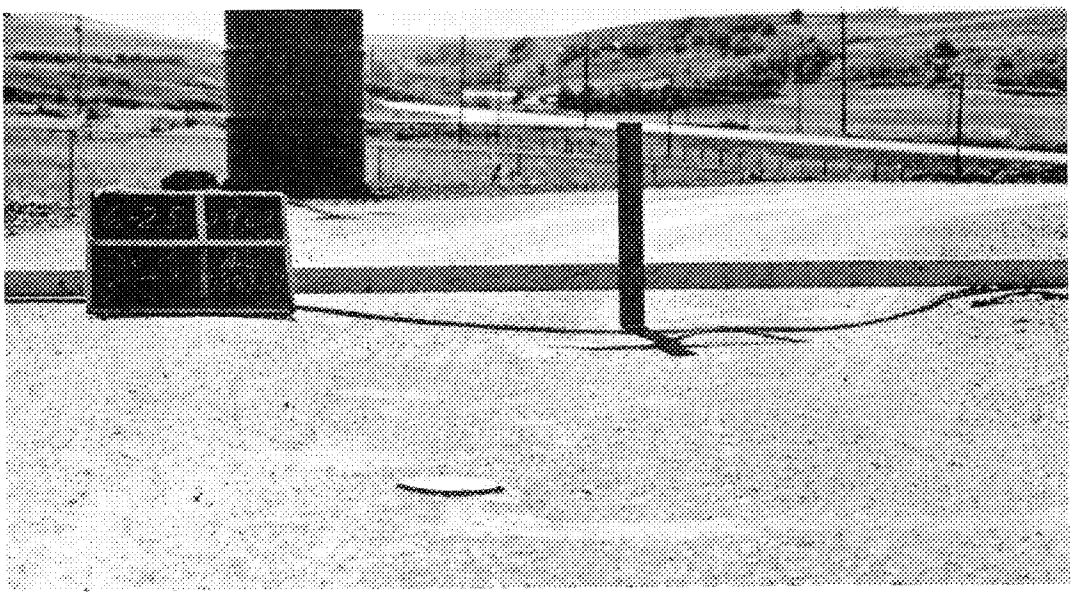

FIGURE 38. CONTINUED SETTLEMENT OF THE PAVEMENT IN SECTION 3 AFTER 780,987 WHEEL LOADS, JUNE 25, 1968.

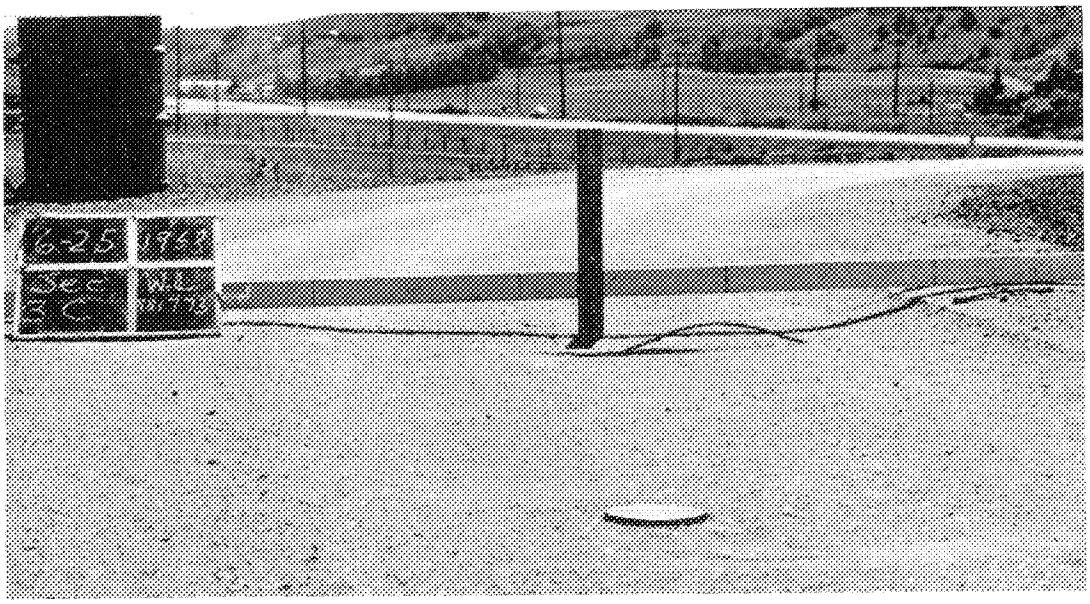

FIGURE 39. CONTINUED SETTLEMENT AND DETERIORATION OF SECTION 3 AFTER 781,773 WHEEL LOAD APPLICATIONS, JUNE 25, 1968.

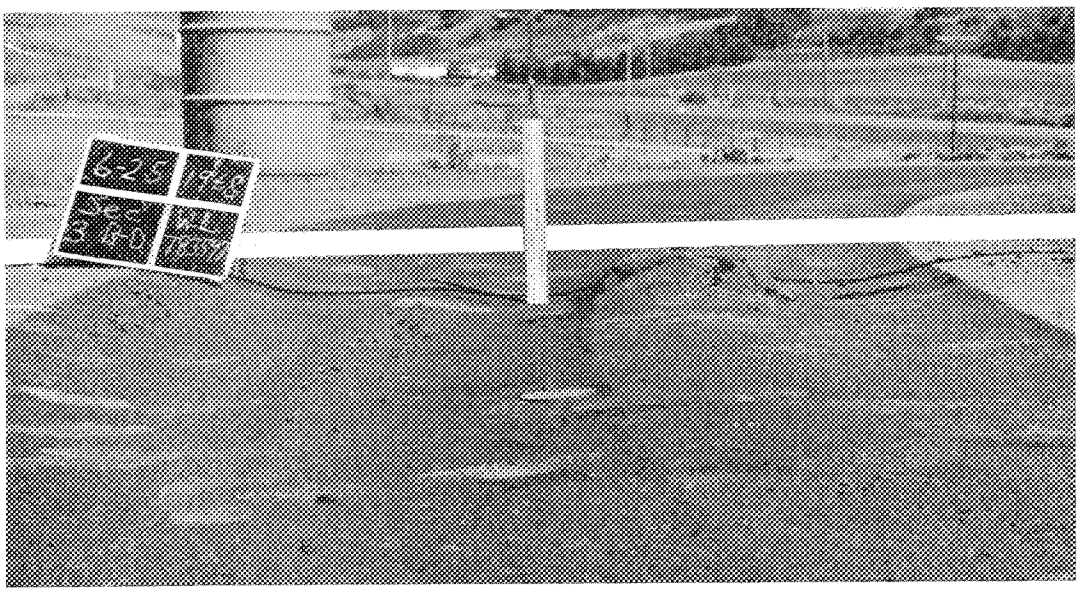

FIGURE 40. "ULTIMATE" FAILURE OF SECTION 3 AFTER 783,597 WHEEL LOADS ON JUNE 25, 1968.

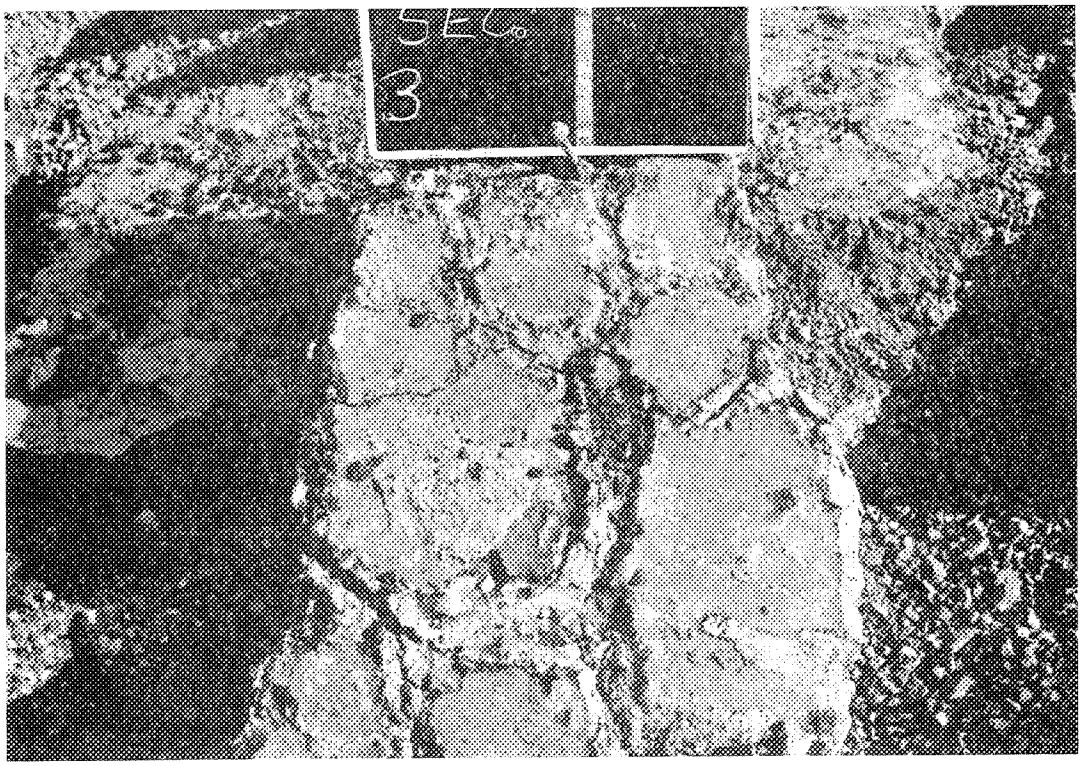

FIGURE 41. THE APPEARANCE OF THE BOTTOM OF SECTION 3 ASPHALT TREATED BASE. NOTE THE FATIGUE CRACKING APPEARANCE AND THE FILLING OF THE CRACKS BY THE SILT SUBGRADE.

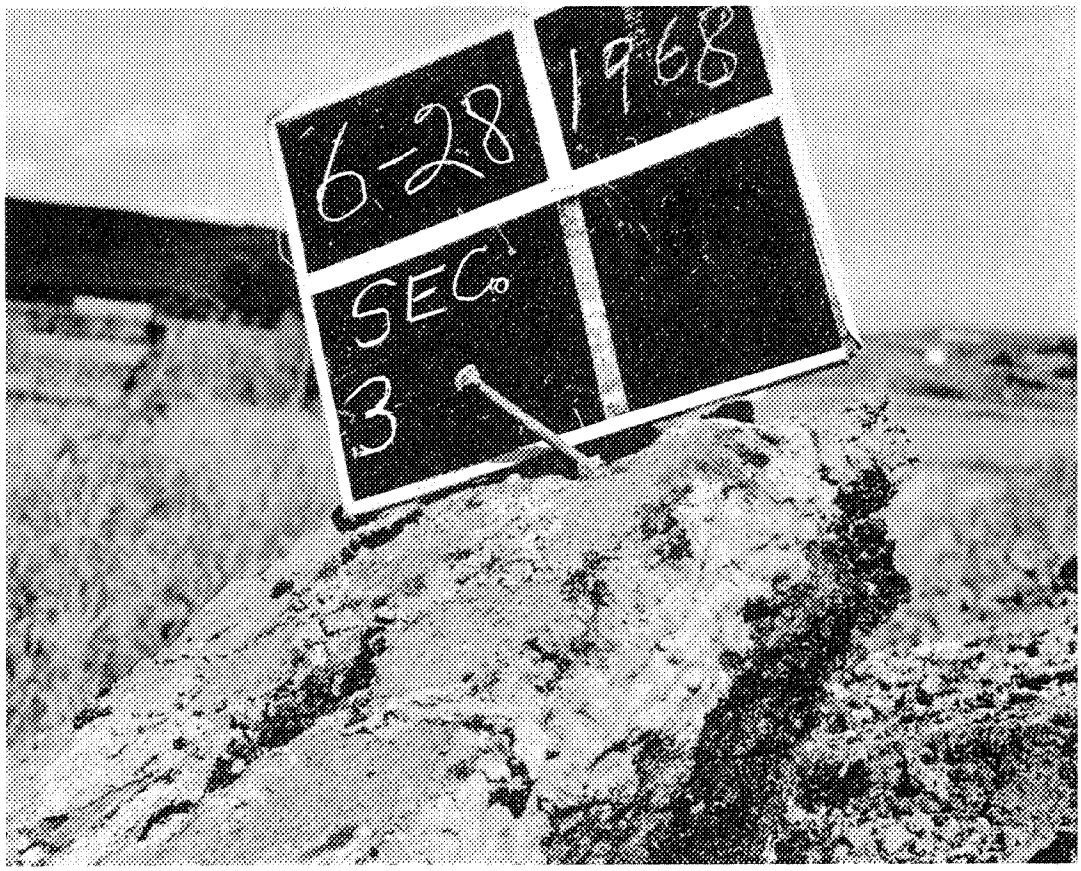

FIGURE 42. SAME MATERIAL AS SHOWN IN PREVIOUS PHOTOGRAPHS. NOTE THE FATIGUE CRACK JOINTS FILLED WITH THE SILT SUBGRADE.

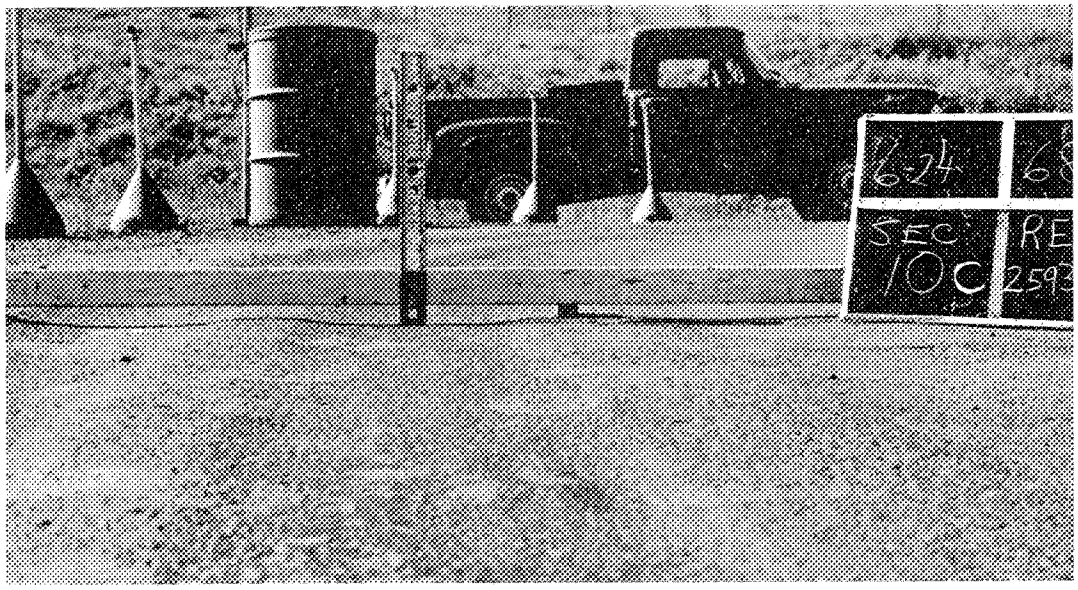

FIGURE 43. RUTTING AND SETTLEMENT IN SECTION 10 (5.0 INCHES OF ETB) ON JUNE 25, 1968, AFTER 778,134 WHEEL LOAD APPLICATIONS.

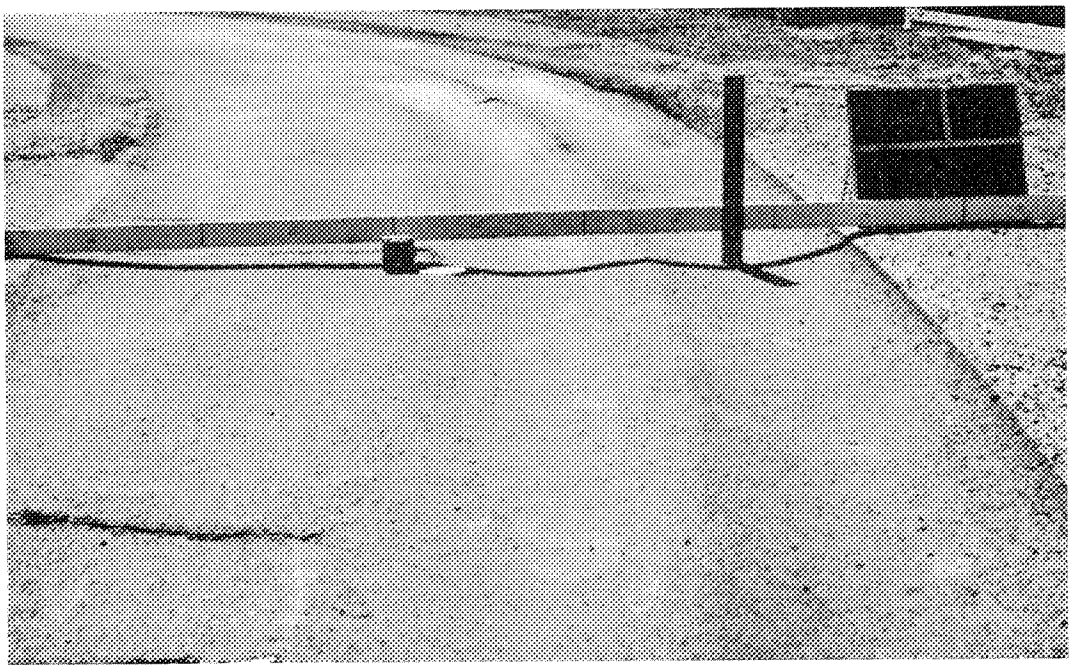

FIGURE 44. APPEARANCE OF SECTION 10 AFTER 794,763 WHEEL LOAD APPLICATIONS ON JULY 9, 1968, AND PRIOR TO PUTTING ON AN ASPHALT "SKIN" PATCH.

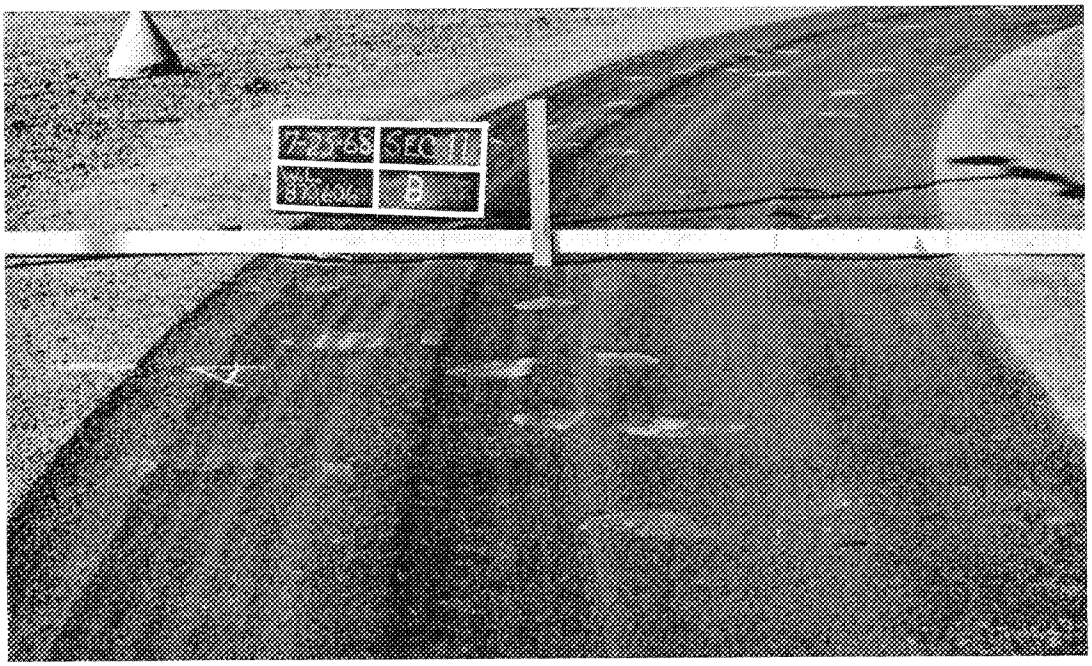

FIGURE 45. FINAL APPEARANCE OF SECTION 11 (7.0 INCHES OF ETB) ON JULY 25, 1968, AFTER 870,606 WHEEL LOAD APPLICATIONS. NOTE THE RUTTING.

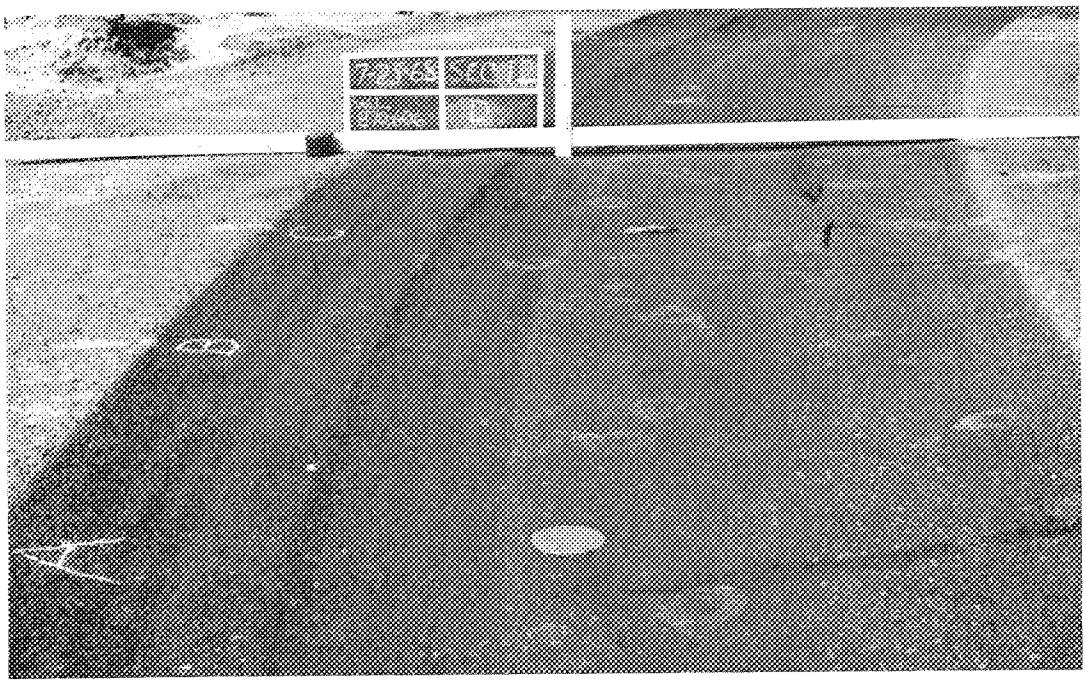

FIGURE 46. FINAL APPEARANCE OF SECTION 12 (9.0 INCHES OF ETB) AFTER 870,606 WHEEL LOADS ON JULY 25, 1968. NOTE THE PERMANENT SETTLEMENT AND THE RUTTING.

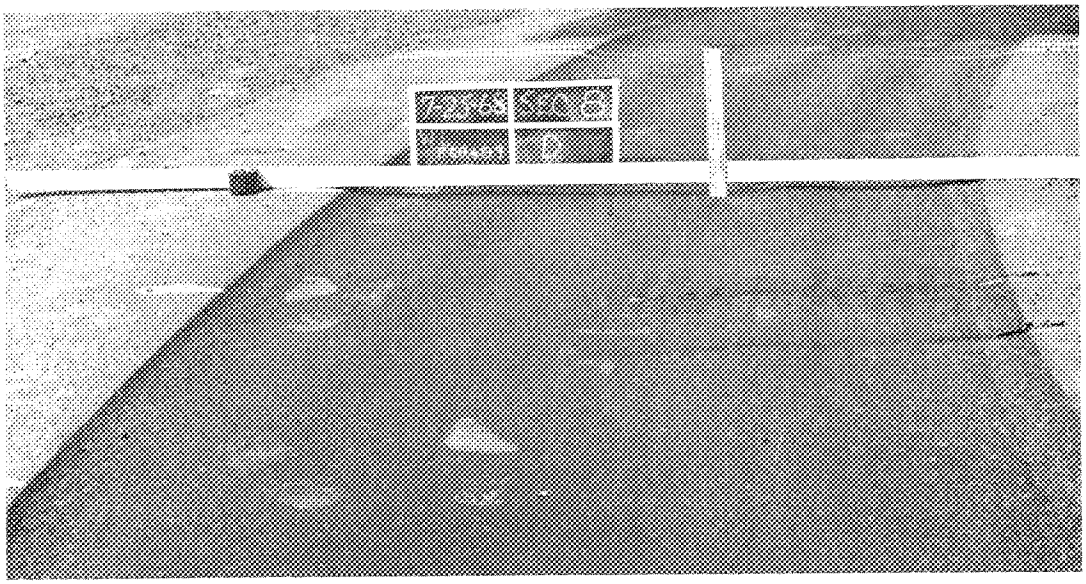

FIGURE 47. FINAL APPEARANCE OF SECTION 8 (12.0 INCHES OF UTB) AFTER 868,689 WHEEL LOADS ON JULY 25, 1968. NOTE THE RUTTING AND PERMANENT SETTLEMENT. THE TRANSVERSE CRACKS FROM LAST FALL HAD HEALED OVER.

FIGURE 48. APPEARANCE OF SECTION 4 (5.0 INCHES OF ATB) AFTER 868,689 WHEEL LOAD REPETITIONS, JULY 25, 1968. NOTE THE RUTTING AND PERMANENT SETTLEMENT.

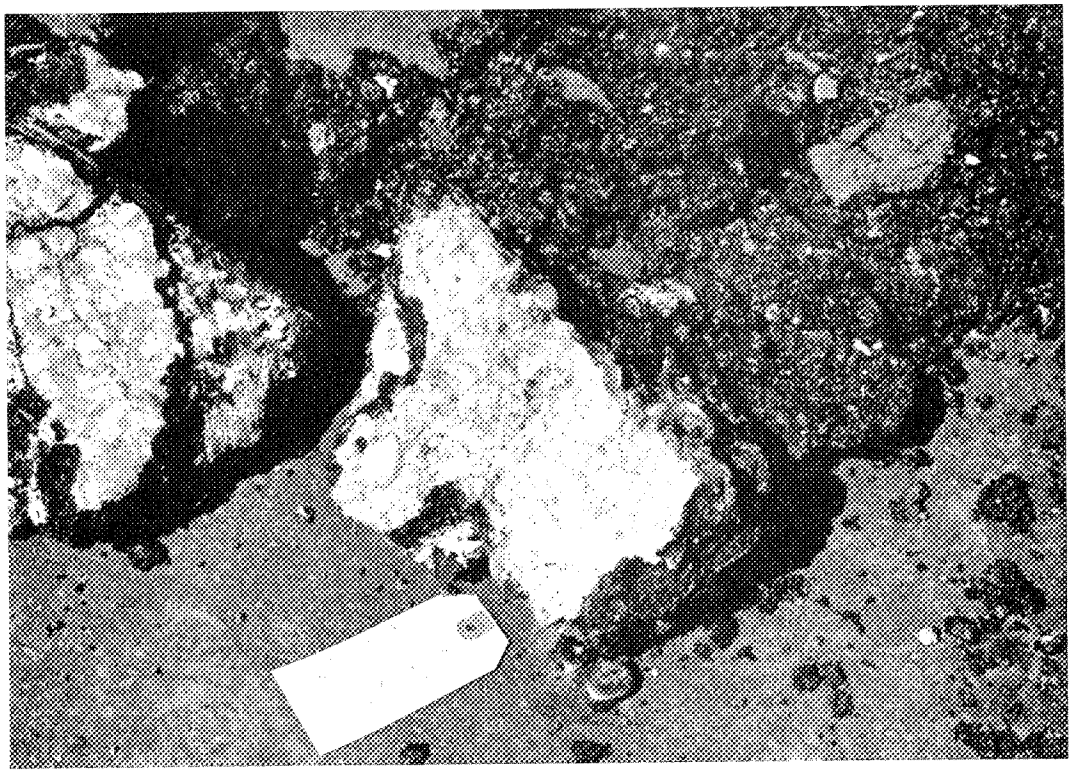

FIGURE 49. APPEARANCE OF THE 5.0 INCH ASPHALT TREATED BASE EXCAVATED FROM SECTION 4. NOTE THE FINE ALLIGATOR CRACKING AT THE BOTTOM OF THE BASE DUE TO FATIGUE CRACKING.

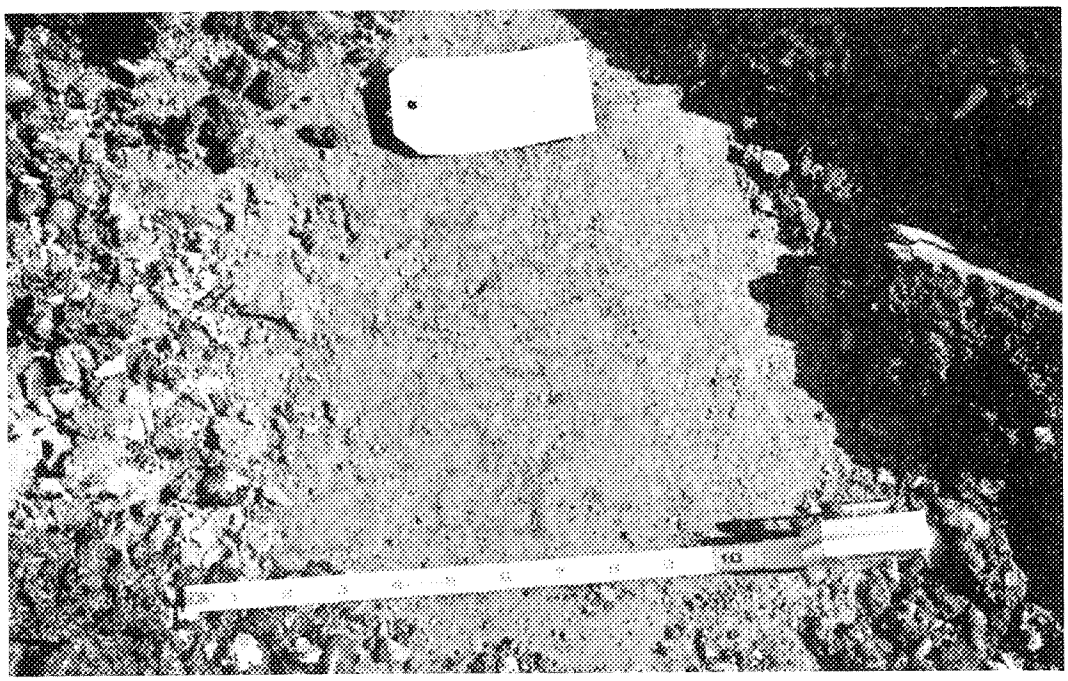

FIGURE 50. APPEARANCE OF THE SUBGRADE AFTER THE BASE IN SECTION 4 WAS REMOVED. NOTE SUPER-IMPOSITION OF FATIGUE CRACKING PATTERN ON THE SUBGRADE.

FIGURE 51. A CROSS SECTION VIEW OF SECTION 10 WITH 5.0 INCHES OF ETB. NOTE THE GRANULAR AND BROKEN APPEARANCE OF THE ETB.

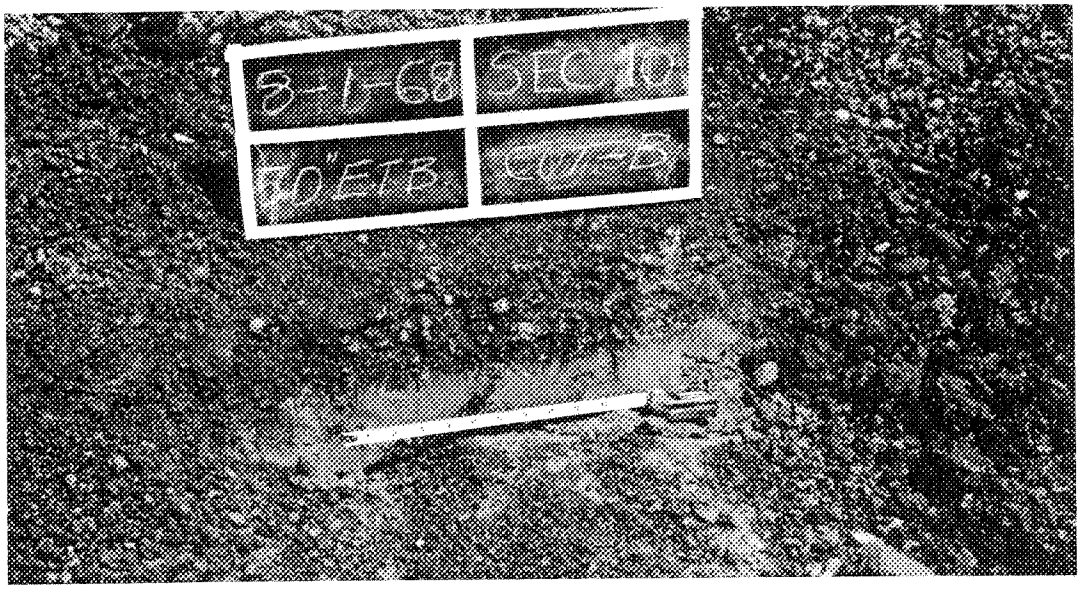

FIGURE 52. A CROSS SECTION VIEW OF SECTION 12 WITH 9.0 INCHES OF ETB. NOTE THE BOTTOM LAYER OF ETB JUST ABOVE THE SILT SUBGRADE HAS A BROKEN APPEARANCE.

2. Very visible flexing of the pavement.

3. The appearance of a few transverse cracks of varying lengths and the pumping of mud through them. Since pumping depends upon wetness, cracking and pumping may or may not occur simultaneously, depending upon environmental conditions.

4. The transverse cracks lengthen and increase in frequency with or without pumping.

5. Longitudinal shear cracks appear at the edge of the dual tires. Some alligator cracking pattern may occur, but is not fully developed.

6. Extensive settlement occurs followed by a longitudinal shear crack on the inside or outside edge of dual tires. The untraveled part of the pavement may bulge.

7. It becomes necessary to fill in the distressed section to keep the frame from dragging. At this point the section is declared failed.

Discussion of Section Failures

Contrasts between fall and spring failures were evident. Table 15 was rearranged into Table 16 to show the number of wheel applications for the different time periods, the time of first distress, and failure. Table 18 shows the amount of wheel loads needed to cause "ultimate" failure after the first appearance of cracking. "Ultimate" failure, as used here, means that the failure of the pavement was taken beyond practical limits reached in regular highway usage; in other words, on a regular highway the pavement would have been repaired long before the "ultimate" failure point was ever reached. Usually, when the skids on the loading arms started to drag on the pavement edge, "ultimate" failure was declared to have occurred. "Ultimate" failure is shown in Figures 24, 29, 30, 36, 40 and 44.

The appearance of transverse cracks in the fall period was usually preceded by visible pavement deflection (over 0.10 inches) and by rutting. The cracks usually started in weak areas located by Benkelman beam rebound measurements. Each section was divided into 5 areas spaced 2-1/2 feet apart and lettered from

A to E as shown in Figure 53; rebound measurements were always taken at each marked line. Relatively higher readings (as compared to the rest) pin-pointed the location of where the first signs of distress would appear. Table 17 gives an indication of the size of these deflections for sections 1 and 6. The relatively higher readings as found in line E of section 6 indicates a variance and a zone of weakness. Initial distress usually started at these points as shown in Figures 20 and 25 (page 44).

Transverse cracks initially appeared between lines C and D, and in line A in section 1 (zero base thickness), line E and between lines B and C in section 6 (7.0 inch untreated base), and in lines A and E in section 5 (4.5 inch untreated base) as predicted by the Benkelman beam readings (see Figures 20 and 25). As the number of wheel loads accumulated, these transverse cracks increased in length and cracks did occur, especially after a rainfall. Permanent settlement of the wheel path increased as shown in Figures 22, 26 and 27. Longitudinal cracks then appeared causing a large sized "alligator" cracking pattern as shown in Figures 23 and 28. Eventually the section serviceability so deteriorated that they had to either be removed and repaired or overlaid. At this time the depth of the ruts for sections 1 and 6 were 2-3/4 and 1-13/16 inches on centerline, respectively. Figures 24 and 29 show the appearance of the two sections just before being declared failed and their removal.

Although transverse cracks did appear in section 5 (4.5 inches of untreated base) at the same time as in section 6 (7.0 inches of untreated base), the cracks did not increase as rapidly as in sections 6 or 1. Parts of section 5 were still serviceable when the failed areas were overlaid with asphalt as shown in Figure 30 (page 49).

Transverse cracks next appeared in section 7 (9.5 inches untreated base) at 636,246 wheel loads in lines B-D. Distress increased rapidly especially

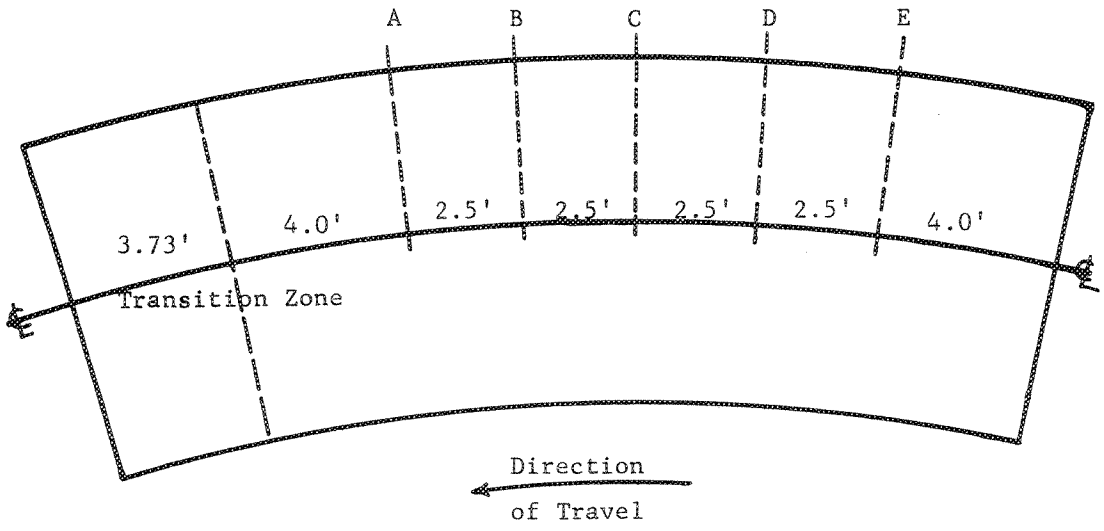

FIGURE 53. LOCATION OF BENKELMAN REBOUND MEASUREMENTS

TABLE 17:

BENKELMAN REBOUND MEASUREMENTS FOR SECTIONS 1 & 6

Wheel Loads		188			325,971			Comment
Section	Line	Air Temp F°	Pavement Temp* F°	Deflection In.	Air Temp F°	Pavement Temp* F°	Deflection In.	
1	A	55	67.0	.040	70	68.5	.060	Transverse cracks started around D, and then in A, then increased from both sides
	B	55	70.0	.040	68	68.5	.052	
	C	54	63.5	.039	65	68.5	.059	
	D	55	70.0	.036	64	68.5	.060	
	E	53	60.5	.037	64	68.5	.051	
		54						
	Avg.	54	66.0	.038	66	68.5	.056	
6	A	56	67.0	.039	71	75.0	.049	Transverse cracks started in E, then in center between B & C, then increased.
	B	53	62.5	.033	71	75.0	.056	
	C	54	62.5	.036	71	75.0	.061	
	D	54	62.5	.044	71	67.0	.055	
	E	52	63.0	.050	71	67.0	.068	
	Avg.	54	63.5	.040	71	72.0	.058	

* Average temperature of A.C. Class"B"wearing course (at 0.0" and 3.0" depth)

at the transition zone end adjoining section 6. This end (see Figure 31) was overlaid with asphalt concrete. The rut depths varied from 1/4 to 11/16 inches on centerline going from A to E respectively.

Section 2 (2.0 inches of special asphalt base) soon began to show signs of distress at Line E. At this point Benkelman beam measurements showed higher readings when compared to the rest of the section measurements. Transverse cracks appeared around this location. At this time, the rut depths varied from 3/8 to 9/16 inches along the centerline. This section was declared failed in the spring after 764,397 wheel load applications.

Section 8 (12 inches of untreated base) developed transverse cracks between lines B, C, and D after 727,161 wheel loads. The remaining sections were in excellent condition, except for section 9 (3.0 inches of emulsion treated base) which had more rutting than the remaining sections. The depth of these ruts measured over 5/8 inches on centerline.

Examination of the failed section 1 (zero base thickness) shows that the moisture contents of the subgrade and shoulder materials did increase but not above optimum moisture levels. Table 20 has the moisture contents found in section 1. Directly under the puddles shown in Figure 24 and right on top of the subgrade surface, moisture contents were high--27.2%--indicating that water seeped downward through the cracks. This moisture content rapidly decreased with depth. On the average, the moisture content in section 1 increased by 4.5% since construction. The shoulders on the outside and inside were fairly dry. It had rained the week before the section was excavated but section 1 failed because of structural deficiencies (lack of base) rather than from subgrade weaknesses.

The failures in the fall were different from those in the spring. The failure mode followed was that as outlined in the previous sections, although rutting and visible pavement deflections were not as evident or prominent as during the spring. Initial cracking often appeared in the spring after 0.10 inches of deflection compared to the fall when cracking appeared after 0.050 inches of deflection. The number of wheel load applications to reach "ultimate" failure was large as compared to the spring period as shown in Table 18.

In contrast, sections 2, 3, 9 and 10, the first two containing the asphalt treated bases and the latter two the emulsion treated bases which failed at the resumption of testing in the spring, failed rapidly. Once initial cracking appeared, "ultimate" failure occurred very rapidly as shown in Table 18 and Figures 32-44 (pages 50-56).

Differences between failures occurring during the two periods were noticeable. During the spring period, shear cracks occurred at the edge of the wheel path as shown in Figure 32. The alligator cracking pattern was not as fully developed as in the section which failed in the fall and shown in Figures 36, 40 and 44. Failure in the fall was slower and progressive, following the failure mode steps mentioned before. The spring failure by-passed some of the failure mode steps and occurred rapidly and spectacularly. Pavement deflections were evident and large with pronounced rutting just before the appearance of cracking as shown in Figures 32, 38, 43, 45, 46, 47 and 48 (page 58).

As soon as testing was resumed in the spring, section 9 (3.0 inches of ETB) started to show extreme deflections and severe rutting in the wheel path. As the wheel moved outward, there was lateral shoving of the subgrade

TABLE 18: PAVEMENT FAILURE SPAN (PFS)[2] - RING #3

Base Type	Section	Base Thickness (Inches)	Wheel Load Applications			PFS	Time Period
			Initial Cracks WL_I	At Failure WL_F	Initial to Failure WL_F-WL_I		
Crushed Surfacing Top Course Untreated UTB	5	4.5	379,047	679,107	300,060	79.2	Fall
	6	7.0	379,047	679,107	300,060	79.2	Fall
	7	9.5	636,246	735,573	99,327	15.6	Fall
	8	12.0	727,161	870,606	143,445	19.7	Fall-Spring
Emulsion Treated ETB	9	3.0	736,737	744,723	7,986	1.1	Spring
	10	5.0	772,746	794,538	21,792	2.8	Spring
	11	7.0	780,000[1]	870,606	90,606	11.6	Spring
	12	9.0	780,000[1]	870,606	90,606	11.6	Spring
Special Aggregate Asphalt Treated ATB	1	0.0	379,047	679,107	300,060	79.2	Fall
	2	2.0	669,579	764,397	94,818	14.2	Fall
	3	3.5	770,244	783,597	13,353	1.7	Spring
	4	5.0	780,000[1]	870,606	90,606	11.6	Spring

[1] Arbitrarily chosen as when rutting became noticeable.

[2] PFS = Wheel load applications (Failure - Initial)/wheel load applications to 1st sign of cracking $= \frac{WL_F - WL_I}{WL_I} \times 100$

TABLE 19: EQUIVALENT THICKNESSES
(3.0" of Class "B" A.C. Wearing Course)

Base Type	Fall 1967 Period[1]		Spring 1968 Period[2]	
	Base Thickness	In Terms of ATB	Base Thickness	In Terms of ATB
Crushed Surfacing Top Course (CSTC) Untreated (UTB)	9.5	4.75	12.0	2.40
Emulsion Treated CSTC ETB	3.0	1.50	9.0	1.80
Special Aggregate Asphalt Treated ATB[3]	2.0	1.00	5.0	1.00

[1] The thinnest sections which survived during this period.

[2] Thickest sections which failed during this time.

[3] Hot mixed.

and base causing uplift of the pavement. The curvature of ruts increased and longitudinal tension surface cracks appeared. Soon afterwards, these increased, followed by transverse cracks, and eventually alligator cracking. The ruts were deep, over 3.0 inches deep at ultimate failure. This is shown in Figures 32-36. Investigation showed that the failure was similar to that which occurred in Ring #2. The failure was very rapid, only some 9,150 wheel loads to failure after the spring start-up. The subgrade was above optimum moisture and the moisture content increased with depth--see Table 19--and moisture content with depth figure. This failure seems to be due to subgrade conditions caused by spring environment. The base may have been inadequate in strength to withstand the extreme deflections thus failing in tension and fatigue. When the emulsion treated base was uncovered, no solid pieces of the base were remaining. The base was broken into chunks 6-8 inches wide indicating an irregular alligator cracking pattern.

In section 2, some transverse cracks had appeared in the fall. Upon resumption of testing, further deterioration of section 2 occurred as shown by Benkelman beam measurements in Table 23. Deflections of the pavement became visible, followed by some rutting and then increased transverse cracks. When this pavement was considered failed, only transverse cracking was visible on the surface with rutting. When the section was excavated, the 2.0 inch asphalt base was completely cracked in an alligator pattern. This cracking pattern did not show up on the wearing course. The cracking pattern of the base indicates that this section may be a base failure caused by fatigue. Investigation of the moisture contents of the subgrade shows that moisture was above optimum and varied from 19.4 to 23.6 per cent, averaging 21.8 (see Table 20). Moisture contents seem to slightly decrease with depth.

TABLE 20: MOISTURE CONTENTS - FAILED SECTIONS

Material	Location Section	Depth Inches	Average Percentage Moisture		
			During Construction	At Failure	Average
Crushed Surfacing Top Course CSTC	1[1]	0-3	About 7.0	4.94	4.94
	5	4.5	About 7.0	7.68	7.86
	6	7.0		6.96	
	7	9.5		8.93	
Palouse Silt	1	0.0	14.3	27.2[2]	19.5[3]
		3.0		18.3	18.8
		6.0		20.7	
		8.0		18.2	
	5	Surface	16.5	20.6	21.6
		3.0		22.6	
		12.0		21.7	
		24.0		21.3	
	6	Surface	15.2	22.2	23.9
		3.0		24.2	
		12.0		25.3	
		24.0		23.7	
	7	Surface	15.2	21.9	22.2
		3.0		21.7	
		12.0		24.1	
		24.0		21.2	
	9	Surface	15.0	21.3	22.1
		3.0		20.9	
		6.0		22.2	
		12.0		22.2	
		24.0		23.8	
	2	Surface	15.0	22.4	21.8
		3.0		22.3	
		6.0		21.9	
		15.0		21.3	
		27.0		20.9	

[1] Shoulders
[2] This was taken in the subgrade directly under the pool of water as shown in Figure 24.
[3] Includes surface moisture.

Pavement behavior observed in section 3 (3.5 inches of ATB) was similar to that exhibited by section 9. Excessive deflection with excessive deformation which caused longitudinal tension surface cracks were observed. The rutting was deep and lateral shoving of the pavement was very pronounced. Uplifting of the pavement occurred on the inside, while in section 9 it occurred on the outside (see Figures 37-40). Transverse cracks appeared followed by alligator cracking pattern throughout the base. This pattern was indented onto the subgrade which showed the rutting contours. This was not observed at any of the other failures. The base in this section probably failed in fatigue and then the individual base entities imprinted and shoved the subgrade aside as shown in Figures 41 and 42. The subgrade moisture content was found to be above optimum.

Section 10 (7.0 inches of ETB) exhibited the same pattern of behavior observed in sections 9 and 3. Excessive deflections with rutting were visible (see Figure 43). Small cracks started to appear, although the hot weather healed them. Benkelman beam readings were also high--between 0.130 to 0.140 inches of deflection. When permanent deformation depth exceeded 2.0 inches as shown in Figure 44 (page 56), this section was overlaid with an asphalt concrete.

Testing halted in July because the four remaining sections showed excessive surface rutting. Rut depths were over 7/8 inches, 7/8 inches, 7/8 inches and 1-1/4 inches in sections 4, 11, 12 and 8 respectively. This is shown in Figures 45-48. These ruts varied with the position of the tires. Benkelman beam measurements indicated that the deflections had stabilized and were rather constant for most of July.

Excavation of the remaining sections revealed several interesting facts. Excavation of section 8 (12.0 inches of UTB) revealed that the C1 "B" AC wearing course peeled off the untreated base without difficulty. The crushed rock base was very highly compacted and could be only removed by pick and back hoe. Moisture content of the untreated base was fairly consistent as shown in Table 21 although the bottom two layers had slightly higher moisture contents. The subgrade moisture contents were higher within the top nine inches and then decreased with depth as shown in Table 21.

Excavation of section 4 revealed that the bottom 5.0 inches of special ATB had tiny alligator cracks as shown in Figure 49. These cracks were superimposed on the subgrade as shown in Figure 50. This also appeared in section 3 when it was excavated. Moisture contents were above optimum and were higher than in some of the other sections. The cracking of the base shows that this is a fatigue phenomena. If testing had continued, the base would have cracked more extensively which could eventually extend to the surface.

Examination of the trench in section 10 (5.0 inches of ETB) showed that there was good bond between the C1 "B" asphalt wearing course and the emulsion treated base (see Figure 51). Removal of the wearing course revealed a longitudinal shear crack along the outside wheel path edge. The top of the ETB looked good, but the trench revealed poor cohesion and extensive cracking of the base. The emulsion base was shattered in large pieces compared to section 9 (3.0 inches ETB) which was shattered in small pieces. This cracking was probably due to fatigue caused by wheel load repetition and excessive deflections and deformations. The moisture content of the emulsion treated base was higher on the bottom than on top. The subgrade moistures decreased with depth (see Table 22).

TABLE 21: VARIATIONS IN MOISTURE CONTENTS IN THE PALOUSE SILT WITH DEPTH
REMAINING SECTIONS
RING #3

Depth	4	8	10	11	12
0"	--	21.6	--	21.3	--
3"	22.2	22.3	22.8	21.2	22.4
6"	24.4	24.0	23.8	21.4	21.7
9"	24.5	23.8	22.6	21.2	22.1
12"	23.4	21.1	22.6	21.3	23.0
2.0'	20.9	21.8	22.7	21.1	22.5
4.0'	22.9	19.9	22.0	21.9	25.4
6.0'	24.7	20.5	21.7	24.5	27.1

TABLE 22: MOISTURE CONTENTS IN BASE MATERIALS
RING #3
DEPTH - INCHES

Section	Material & Base Depth	0-3	3-6	6-9	9-12
8	12.0" UTB	6.24	6.25	6.52	6.67
10	5.0" ETB	3.74	4.18		
11	7.0" ETB	2.00	2.87		
12	9.0" ETB	5.86	4.89	5.36	

Sections 11 and 12 (7.0 and 9.0 inches of ETB) also revealed several differences. There was good bond between the wearing course and both emulsion bases. Trenching revealed that in section 11, the top of ETB to be intact but the bottom two layers were cracked in an alligator pattern. There was poor bond between the emulsion layers in section 12, but not in section 11. In section 12, only the bottom layer was cracked. This cracking was probably due to fatigue (see Figure 52). The emulsion treated base in section 11 had less moisture than section 12. Another interesting difference revealed that the subgrade in section 12 had higher moisture contents than section 11. An interesting observation to this was that during construction of Ring #4, a soft spot developed in section 12 which had to be excavated.

As far as riding qualities are concerned, sections 4, 12 and 8 seem to be about equal. Section 11 may have been in slightly worse condition. The base underneath was cracked more extensively than section 12 or 4. Although the wearing course of section 8 was cracked early in the testing period, the riding quality remained quite good (9).

The difference in modes of failure is probably due to the difference in environmental conditions. An interesting observation came out of the adjustment of the LVDT gages in Ring #4 prior to testing. Adjustments had to be made which indicated that the pavements had risen by 1/16 to 1/8 of an inch. This seems to indicate that the pavements were uplifted by that amount during the winter (10). This may explain why such rapid failures occurred. Differential recompaction of the saturated subgrade from the transversed part of the pavement to the non-transversed part may have occurred, causing localized stresses at the edge of the wheel track thereby bringing about a punching shear situation. The semi-rigidity of the emulsion-treated and special asphalt treated bases may

have changed the rate of failure. The fact that section 8 with 12 inches of untreated base has been able to survive even when cracked indicates that the structure of its base enables it to follow the compaction and contours of subgrade.

The concept of "Pavement Failure Span" (PFS) was originally brought out in the report on Ring #2 (1) and is shown in Table 18 for Ring #3. The table shows that for some sections almost as many wheel applications were needed to reach "ultimate failure" as to cause initial cracking. The table also shows that the more rigid pavement sections (2-4 and 9-12) did not have large pavement failure spans. Contributing factors should be considered in evaluation of PFS. These factors are type and thickness of base, environmental conditions of temperature and moisture at time of testing. In addition, "ultimate failure" point is somewhat arbitrary. The researchers believe that the concept does indicate a relationship of interest.

The equivalency thickness is shown in Table 19. The equivalencies obtained for the fall period of 1967 are based on the thinnest surviving sections. The 1968 spring equivalencies are based on the thickest section that failed during this period.

Load Response Characteristics

Temperature Variables

During the 1967 fall period, air temperatures were fairly high until about October 24 when the temperatures started to fall and the rain began. The pavement temperatures seemed to vary as a direct result of varying air temperatures and solar radiation. The 1967 testing period can be divided into two periods--early and late fall, that is, prior to and after November 14 when

the rains fell. Changes in instrument reading results may be attributed to the break in temperatures and the steady rainfall (see Table 14, page 39).

During the 1968 spring period, the air temperatures in May and early June were fairly consistent. The minimum daily temperature started to rise. High summer temperatures continued to the end of testing as shown in Table 14. The 1968 testing period can be subdivided into spring and early summer periods. Benkelman beam readings stabilized during the latter subperiod. Temperatures did affect the stress and strain readings, but they may not have played a significant part in the early spring pavement section failures. The high temperatures may have helped to increase the rutting phenomena in the remaining sections.

Moisture Contents

Moisture contents were measured by moisture tensiometer methods and by regular sampling methods. Samples of bases and subgrade were taken for the measurement of moisture contents after the existing section was removed.

During construction the moisture contents of the Palouse silt subgrade was found to be on the dry side. This slowly changed with time and the weather. Measurements with individual moisture tensiometers, as shown in Figure 54, show that the moisture content built up with time. According to the probes, the moisture content in section 2 was on the dry side and slowly increased, while sections 3 and 6 were on the higher moisture side. There seemed to be a sudden rise in moisture content after October 18 in sections 3, 6 and 10 although it did not rain that much. The only explanation is that the probes may have been purged at that time thus giving higher than normal readings. There was an adjustment in a few days as shown in Figure 54.

Figure 55 shows the correlation of moisture content in the subgrade with precipitation. After October 15, the subgrade was being saturated, either by moving through the shoulders or through natural moisture movement through the

subgrade. Some may have moved in through the cracks as in section 1. The moisture content under the asphalt treated bases seems to be lower than for the rest of the sections (see Tables 20 and 21). These tables seem to indicate that moisture contents decrease somewhat with depth.

Samples taken from the untreated crushed surfacing top course bases indicate that moisture contents were high (Table 22) and may have been a partial cause of subgrade saturation. The subgrade moisture contents were higher but this may be due to the boundary conditions caused by the vicinity of the concrete tunnel.

The moisture contents in the emulsion treated bases as shown in Table 22 varied in the sections. The thickest section, 12, had more moisture than the emulsion base in section 11. The bottom layers were wetter than the upper layers which may be due to the saturated subgrade. Section 10 was also wetter than section 11, but not wetter than section 12.

High moisture contents in the subgrade and the bases indicate that moisture played an important role in the failures of the sections. The fact that moisture contents were above those during construction and above optimum during the two testing periods implies the subgrade bearing strength was weakened, which could have led to the rapid failures during the spring testing period.

Static Deflections

*Benkelman beam rebound measurements using the Canadian Good Roads Association procedure (11) were taken at five selected intervals per section as shown in Figure 53. This was done to check the homogeneity of the test pavement section and to obtain a better rebound average for that test section.

Rebound measurements were taken before testing commenced and continued throughout the testing period in the fall and spring. Pavement temperatures

*See Appendix.

FIGURE 54. MOISTURE CONTENT VS. DAY OF OCTOBER
(Individual Probes)

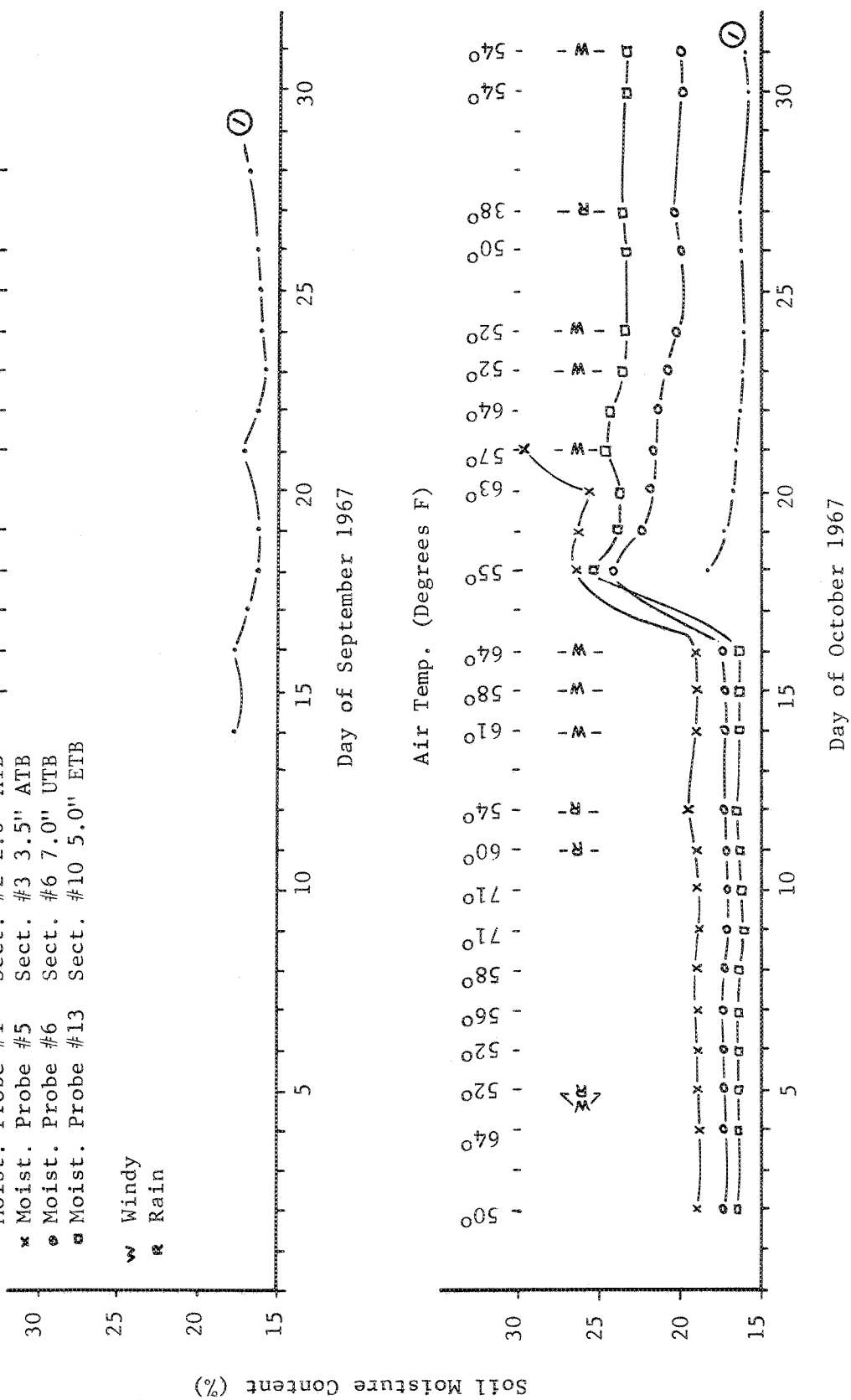

FIGURE 55. MOISTURE CONTENT & PRECIPITATION
RING #3 - SECTIONS 3, 6 AND 10

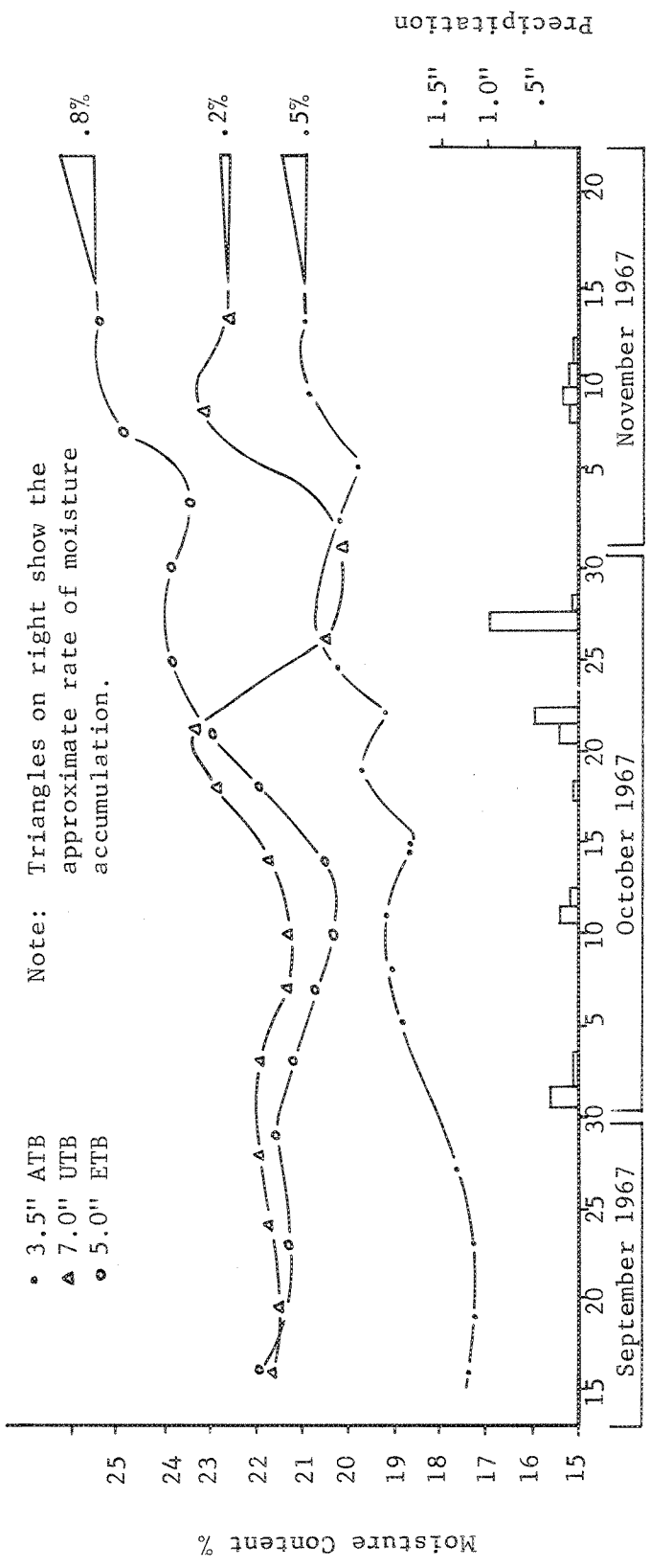

were obtained from thermocouples in the pavement and were averaged out for the pavement system. Using the Asphalt Institute's temperature correction procedure, all Benkelman readings were corrected to 70° temperature (12). Some typical readings are shown in Table 17 (page 63).

Table 23 shows the Benkelman beam rebound measurements obtained during the fall of 1967. Since the foundation was in good shape and in a dry condition, temperature correction curve A in the reference (12) was used for adjusting the deflections to a standard 70°F. The table shows that cracking started usually when deflection of 0.050 inches had been reached. In general, deflections increased with wheel load applications. Once a pavement cracked, deflections increased and sometimes decreased depending upon the extent of the cracked pavement area. Figures 56-58 show the unadjusted rebound deflections (page 82).

Table 24 shows the Benkelman beam rebound measurements obtained during the spring. Deflections were frequently two to four times greater than those obtained in the fall. This is probably due to the existence of a saturated subgrade thus causing a loss of support. To adjust the deflections for temperature, curve B in reference (12) was used. Cracks seem to occur after deflection of 0.080 inches have been reached. The deflections seemed to stabilize as testing continued into the summer period. Although the subgrade was saturated as revealed by sampling, the subgrade probably had reached its limit of deformation for the surviving sections.

Dynamic Deflections

Dynamic deflections were measured by Sanborn linear variable displacement transducers (LVDT) in sections 3, 6, 10 and 12 (3.5 inches of special aggregate asphalt treated base, 7.0 inches of untreated base, 5.0 inches and 12 inches of emulsion treated base, respectively) during the period when strain gage readings were taken and during a continuous time period. The deep LVDT gages

TABLE 23: SUMMARY OF FALL 1967 BENKELMAN BEAM REBOUND DEFLECTIONS* - RING #3

Date:		09-11	09-18	09-19	09-20	09-22	09-25	09-27	10-09	10-13	10-16	10-24	10-31	11-06	
Wheel Loads x 10^3		.1	72.4	92.6	116.8	152.8	199.4	240.9	326.0	396.2	442.4	543.5	595.8	640.2	
Section	Base														
	ATB														
1	0.0"	.039	.041	.046	.042	.059	.057	.060	.056	.056**	.059	.057	.057	.068	cracked
2	2.0"	.035	.043	--	.044	.0505	.047	.052	.047	.049**	.058	.050	.052	.0515	
3	3.5"	.026	.039	--	.039	--	.044	.039	.038	--	.0375	.034	.037	.033	
4	5.0"	.024	.021	--	.019	--	.027	.027	.021	--	.029	.015	.019	.014	
	UTB														
5	3.5"	.039	.040	.040	.045	.048	.047	.050	.043	.044**	.046	.045	.0615	.0605	cracked
6	7.0"	.042	.0405	.040	.040	.050	.0495	.065	.056	.065**	.075	.091	.081	.092	
7	9.5"	.035	.031	--	.028	--	.041	.048	.041	--	.045	.037	.059	.062**	
8	12.0"	.031	.026	--	.027	--	.035	.036	.033	--	.036	.043	.041	.041	
	ETB														
9	3.0"	.032	.040	--	.034	--	.043	.047	.041	--	.043	.043	.045	.040	
10	5.0"	.031	.032	--	.034	--	.037	.041	.042	--	.036	.038	.035	.035	
11	7.0"	.028	.028	--	.023	--	.029	.032	.029	--	.030	.024	.025	.025	
12	9.0"	.0235	.019	--	.019	--	.023	.027	.021	--	.023	.021	.022	.021	

* Corrected to 70°F using the Asphalt Institute Method, Curve A. Deflections are in inches.

** Cracks were present.

TABLE 24: SUMMARY OF SPRING 1968 BENKELMAN BEAM REBOUND DEFLECTIONS[1] - RING #3

Date:		04-23	05-10	05-22	06-20	06-24	07-08	07-11	07-15	07-17	07-19	07-23
Wheel Loads x 1000		735.6	736.7	745.0	766.1	777.5	789.0	801.9	815.6	828.1	840.8	863.2
Section	Base											
1	ATB 0.0"	.032[2,3]	--	--	--	--	--	--	--	--	--	--
2	2.0"	.120[2]	.109	.094[3]	--	--	--	--	--	--	--	--
3	3.5"	.090	.071	.073	.073	.087[2,3]	--	--	--	--	--	--
4	5.0"	.054	.038	.045	.049	.050	.054	.049	.052	.053	.050	.0515
5	UTB 3.5"	.100[2,3]	--	--	--	--	--	--	--	--	--	--
6	7.0"	.147[2,3]	--	--	--	--	--	--	--	--	--	--
7	9.5"	.079[2,3]	--	--	--	--	--	--	--	--	--	--
8	12.0"	.073[2]	.045	.077	.048	.048	.056	.0425	.055	.050	.0485	.046
9	ETB 3.0"	.124	.219[2,3]	--	--	--	--	--	--	--	--	--
10	5.0"	.100	.078	.065	.088	.080[2]	.121	.080[4]	.097	.087	.076	.078
11	7.0"	.067	.051	.049	.051	.050	.0675	.058	.069	.043	.055	.060
12	9.0"	.071	.048	.055	.051	.055	.062	.060	.062	.0515	.054	.059

[1] Corrected to 70°F using the Asphalt Institute Method, Curve B as subgrade was saturated. Deflections are in inches.
[2] Cracked--in sections 1, 2, 5, 6, 7 and 8--cracks first appeared in Fall 1967.
[3] Replaced.
[4] An AC overlay was placed.

FIGURE 56. BENKELMAN BEAM REBOUND DEFLECTIONS VS. WHEEL LOADS
Ring #3--September 1967-July 1968
(Not corrected for temperature)

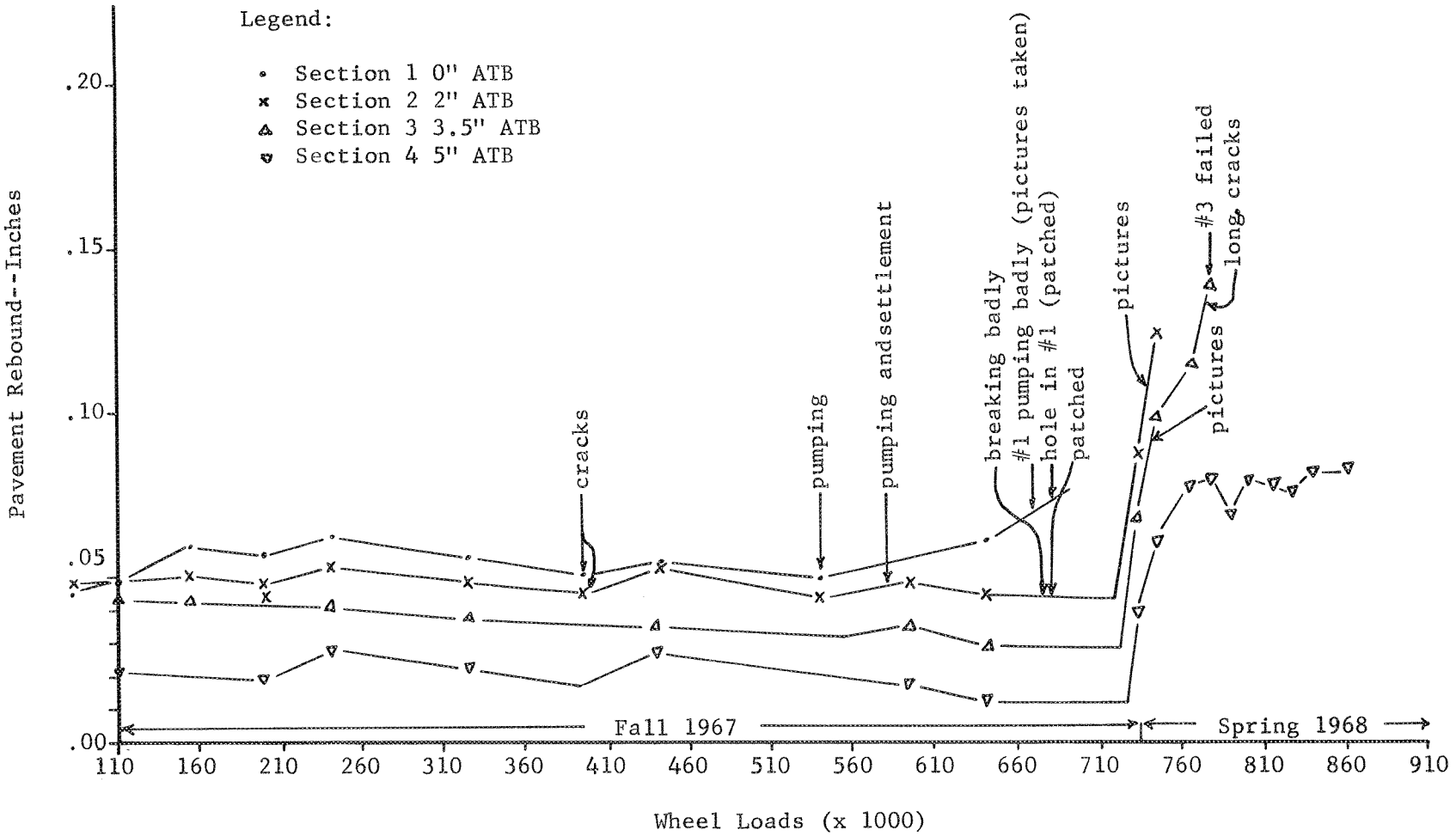

FIGURE 57. BENKELMAN BEAM REBOUND DEFLECTIONS VS. WHEEL LOADS

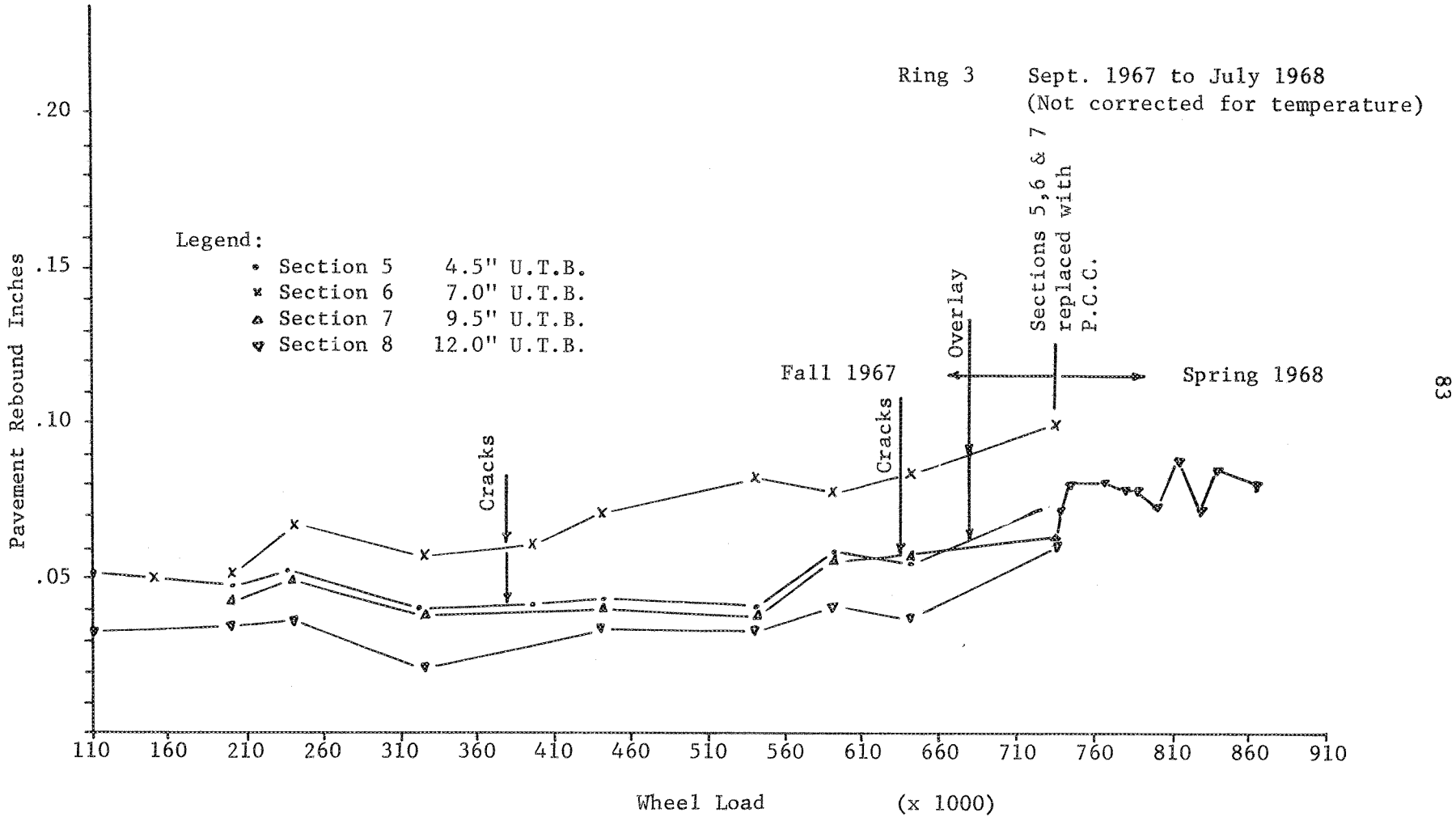

FIGURE 58. BENKELMAN BEAM REBOUND DEFLECTIONS VS. WHEEL LOADS

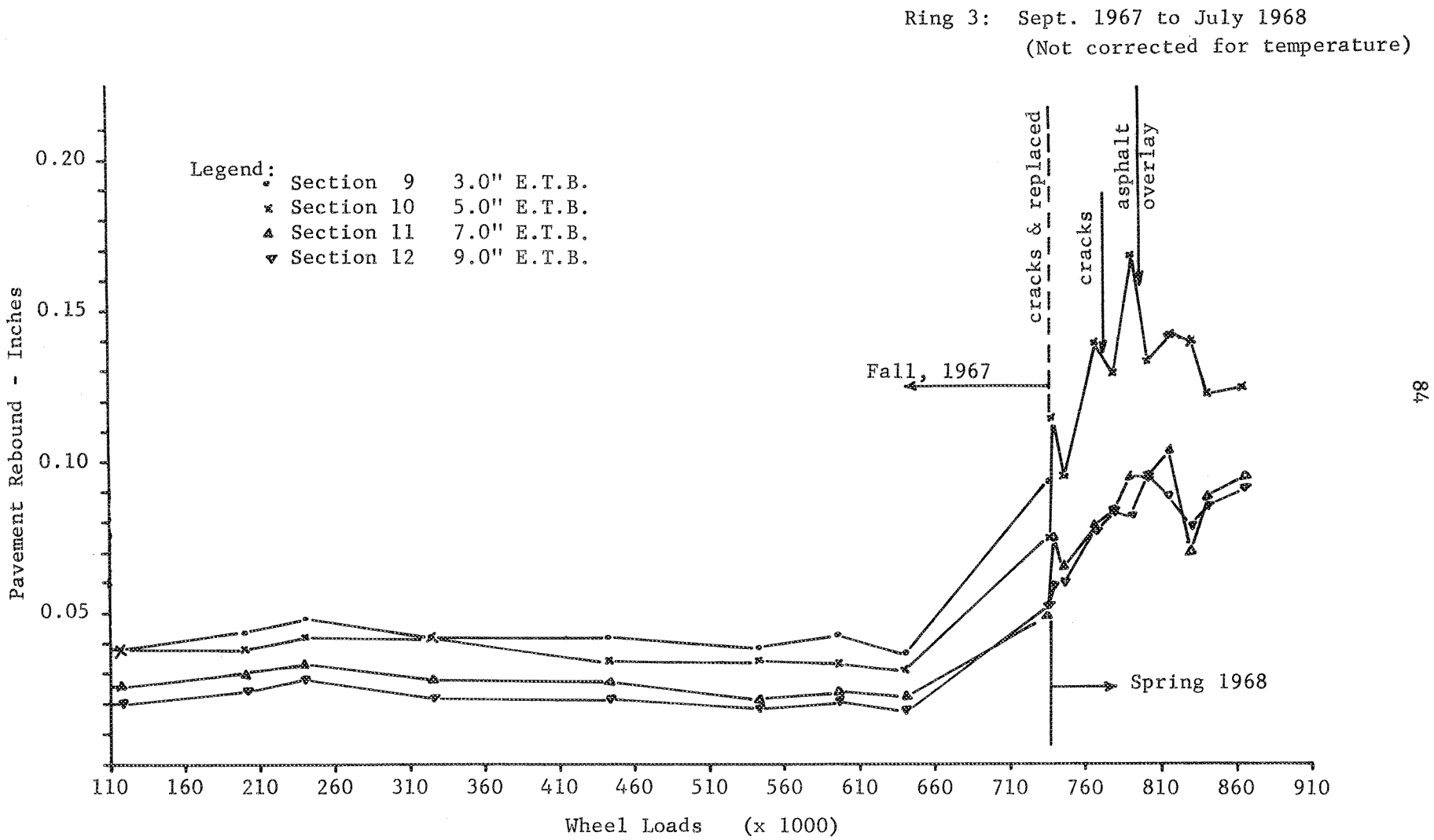

measured movement of the pavement system including subgrade; the shallow gages measured movement of the surface and base layers only. Some dynamic deflections were taken in conjunction with Benkelman beam measurements to check out the deep LVDT gages and installations. The correlation was good.

The fall testing period was divided into early and late fall. This was done on the basis of rainfall and temperature. There was not much use in dividing the spring-summer testing period because by that time most of the LVDT gages were inoperative by early June. Most of the deflections were plotted from continuous time readings. Readings taken in the fall were usually at 20 mph unless otherwise stated; in the spring the operating speed was 10 mph. Figure 59 shows the dimension of the dual tires.

Figures 60 and 61 show the variation in dynamic deflections with transverse distance and with temperature as shown by the different time periods for LVDT #1 and #2 in section 3 containing the 3.5 inches of ATB. The pavement temperatures here are an average of temperatures measured on the surface, top of base, and bottom of base. The results show that deflections were affected by pavement temperatures during the fall but the variation was not that large as shown by the different fall periods. When the temperature was low, the pavement structure (wearing course plus base) deflection measured by LVDT #1 was very low with respect to the total pavement system deflection which was measured by LVDT #2. During the early fall period deflections occurring within the pavement and base was only 8.8% of the total pavement system; this ratio is called the dynamic deflection ratio. This decreased to 5.2% in the late fall period. In the spring, the dynamic deflections increased about 10 times for the pavement structure and about doubled for the total pavement structure. Forty-four percent of the deflections occurred within the pavement structure. This seems

FIGURE 59. DIMENSIONS OF DUAL TIRES

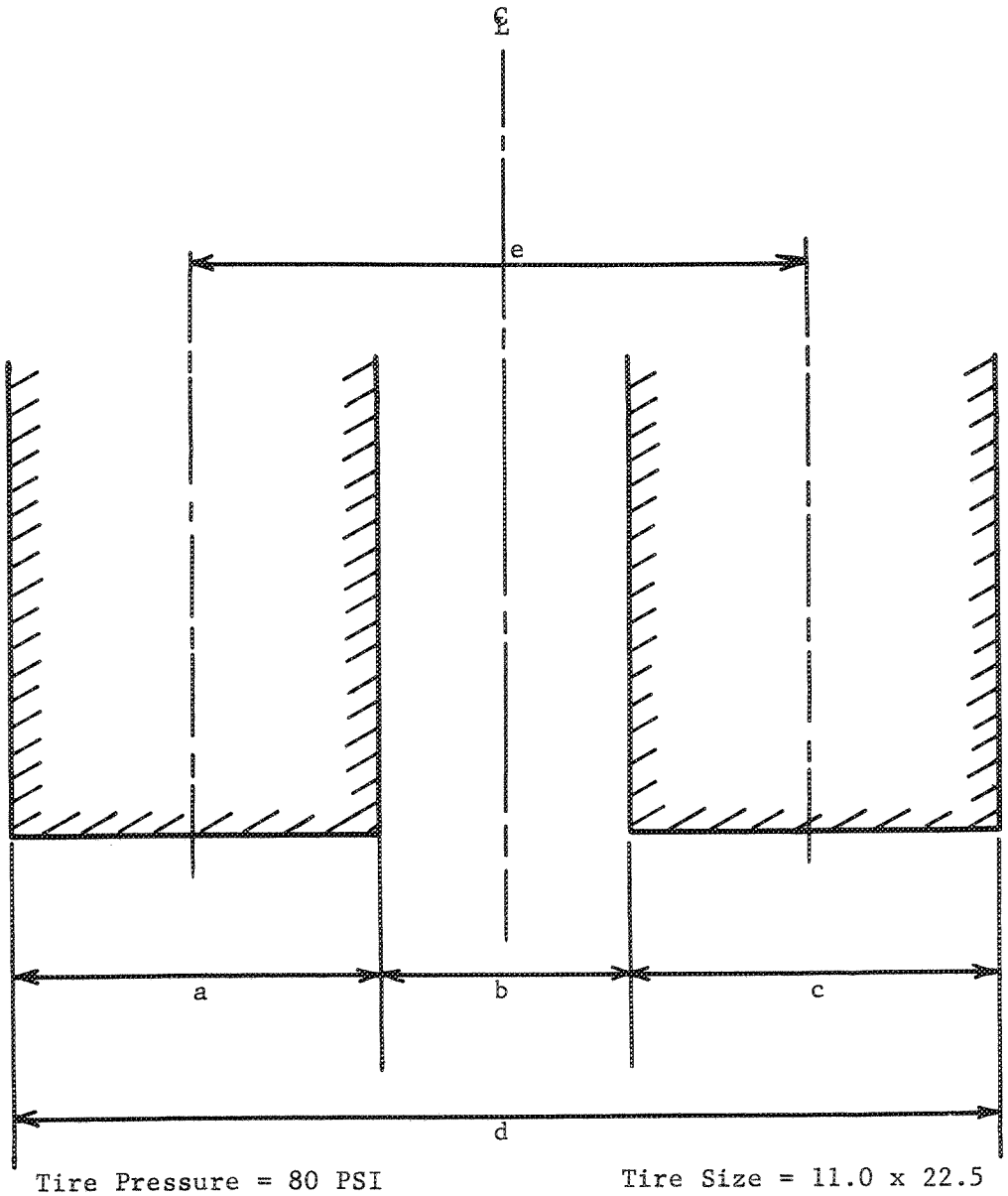

Tire Pressure = 80 PSI
Length of Tire = 11 "
a = c = 7.75" = 0.65'
b = 5.25" = 0.43'
d = 20.75" = 1.73'
d/2 = 10.37" = 0.86'
e = 13.0"

Tire Size = 11.0 x 22.5
Wheel Load = 5300 lbs.
Dual Load = 10,600 lbs.
Single Axle Load = 21,200 lbs.
Contact Area/Tire = 85.25 sq. in.

Scale: 1" = 4.0"

FIGURE 60. DYNAMIC DEFLECTION VARIATIONS VS. TRANSVERSE DISTANCE
RING #3

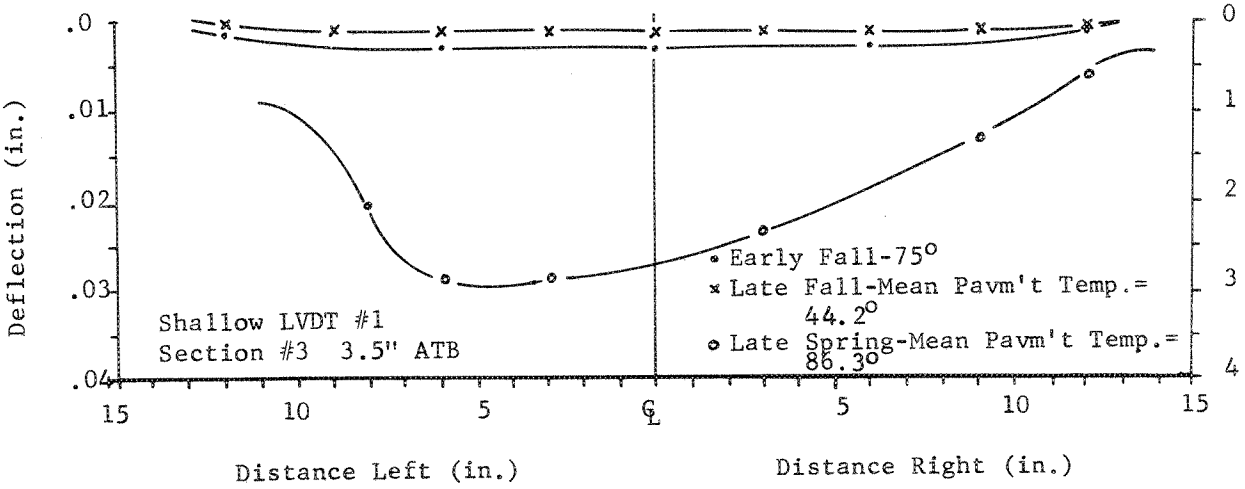

FIGURE 61. DYNAMIC DEFLECTION VARIATIONS VS. TRANSVERSE DISTANCE
RING #3

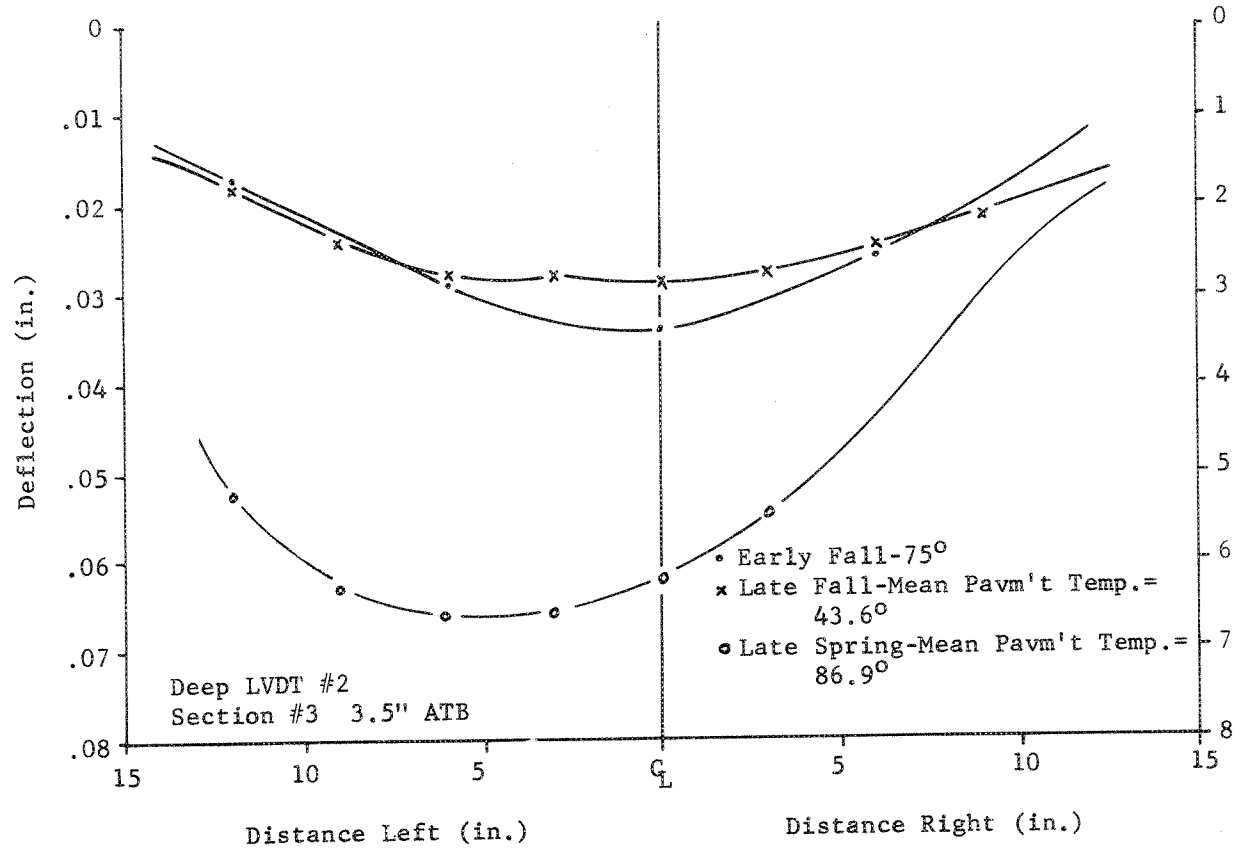

to indicate that whole pavement structures become more flexible under wheel load applications in a wet environment. The fact that the pavement structure deflection increased with respect to the subgrade by some 30% seems to indicate that pavement was taking up more of the load and the subgrade less. The mode of failure shown in Figures 37-40 seems to bear out that the subgrade was displaced because the pavement structure was unable to continue taking the wheel load applications. The maximum deflection occurred in the fall under the center of the duals; while in the spring, maximum deflection occurred under the inside edge of the outside dual tire.

The deflection curves data for the 7.0 inches of untreated crushed rock base, section 6, is shown in Figures 62 and 63. No deflections were available in the spring since this section had failed in the fall. Higher deflections were obtained in the late fall period, both for the shallow and deep gages. The readings for the late fall are after the pavement section had cracked and just before "ultimate" failure was reached. Deflection readings were higher than those obtained prior to cracking. In fact, once initial cracks occurred, immediately the shallow and deep deflections increased. This may be due to the pavement now acting as separate slabs rather than one continuous beam. During the early fall period deflections occurring within the pavement structure were 34% of the total pavement system. After initial cracking, this dynamic deflection ratio had increased to 51.8%, and prior to ultimate failure, this ratio was 46.5%. Just before the initial cracks appeared, the shallow and deep deflections were 0.0112 and 0.0464 inches, respectively, and the pavement temperature was 64°F. Seven hours earlier the pavement temperature was 57°F with the shallow and deep deflection 0.0158 and 0.0464 inches, respectively. More and more of the total deflection was being taken by the pavement

FIGURE 62. DYNAMIC DEFLECTION VARIATIONS VS. TRANSVERSE DISTANCE
RING #3

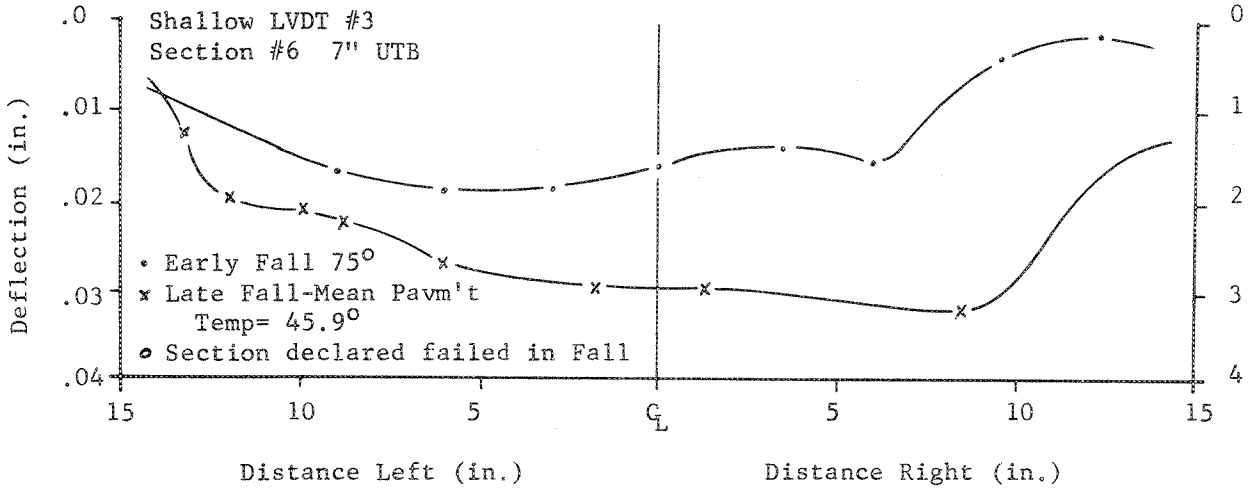

FIGURE 63. DYNAMIC DEFLECTION VARIATIONS VS. TRANSVERSE DISTANCE
RING #3

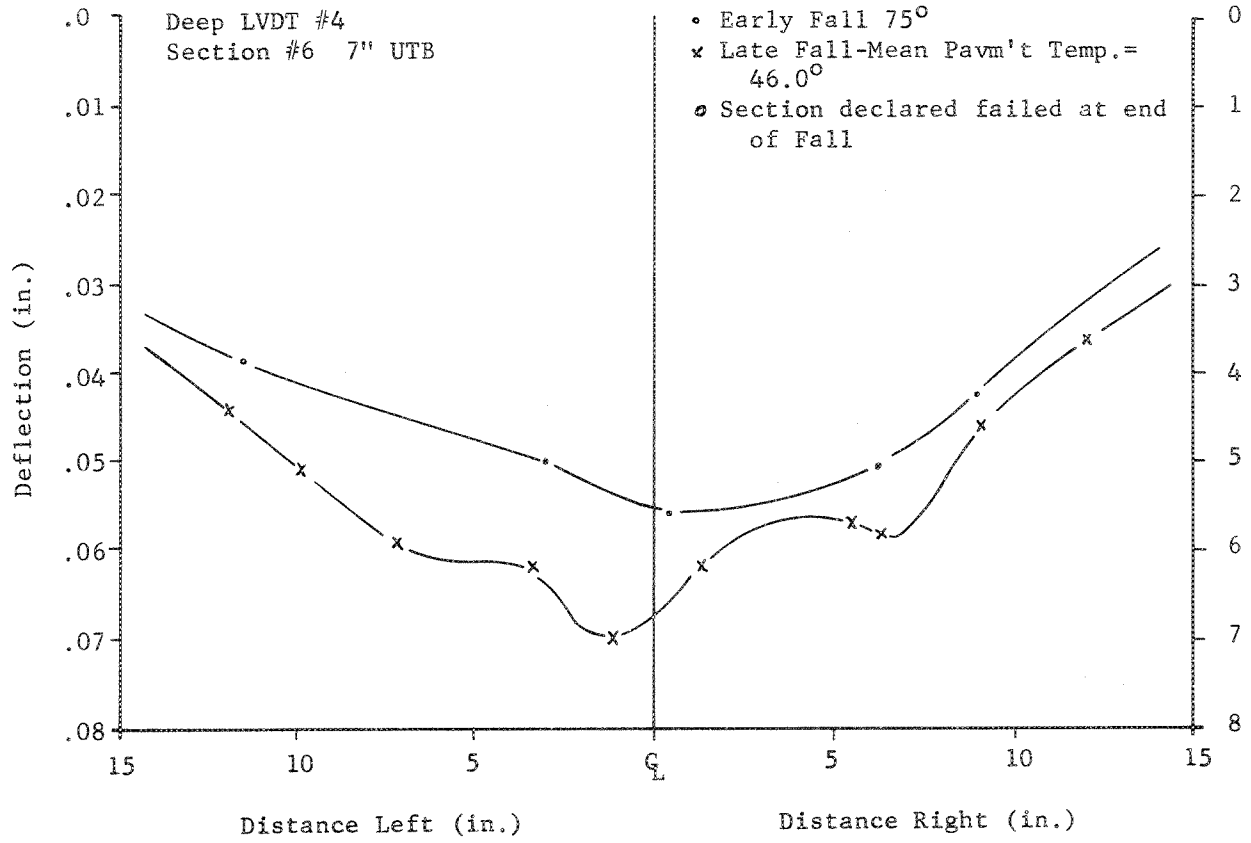

system prior to the appearance of the initial cracks. The maximum deflections seem to occur when the inside edge of the outside tire is over the LVDT gages. The high deflections seem to indicate a deterioration in the subgrade support in section 6 and is probably due to the nature of untreated base, the thickness and the environmental conditions.

Measured dynamic deflections for the 5.0 and 10.0 inch emulsion treated base, sections 10 and 12, are shown in Figures 64 and 65 and Figures 66 and 67, respectively. These figures show that the temperature during the fall period did affect the deflection readings, and that deflection doubled and tripled in the spring period thus indicating a change in the subgrade. Initially, most of the deflections occurred within the pavement system with very little occurring within the pavement structure. The ratio for section 10 during early fall, late fall and early spring was 2.1%, 14.8% and 57%, respectively. For section 12 the ratio in the spring was 36.8%. Maximum deflection usually occurred under the tires.

Table 25 shows the maximum LVDT deflection values obtained during different time periods. Maximum deflection occurred under the tires as borne out in the Shell Avenue Test Road (13). The table bears out that deflection increased rather dramatically during the spring and that during the coldest time deflection was at a minimum. The deflection difference during the different time period may have also been partly responsible for the different failure mode.

Deflections seem to have increased with wheel load repetitions but this may not be a function entirely due to wheel loads but to other factors such as the thickness and type of base, and the most important, the changing environmental conditions. The latter, especially during the spring, caused

FIGURE 64. DYNAMIC DEFLECTION VARIATIONS VS. TRANSVERSE DISTANCE
RING #3

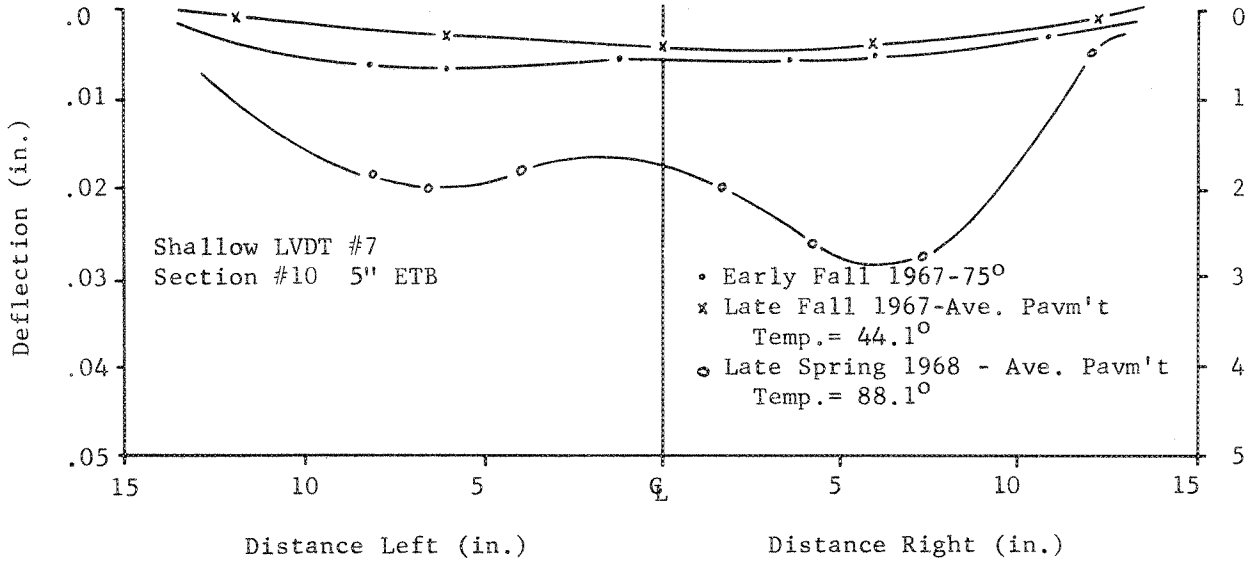

FIGURE 65. DYNAMIC DEFLECTION VARIATIONS VS. TRANSVERSE DISTANCE
RING #3

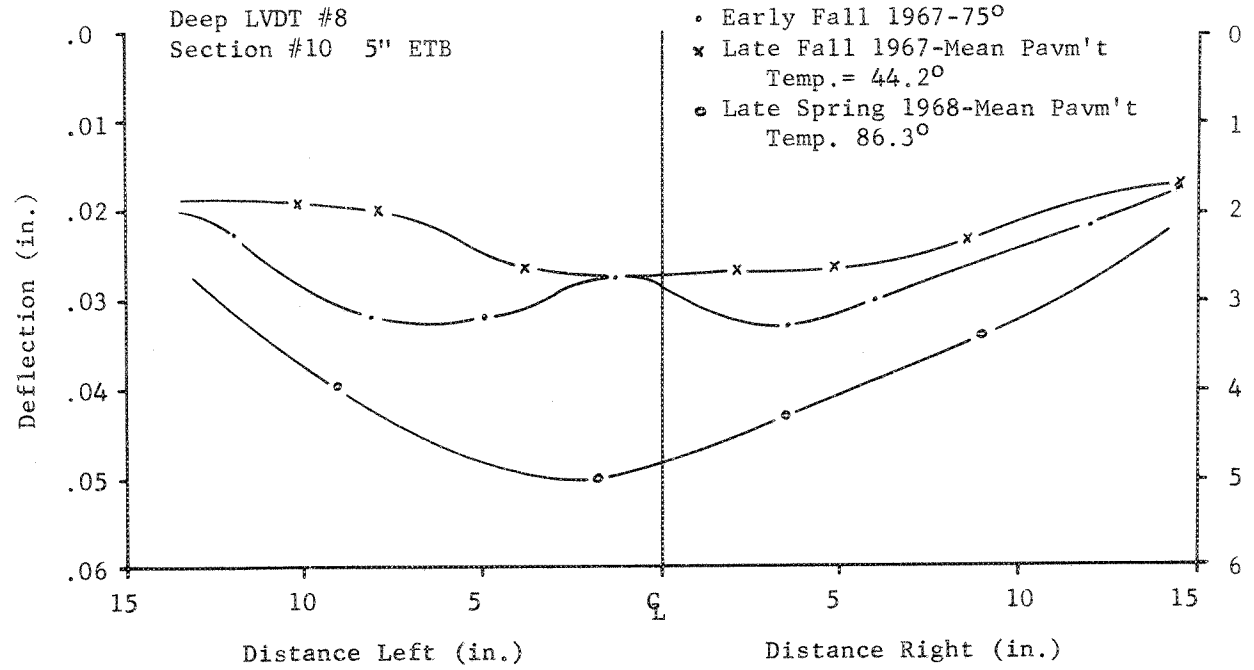

FIGURE 66. DYNAMIC DEFLECTION VARIATIONS VS. TRANSVERSE DISTANCE
RING #3

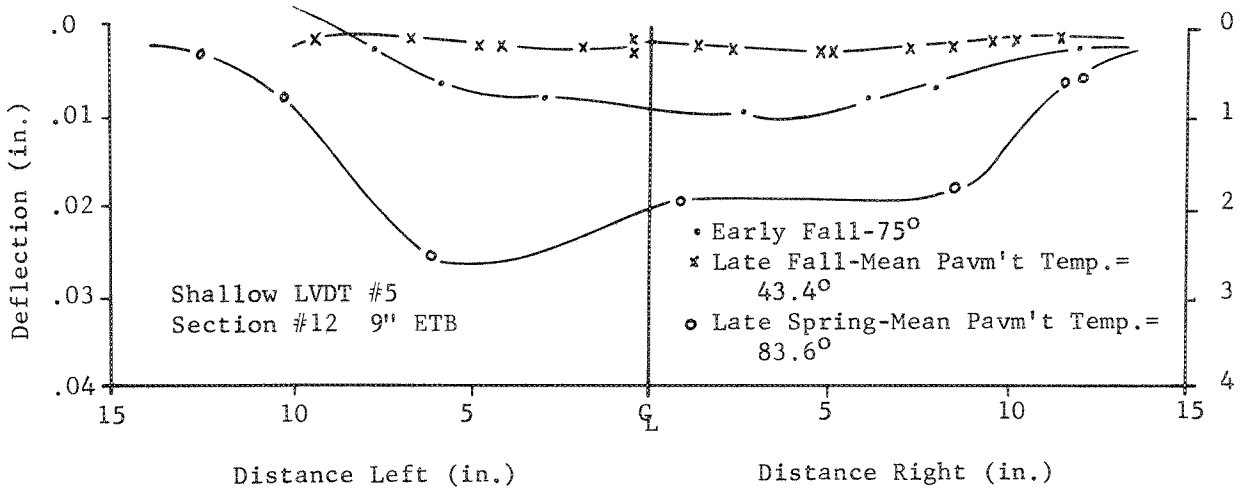

FIGURE 67. DYNAMIC DEFLECTION VARIATIONS VS. TRANSVERSE DISTANCE
RING #3

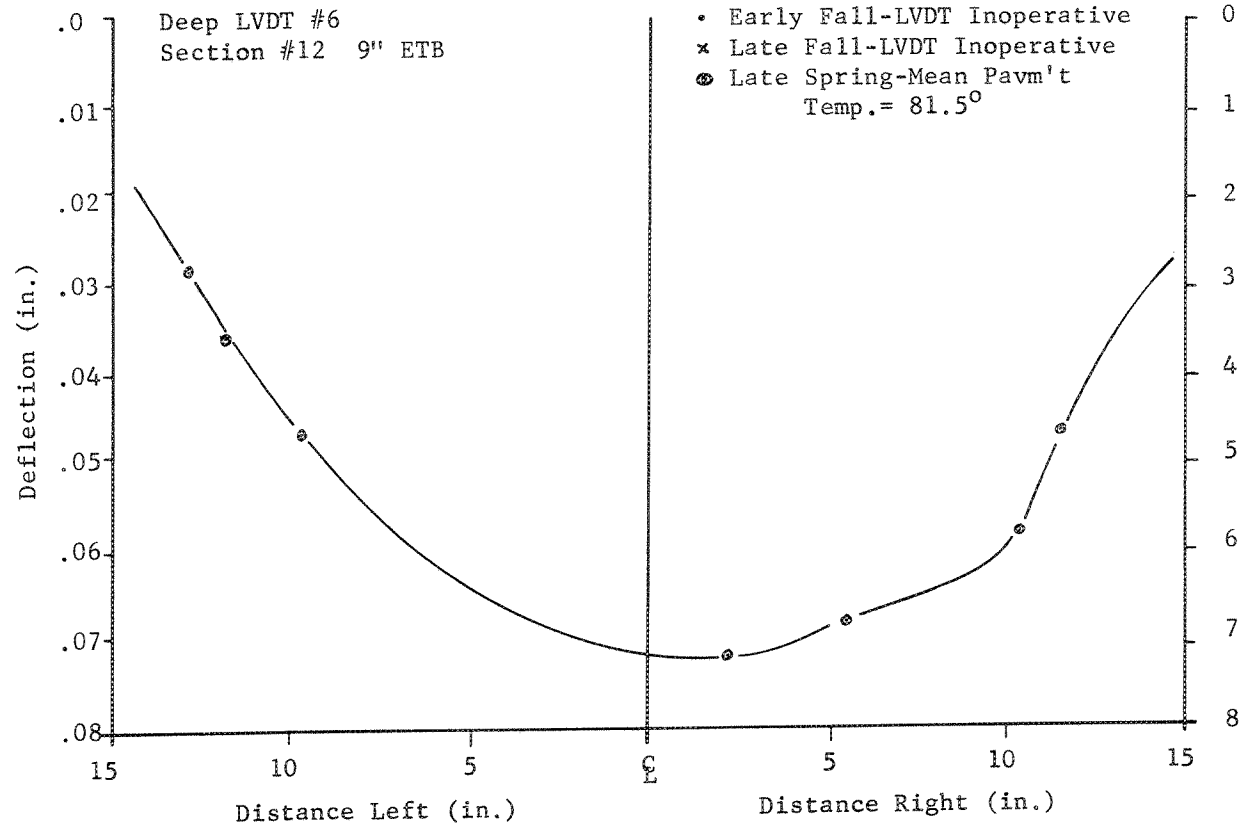

TABLE 25: SUMMARY OF LVDT DEFLECTION MAXIMUM MEASUREMENTS
RING #3

Section	LVDT	Position	Period	Deflection Under Tire Inches	Deflection $\mathbb{Q}_L$ Duals Inches	Average Pavement Temp.
3	1	Shallow	Late Sept.	.009	.004	80°
			Late Nov.	.002	.001	66°
			Spring	.029	.027	86°
	2	Deep	Late Sept.	.036	.033	102°
			Late Nov.	.039	.035	57°
			Spring	.107	.093	71°
6	3	Shallow	Late Sept.	.019	.017	79°
			Early Oct.	.026	.021	55°
			Late Nov.	.037	.037	37°
	4	Deep	Late Sept.	.068	.061	99°
			Early Oct.	.0893	.082	55°
			Late Nov.	.075	.075	41°
10	7	Shallow	Late Sept.	.010	.007	77°
			Late Nov.	.004	.003	44°
			Spring	.035	.028	88°
	8	Deep	Late Sept.	.043	.029	101°
			Late Nov.	.029	.026	40°
			Spring	.054	.048	88°
12	5	Shallow	Late Sept.	.018	.014	73°
			Late Nov.	.0028	.0024	35°
			Early Spring	.017	.011	74°
			Late Spring	.075	.052	103°
	6	Deep	Early Spring	.043	.043	64°
			Late Spring	.089	.071	82°

a saturated subgrade which may have caused a decrease in pavement and subgrade modulus and strength.

Although this was not examined, speed and temperature do affect the pavement deflection. Static deflections measured with a Benkelman beam usually are higher than those measured by LVDT gages under dynamic conditions. Usually the correlation between the LVDT deflections and the Benkelman beam deflections were good. As an example, over the deep LVDT gage #2, the LVDT reading was 0.1142 inches while the Benkelman beam measurement was 0.110 inches at 756,737 wheel loads.

With time and wheel load applications, the pavement structure was called upon to take up more and more of the total pavement system deflection. This dynamic deflection ratio will increase and cause more and more flexure in the pavement structure thus inducing fatigue failure in the pavement. This was shown in Figures 41, 42 and 49 to 52, in sections 3, 4, 11 and 12. Here we can see that fatigue cracking had started at the bottom of the pavement structure.

Strain Gage Data

The strain gage data was plotted against lateral wheel placement by fall and spring periods. The data came from continuous readings, that is, readings taken every half-hour or so during a 24-hour day or longer, along with temperature readings. The strain data also came from runs, that is, during a certain period of the day all the instruments were read. The combined data was often plotted together to be able to sort out the different variations due to temperature and lateral tire distance from the gage. In these series, accumulated wheel loadings were not considered. Operating speeds were 20 mph through November 2, 15 mph until November 8, then 10 mph through December 3.

The pavement temperature is the average of temperatures measured at the pavement surface, top of base and bottom of base, except in the untreated sections where the pavement temperature was taken as an average between top and bottom temperatures of the wearing course.

From the data, maximum longitudinal and transverse strains were tabulated into Table 26. The different periods were divided into subperiods, especially for the sections which developed signs of failure in the fall. From Table 26, one can see that usually maximum strain readings occurred when one of the tires was over the strain gage. The table also shows that temperature affected strain values with higher strains usually associated with high temperatures and vice versa. The strains were usually higher during the spring period thus indicating that structural conditions had changed. Tensile strains measured at the bottom of the untreated bases are those measured by the extensiometers; untreated bases cannot tolerate tensile strains because of their nature.

Table 26 shows that strains increased by wide margins prior to initial cracking as indicated by the different sections. Tensile strain was greater in the longitudinal direction than in the transverse direction; these strains increased with depth. This may explain why transverse cracks appeared rather than longitudinal cracks, and why fatigue failure occurred in the bottom and worked its way upward to the surface. Another interesting fact from Table 26 is that prior to initial cracking, strains (both in compression and tension) became very large and gages frequently became inoperational thereafter thus indicating that the strain gage had reached its strain limit.

The graphs show that transverse strain gage data was very complex and that the lateral position of the tires and also depth greatly affected its magnitude, mode and reversal of the strains. The lateral position of the wheels

TABLE 26: SUMMARY OF MAXIMUM LONGITUDINAL AND TRANSVERSE STRAIN GAGE MEASUREMENTS - RING #3[1]
(Readings are maximum values taken in longitudinal direction)

Section	Position	Period	Longitudinal Maximum Values				Pavement[3] Temp. °F		Transverse Maximum Values				Pavement[3] Temp. °F	
			Measurements		Lateral Pos.[2]				Measurements		Lateral Pos.[2]			
			C	T	C	T	C	T	C	T	C	T	C	T
1	Surface	Sept.	950	300	U.T.	U.T.	73	97	440	120	B.T.	U.T.	102	91
0.0"		Early Oct.[4]	1650	390	U.T.	N.D.	69	89	600	215	U.T.	U.T.	64	66
ATB		Late Oct.[5]	800	60	U.T.	B.T.	71	71	220	110	U.T.	U.T.	70	70
2	Surface	Sept.	600	70	N.D.	U.T.	73	83	580	260	B.T.	B.T.	95	95
2.0"		Early Oct.	700	70	B.T.	B.T.	72	66	260	100	B.T.	U.T.	72	66
ATB		Late Oct.	440	--	U.T.	--	71	--	400	140	U.T.	U.T.	71	71
		May	1900	850	U.T.	B.T.	91	97	1100	700	U.T.	U.T.	76	76
		June	650	500	B.T.	U.T.	70	83	600	140	U.T.	U.T.	97	83
3	Surface	Sept.	170	70	B.T.	B.T.	78	78	320	--	U.D.	--	89	--
3.5"		Oct.	190	150	B.T.	[6]	71	60	360	60	U.T.	U.T.	72	58
ATB		Nov.	110	60	U.T.	U.T.	66	66	180	--	U.T.	--	66	66
		May	600	200	B.T.	U.T.	92	88	600	120	U.T.	U.T.	88	96
		Early June[6]	1000	200	B.T.	U.T.	96	83	600	120	U.T.	B.T.	83	96
		Late June[7]	1700	300	U.T.	U.T.	108	82	1600	320	U.T.	U.T.	97	108
	Base Top	Sept.	320	140	U.D.	U.D.	101	101	270	500	U.T.	U.D.	90	101
		Oct.	70	90	B.T.	[6]	75	55	90	50	U.T.	B.T.	65	75
		Nov.	--	20	--	B.T.	--	66	80	250	U.T.	U.T.	66	45
		May	140	120	U.T.	U.T.	96	96	420	60	U.T.	B.T.	88	92
		Early June	60	220	U.T.	U.T.	84	84	200	120	U.T.	B.T.	84	99
		Late June	100	1700	U.T.	U.T.	86	90	400	1000	U.T.	U.T.	82	90
	Base Top	Sept.	50	280	U.T.	U.D.	90	101	190	140	U.T.	U.D.	90	101
		Oct.	30	170	U.T.	U.T.	55	55	65	60	U.T.	B.T.	54	54
		Nov.	50	250	U.T.	U.T.	66	45	80	--	U.T.	--	66	--
		May	200	440	U.T.	U.T.	73	73	--	--	--	--	--	--
		Early June	140	1000	N.D.	N.D.	84	84	--	--	--	--	--	--
		Late June	120	560	U.T.	U.T.	82	82	--	--	--	--	--	--

TABLE 26 CONTINUED:

Section	Position	Period	Longitudinal Maximum Values: Measurements C	Longitudinal Maximum Values: Measurements T	Longitudinal Maximum Values: Lateral Pos.[2] C	Longitudinal Maximum Values: Lateral Pos.[2] T	Pavement[3] Temp. °F C	Pavement[3] Temp. °F T	Transverse Maximum Values: Measurements C	Transverse Maximum Values: Measurements T	Transverse Maximum Values: Lateral Pos.[2] C	Transverse Maximum Values: Lateral Pos.[2] T	Pavement[3] Temp. °F C	Pavement[3] Temp. °F T
	Base Bottom	Sept.	160	460	U.T.	U.T.	101	101	120	310	B.T.	U.T.	78	74
		Oct.	--	--	--	--	--	--	100	140	U.T.	U.T.	59	57
		Nov.	--	--	--	--	--	--	50	140	B.T.	N.D.	41	45
		May	--	--	--	--	--	--	240	360	B.T.	U.T.	92	96
	Base Bottom	Sept.	--	--	--	--	--	--	70	200	B.T.	[illegible]	78	101
		May	--	--	--	--	--	--	120	600	B.T.	U.T.	92	74
		Early June	--	--	--	--	--	--	200	180	B.T.	[illegible]	99	84
		Late June	--	--	--	--	--	--	160	400	U.T.	U.T.	82	97
4 5.0" ATB	Surface	Sept.	500	50	N.D.	N.D.	90	84	--	--	--	--	--	--
		Oct.	110	30	U.T.	U.T.	71	71	180	520	N.D.	U.T.	65	74
		Nov.	--	--	--	--	--	--	60	--	B.T.	--	64	--
		May	--	--	--	--	--	--	320	--	[illegible]	--	90	--
		Early June	100	--	B.T.	--	93	--	180	200	U.T.	U.T.	91	81
		Late June	400	100	U.T.	U.T.	84	81	800	60	U.T.	B.T.	84	96
	Base Top	Sept.	--	--	--	--	--	--	260	80	U.T.	B.T.	100	90
		Oct.	--	--	--	--	--	--	100	25	U.T.	U.T.	56	74
		Nov.	--	--	--	--	--	--	30	--	B.T.	--	64	--
		May	--	--	--	--	--	--	150	--	[illegible]	--	90	--
		Early June	--	--	--	--	--	--	100	60	B.T.	U.T.	93	81
		Late June	--	--	--	--	--	--	240	60	B.T.	U.T.	106	81
5 9.5" UTB	Surface	Sept.	600	110	U.T.	U.T.	96	78	750	100	U.T.	U.T.	96	100
		Early Oct.	570	170	U.T.	U.T.	71	71	650	180	U.T.	U.T.	68	73
		Late Oct.	250	70	B.T.	U.T.	72	45	140	50	B.T.	B.T.	72	71
6 7.0" UTB	Surface	Sept.	360	480	B.T.	U.T.	99	96	400	210	U.T.	U.T.	61	70
		Early Oct.	320	140	N.D.	N.D.	74	74	1000	120	U.T.	B.T.	79	64
		Late Oct.	160	105	U.T.	U.T.	72	72	650	30	U.T.	U.T.	72	61
	Base Top	Sept.	250	600	U.T.	U.T.	95	95	140	540	B.T.	U.T.	100	99
		Early Oct.	200	540	N.D.	N.D.	74	74	120	200	N.D.	U.T.	74	77
		Late Oct.	--	--	--	--	--	--	--	460	--	U.T.	--	64

TABLE 26 CONTINUED:

Section	Position	Period	Longitudinal Maximum Values				Pavement[3] Temp. °F		Transverse Maximum Values				Pavement[3] Temp. °F	
			Measurements		Lateral Pos.[2]				Measurements		Lateral Pos.[2]			
			C	T	C	T	C	T	C	T	C	T	C	T
	Base Bottom	Sept.	40	260	U.T.	U.T.	107	107	130	140	B.T.	U.T.	73	107
	Base Bottom	Sept.	160	600	U.T.	U.T.	99	99	160	100	B.T.	U.T.	95	95
		Early Oct.	--	--	--	--	--	--	160	100	B.T.	U.T.	64	78
		Late Oct.	--	--	--	--	--	--	35	50	U.T.	U.T.	61	60
7 9.5" UTB	Surface	Sept.	280	80	U.T.	B.T.	77	77	850	140	U.T.	B.T.	76	98
		Early Oct.	270	220	B.T.	U.T.	64	74	520	150	U.T.	U.T.	74	77
		Late Oct.	320	160	U.T.	U.T.	75	75	1000	140	U.T.	B.T.	75	56
		Nov.	280	200	U.T.	U.T.	31	59	760	60	U.T.	U.T.	65	61
8 12.0" UTB	Surface	Sept.	490	160	U.T.	U.T.	94	106	540	460	U.T.	U.T.	73	94
		Early Oct.	250	70	U.T.	U.T.	62	73	410	50	U.T.	U.T.	67	76
		Late Oct.	--	--	--	--	--	--	180	--	U.T.	--	63	--
	Base Top	Sept.	180	450	U.T.	U.T.	102	102	--	200	--	U.T.	--	94
		Oct.	100	200	U.T.	U.T.	67	67	--	--	--	--	--	--
		Nov.	120	220	U.T.	U.T.	72	72	--	--	--	--	--	--
		May	150	600	N.D.	N.D.	80	80	--	--	--	--	--	--
9 3.0" ETB	Surface	Sept.	500	240	B.T.	U.T.	105	95	1000	1500	U.T.	B.T.	93	105
		Oct.	220	160	U.T.	U.T.	75	75	720	110	U.T.	B.T.	75	70
		Nov.	180	70	N.D.	N.D.	47	47	200	80	N.D.	B.T.	47	64
		May	900	400	B.T.	B.T.	100	100	1700	--	B.T.	--	100	--
10 5.0" ETB	Surface	Sept.	440	80	U.T.	U.T.	74	77	480	180	U.T.	U.T.	74	86
		Oct.	540	120	U.T.	U.T.	68	68	500	20	U.T.	B.T.	67	61
		Nov.	150	50	U.T.	B.T.	46	66	240	65	U.T.	B.T.	46	66
		May	650	250	B.T.	B.T.	77	77	500	200	℄	℄	99	99
		June	1600	500	U.T.	B.T.	80	107	--	--	--	--	--	--
	Base Top	Sept.	120	260	B.T.	U.T.	95	77	165	500	B.T.	U.T.	80	77
		Oct.	190	260	B.T.	U.T.	60	67	55	290	B.T.	N.D.	61	69
		Nov.	60	220	B.T.	B.T.	66	66	110	30	B.T.	B.T.	66	66

TABLE 26 CONTINUED:

Section	Position	Period	Longitudinal Maximum Values: Measurements C	Measurements T	Lateral Pos.[2] C	Lateral Pos.[2] T	Pavement[3] Temp. °F C	Pavement[3] Temp. °F T	Transverse Maximum Values: Measurements C	Measurements T	Lateral Pos.[2] C	Lateral Pos.[2] T	Pavement[3] Temp. °F C	Pavement[3] Temp. °F T
		May	120	280	℄	℄	99	99	--	--	--	--	--	--
		June	200	200	U.T.	U.T.	107	107	--	--	--	--	--	--
11 7.0" ETB	Surface	Sept.	310	70	U.T.	U.T.	88	90	850	40	U.T.	B.T.	88	74
		Oct.	230	65	U.T.	U.T.	71	71	460	20	U.T.	B.T.	71	66
		Nov.	100	30	U.T.	U.T.	47	47	80	--	U.T.	--	47	--
		May	300	180	U.T.	U.T.	94	94	180	60	U.T.	U.T.	81	81
		June	750	300	U.T.	B.T.	94	100	1600	160	U.T.	B.T.	94	91
12 9.0" ETB	Surface	Sept.	340	170	U.T.	U.T.	93	80	1050	150	U.T.	U.T.	80	98
		Oct.	145	90	U.T.	U.T.	52	62	520	60	U.T.	U.T.	70	70
		Nov.	120	50	U.T.	U.T.	59	59	160	--	U.T.	--	59	--
		May	400	120	N.D.	N.D.	85	85	100	--	U.T.	--	60	--
		June	650	160	N.D.	U.T.	106	91	1150	200	U.T.	U.T.	85	97
	Base Top	Sept.	200	280	U.T.	U.T.	98	86	420	360	U.T.	U.T.	98	93
		Oct.	125	110	B.T.	U.T.	72	72	55	85	B.T.	U.T.	72	59
		Nov.	70	70	U.T.	U.T.	59	59	--	50	--	N.D.	--	45
		May	160	320	N.D.	N.D.	85	85	--	--	--	--	--	--
		June	160	1500	B.T.	U.T.	78	94	--	--	--	--	--	--
	Base Bottom	Sept.	170	280	U.T.	U.T.	74	88	40	260	U.T.	U.T.	66	87
		Oct.	50	500	U.T.	N.D.	62	59	100	200	B.T.	U.T.	73	72
		Nov.	--	--	--	--	--	--	--	150	--	U.T.	--	59

[1] The speed for September and October was 20 mph; for November, 10 to 15 mph; and for May onward the speed was 10 mph.

[2] U.T. means under tire, B.T. means beyond the inside or outside edge of tire with respect to gage, N.D. means not defined precisely but the gage is somewhere inside center line of duals, and ℄ means center line of duals is center line with gage.

[3] This is an average temperature of pavement surface, top of base and bottom base. In the U.T.B. section, the temperature is an average of top and bottom of wearing course.

[4] Up to October 13.

[5] After October 13.

[6] Up to June 15.

[7] After June 15 and includes July data, if any.

C means compression.

T means tension.

did not seem to affect the longitudinal strain as much. But the graphs do show that lateral tire position affected the strains and also the mode.

Figures 68-71 (page 106) show the change in surface strain during the continuous run for section 1. Temperature effects on strain are also shown.

Figures 70 and 71 (page 107) show that strains increased just before initial cracking. Figures 72-75 show the surface strains obtained from sections 2, 3 and 4. Strains were lower on the surface in the thicker sections than in thinner sections. This is also borne out by the strains in Table 26. Figures 76-81 show the magnitude of strains with depth. They show that tensile strains increase with depth and the complexity of strain in the lateral direction. Figure 98 shows a cross-section of strain with depth for both transverse and longitudinal directions.

Figures 82-89 show the longitudinal and transverse surface strain magnitudes with lateral distance for the untreated base sections. It can be seen that maximum strain values occur with tires over the gage, and that temperature does affect readings to some extent. Since strain data was scarce due to premature failure of the depth strain gages, no other graphs are included. Figure 100 shows strain with depth for section 6. Tensile strains seem to be less on the bottom but this may be due to the nature of the extensiometers and the granular base, and hence may be low.

The longitudinal and transverse strains on the surface for the emulsion treated bases, sections 9-12, are shown in Figures 90-97 (page 120). These show that the strains were usually at a maximum when the tires were over the gages, that temperature affected the readings, and that the lateral tire distance affected the readings. Figure 99 shows the strain values with depth for section 12, and shows that tensile strains at the bottom were larger on the longitudinal than on the transverse direction.

Examination of the strains from the continuous strain gage data seems to show that strain readings were not always symmetrical. Some of this hysteresis effect may be due to temperature effects which caused strain changes, and perhaps to the wheel loads. Another reason is that as the duals moved laterally the weight distribution may have changed due to transverse load placement. The camber of the wheels was set to the slope of the pavement so that weight distribution on each wheel was equal; as the pavement became rougher, the load on each wheel may have shifted due to this camber thus causing some variations in strains, both in longitudinal and transverse directions. However, the continuous strain gage readings did show up the various patterns of reversals of strain with lateral distance, and also showed the temperature effects.

Comparison with maximum strains obtained from Ring #2 (1) shows that maximum strains for Ring #3 were higher. It is difficult to explain why, but some of the reason may be that the testing period was longer, hence more data was obtained giving more values under all temperatures, the temperatures generally were higher, hence giving higher readings, and the pavements lasted longer thus the strain gages survived longer. Thus the maximum readings may give us better values for determination of initial strain values for design and failure.

Stress Data

Measurements of vertical stress were obtained from the WSU strain gage pressure cells and from the WSU hydraulic pressure cells taken on a continuous basis during a day or a period of days and also during runs along with other instrument readings. Unfortunately, operational difficulties with the WSU

TABLE 27: SUMMARY OF MAXIMUM MEASURED VERTICAL STRESSES

Section	Period	Gage Depth Inches	Vertical Stresses PSI	Lateral Position to ℄ Duals (Feet)	Temp. at Gage °F	Speed MPH
3 - 3.5" A.T.B.	Sept.	6.5"	33.0	0.10	86	20
	Oct.		12.0	0.30	53	20
	Nov.		11.0	0.15	36	10
	May		53.0	0.10	82	2
			27.0	0.15	74	10
	June		29.0	0.05	72	10
6 - 7.0" U.T.B.	Sept.	10.0"	19.3	0.06	74	20
	Oct.		13.3	0.25	63	20
	Late Oct.		21.0	0.30	56	20
	Nov.		33.8	0.02	45	10
8 - 12.0" U.T.B.	Sept.	15.0"	9.7	℄	72	7
	Oct.		9.0	0.30	64	20
	Nov.		10.0	0.50	48	10
	May		17.3	0.65	68	10
	June		24.0	0.65	77	10
	July		27.0	0.55	84	10
10 - 5.0" E.T.B.	Sept.	8.0"	16.75	0.25R	74	20
	Oct.		24.3	0.20	62	20
	Nov.		17.25	0.50	46	10
	May		29.4	0.68	70	20
	June		22.0	0.50	75	10
	July		23.0	℄	84	10
	July after overlay		21.0	0.80	99	10
12 - 9.0" E.T.B.	Sept.	3.0"	58.8	0.45	117	20
	Oct.		18.3	0.42	69	5
	Nov.		16.0	0.12	35	10
	May		50.9	0.30	77	10
	June		55.6	0.18	108	10
	July		66.8	0.63	106	10

hydraulic pressure cells developed which resulted in insufficient data for inclusion in this report.

Table 27 (page 102) summarizes the maximum stress value obtained during different periods of testing. Figures 101-105 (page 125) are curves which show the distribution of the stress values with lateral distance and temperature for the different base types. Stresses were measured on the top of the subgrade in sections 3, 6, 8 and 10. In section 12, vertical stresses were measured on top of the 12-inch emulsion base; the cell in the subgrade failed to respond.

The stress data showed that vertical stress varied with lateral position of the duals, speed, temperature, subgrade moisture, type of base material and with environment. Maximum stress values were obtained when the duals were usually over the cells in the subgrade. This was true only for the cells placed in the subgrade. The maximum values for the cell on top of the base in section 12 and shown in Figure 105 were obtained when the tire was over the cell. It was noticed that speed affected the values; lower speeds usually gave higher stresses and vice versa. Temperature, since it affects the modulus of the pavement structure, also affected the vertical stresses. Stresses usually increased as the temperature increased. Since moisture affects the resilient modulus of the subgrade, this in turn affects the vertical stress which will increase as the resilient modulus decreases. All this is affected by the environment which is made up of different variables, and hence affects the vertical stresses and strains.

Vertical stresses were measured in the 7.0- and 12.0-inch untreated crushed rock base sections 6 and 12 respectively, and are shown in Figures 101 and 102 (page 123).

The figures show that for the early fall period the 5.0 inches of crushed rock more in section 12 reduced the vertical stress at the subgrade by approximately 50%. This percentage may have increased in spring, but comparison is difficult since section 6 had failed in the fall. Figure 101 shows the different stress levels with temperature and time for section 6. Curve 1 is interesting in that it shows the stresses obtained prior to initial cracking. It is interesting that stresses increased after initial cracking and reached maximum values prior to "ultimate" failure. The reason for this phenomena may be that as the pavement system starts to break up the pavement no longer acts as a continuous slab, but now acts as a series of separate entities, which may act individually or collectively on the subgrade as pressure points thus giving higher stress values. Stresses in section 12 in the fall seem to increase slightly as the temperature fell. Some of this may be due to increased moisture in the subgrade which came from increased rainfall. In the spring, due to the saturation of the subgrade, environmental conditions and decrease in base modulus, stresses increased almost two to three times. Temperature effects decrease with depth as shown by Figures 101-104 (page 124).

In section 6, as shown in Figure 103, vertical stresses increased as temperatures decreased in the fall; this is shown by curves 1 and 2. The reasons for this may be due to increased moisture content in the subgrade and increased wheel loads. In the spring the vertical increased by more than two times. The fact that the spring vertical stresses were higher than those for the 5.0-inch E.T.B. (section 10) and shown in Figure 104 may account for the fact that section 3 failed before section 10.

Figure 104 shows the stresses obtained from section 10 for the fall and spring periods. The stresses increased in the spring by a factor of two over those measured in the fall, thus indicating that environmental conditions had affected that shear strength of the subgrade. Curve 3 shows that an asphalt overlay reduced vertical stress by some 25%.

Figure 105 is of interest in that it shows the effect of temperature on vertical stresses rather well. The figure also shows that the individual tires did cause higher stresses than the center of the duals. This may have been a function of the depth of the cell. Spring vertical stresses were very high and increased by over five times those measured in the fall.

Increased vertical stresses in the spring perhaps is an indication why different modes of failure occurred in spring as compared to the fall. The spring stress level was beyond critical values obtained in the AASHO Road Test (14) and reported on by Vesic and Domaschuk (15). These critical stress values ranged between 9 to 11 psi. If stress values are above this figure, rutting usually increases rapidly and with a relatively weak, compressible subgrade and strong, well-compacted thin pavement structure, structural failure may occur mainly due to punching shear. This occurred in the spring break-ups in Rings #2 and #3. Rutting is then due to primarily compression and distortion of the subgrade soil. The fall stress values were usually below the critical stress values except just prior to initial cracking as shown in section 6. Then the critical stress value was reached. Hence, failure was due to other factors besides excessive vertical stresses, and environmental conditions such as additional moisture, lower temperatures, increased wheel loads, along with thin sections may have been responsible for the different failure mode.

FIGURE 68. STRAIN VS. LATERAL DISTANCE
Section #1 - No Base
Longitudinal Strain Gage A-6-L Surface
20 mph Oct. 5, 1967
261,330 Wheel Loads

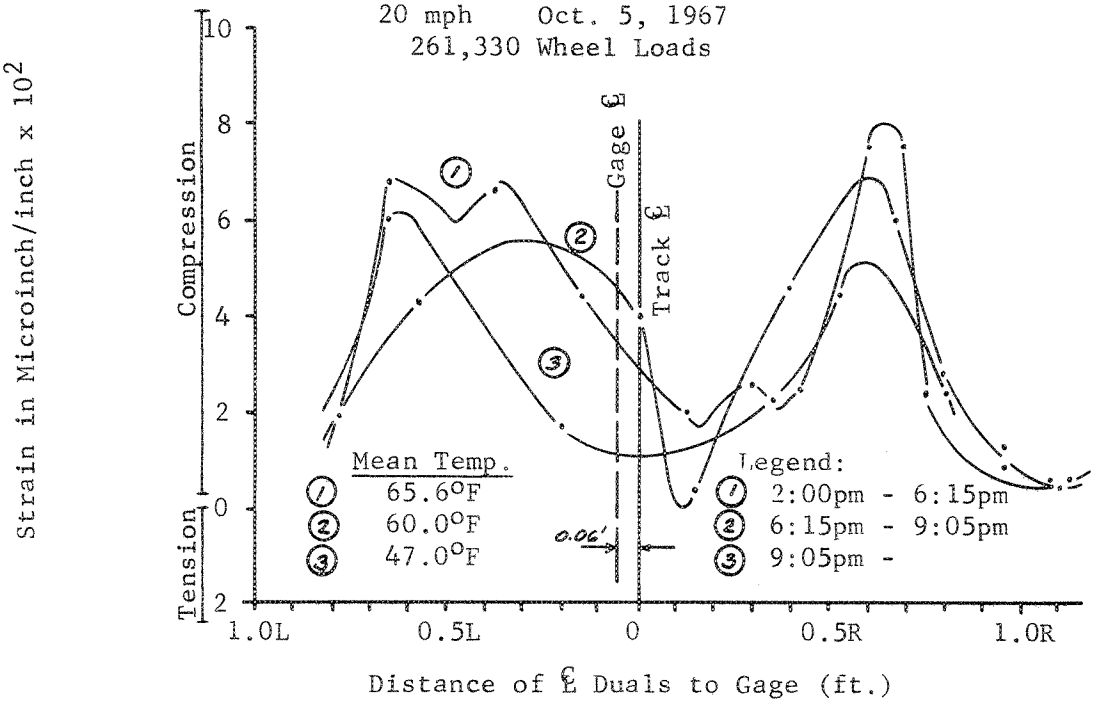

FIGURE 69. STRAIN VS. LATERAL DISTANCE
Section #1 - No Base
Surface Transverse Strain Gage A-7-T
20 mph Oct. 5, 1967
261,330 Wheel Loads

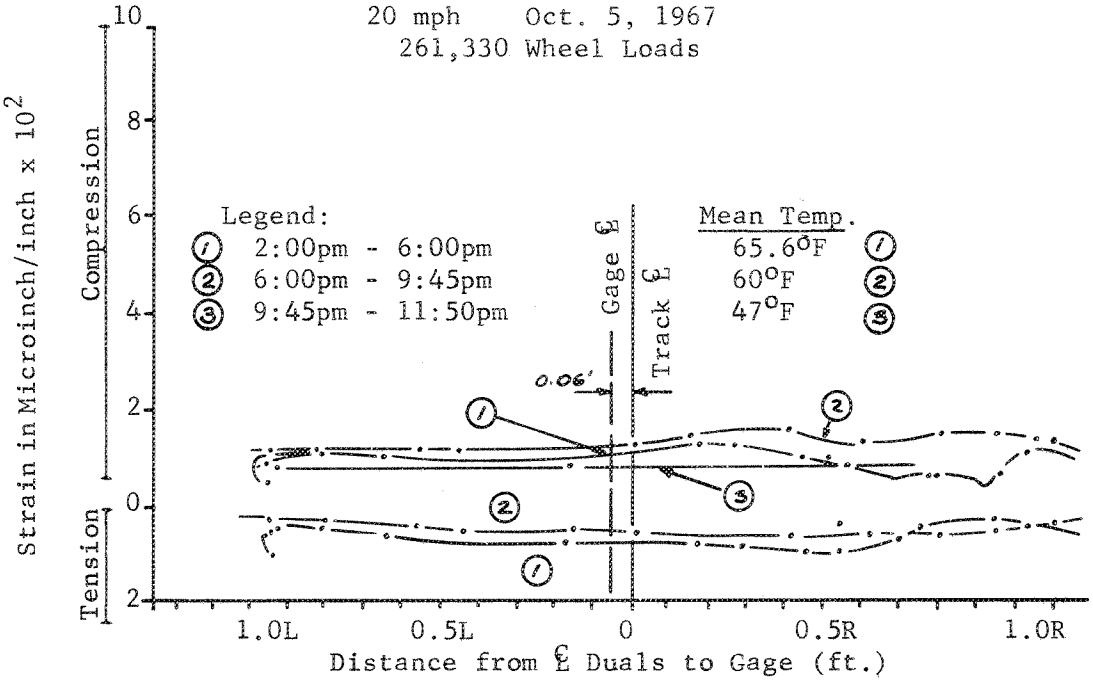

FIGURE 70. STRAIN VS. LATERAL DISTANCE
Section #1 - No Base
Longitudinal Strain Gage A-6-L-Surface
20 mph Oct. 8, 1967
309,792 Wheel Loads

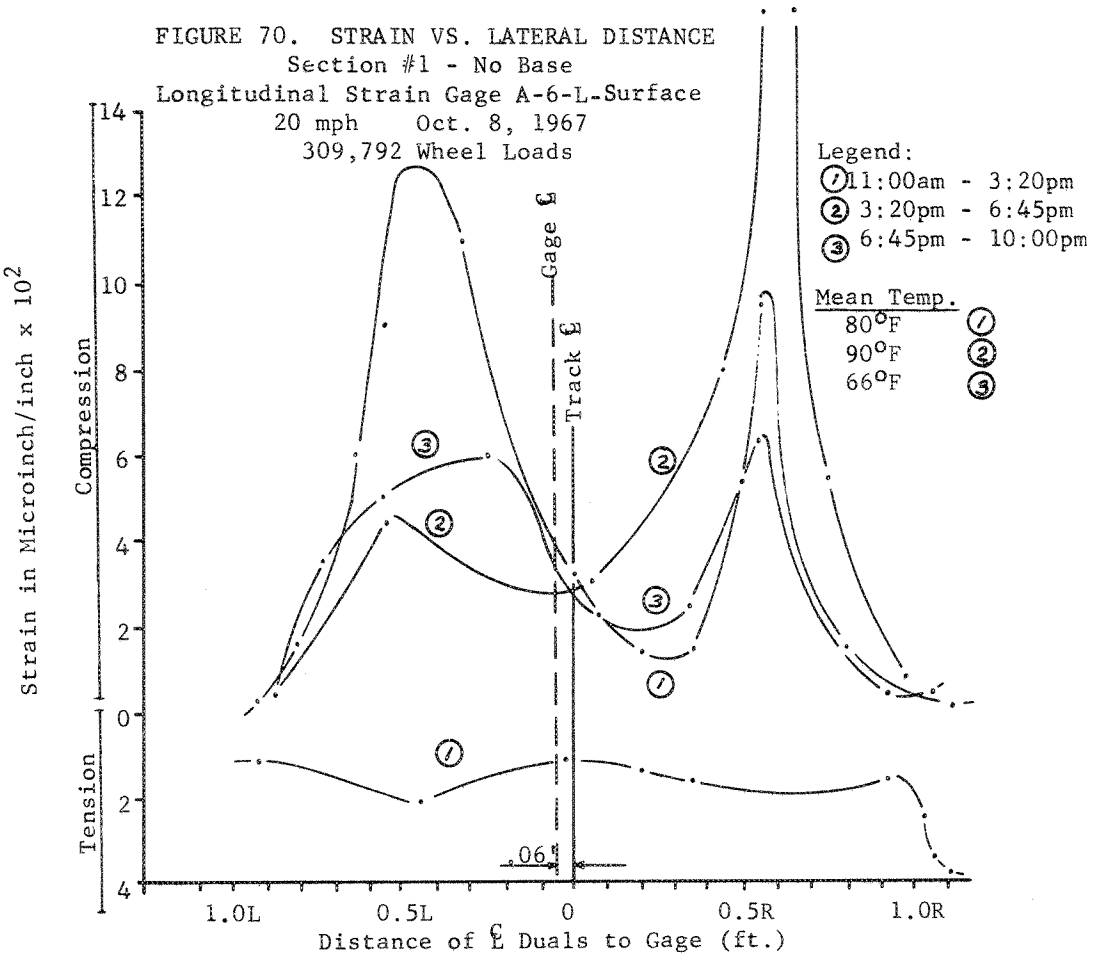

FIGURE 71. STRAIN VS. LATERAL DISTANCE
Section #1 - No Base
Surface Transverse Strain Gage A-7-T
20 mph Oct. 8, 1967
309,792 Wheel Loads

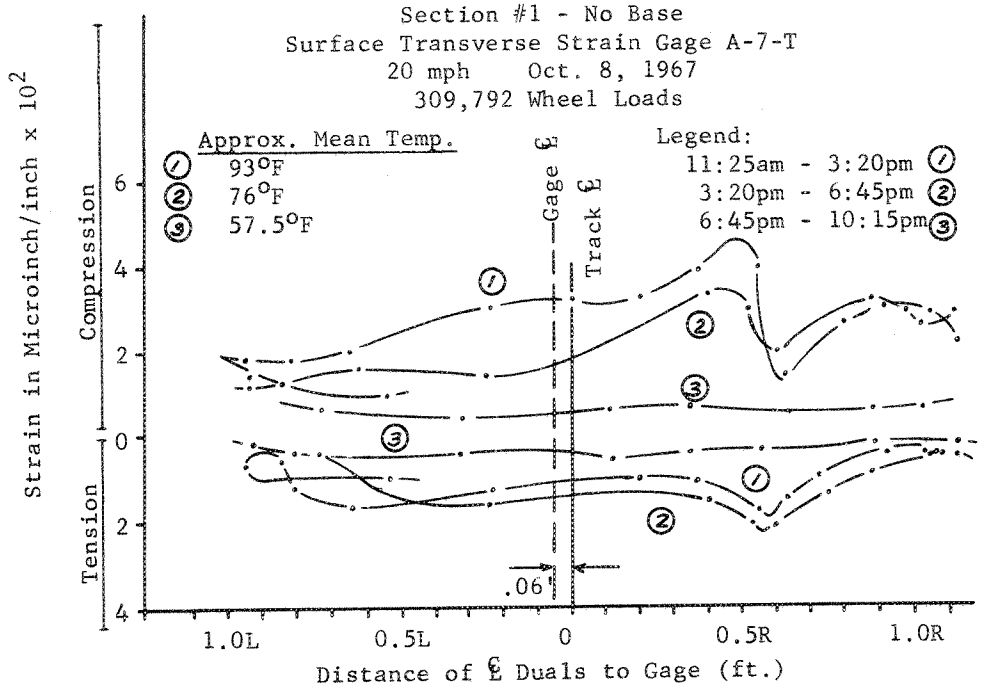

FIGURE 72. STRAIN VS. LATERAL DISTANCE
Section #2 - Ring #3 - 2" A.T.B.
Surface Strain Gages A-8 and A-9*
Oct. 7-17, 1967

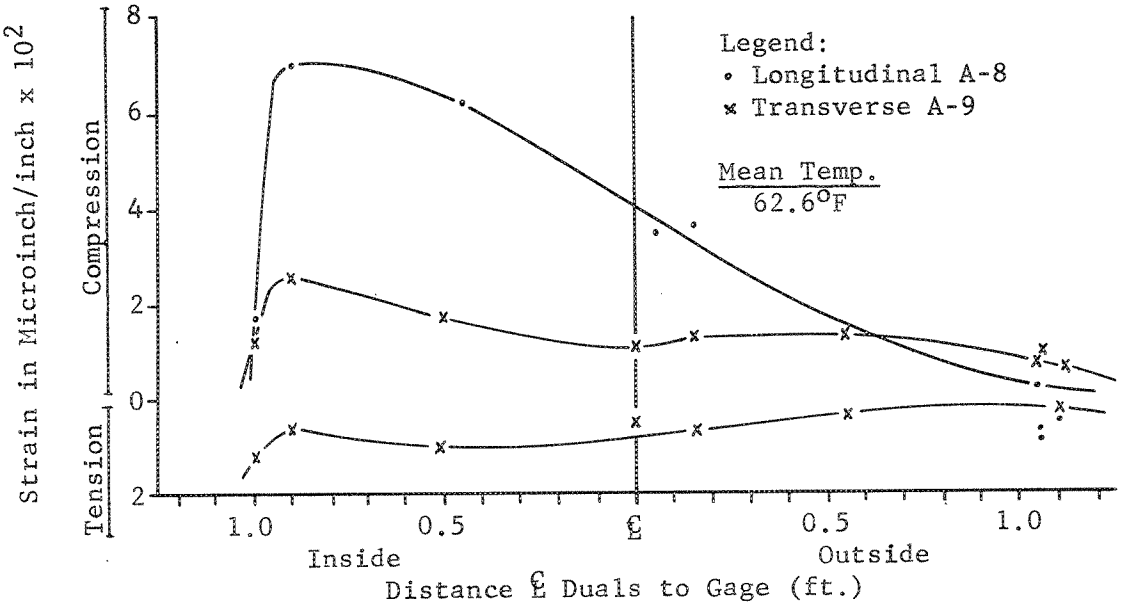

FIGURE 73. STRAIN VS. LATERAL DISTANCE
Section #4 - 5" A.T.B.
Surface Strain Gages B-4 and B-3*

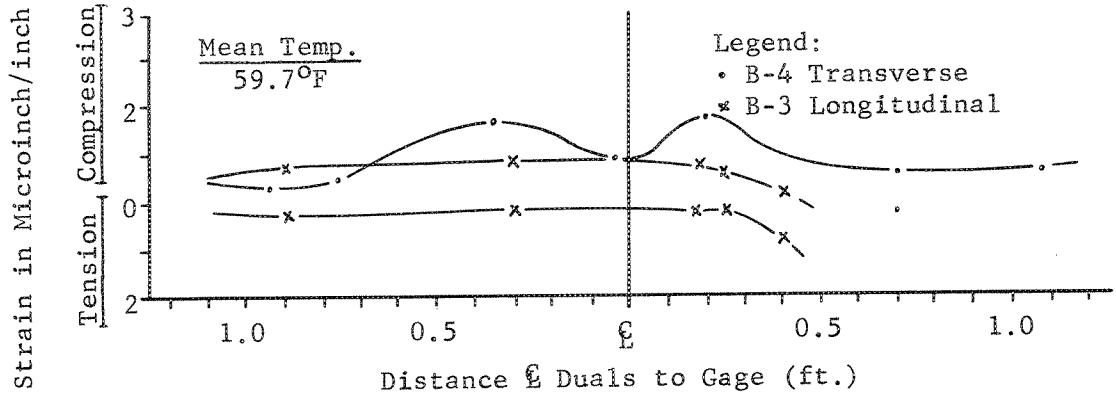

* Data taken from runs, hence wheel load effect is ignored.

FIGURE 74. STRAIN VS. LATERAL DISTANCE
Section #3 - Ring #3 - 3.5" A.T.B.
Surface Transverse Strain Gage B-2
20 mph Oct. 20, 1967
397,589 Wheel Loads

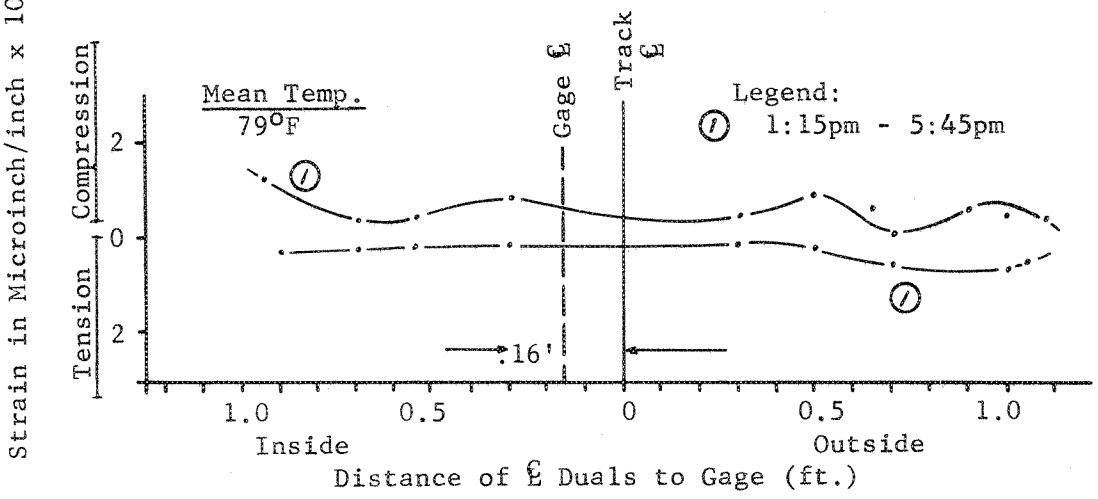

FIGURE 75. STRAIN VS. LATERAL DISTANCE
Section #3 - Ring #3 - 3.5" A.T.B.
Surface Longitudinal Strain Gage B-1
20 mph Oct. 20, 1967
397,589 Wheel Loads

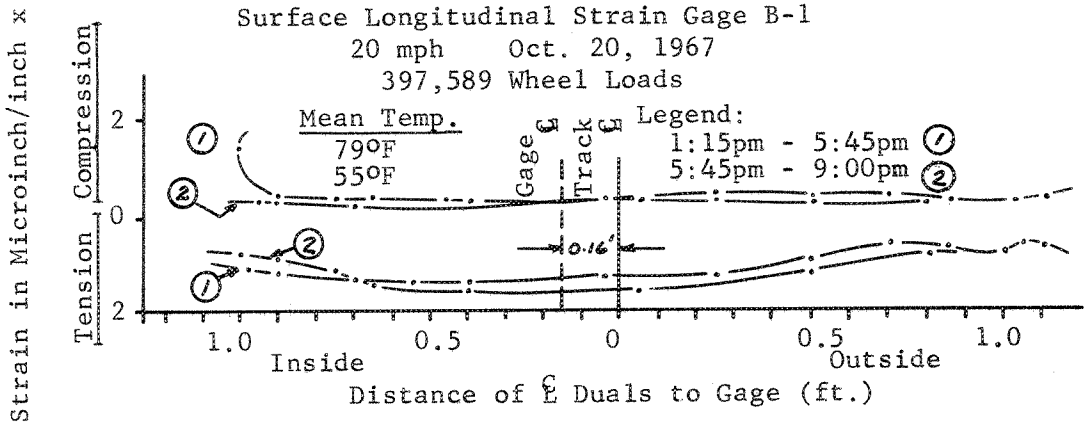

FIGURE 76. LONGITUDINAL STRAIN MEASUREMENTS VS. LATERAL DISTANCE
Section 3 3.5" A.T.B. Depth = 3.0"

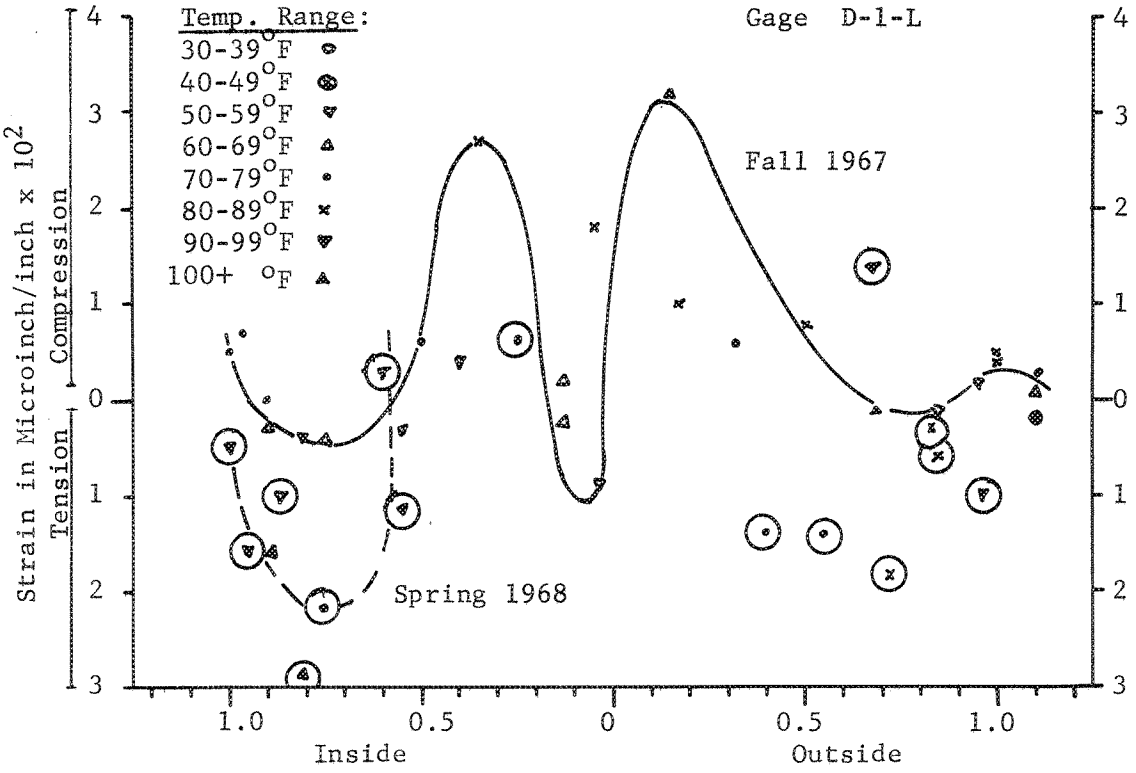

FIGURE 77. LONGITUDINAL STRAIN MEASUREMENTS VS. LATERAL DISTANCE
Section 3 Gage *B-1-L
Depth = 3.0"

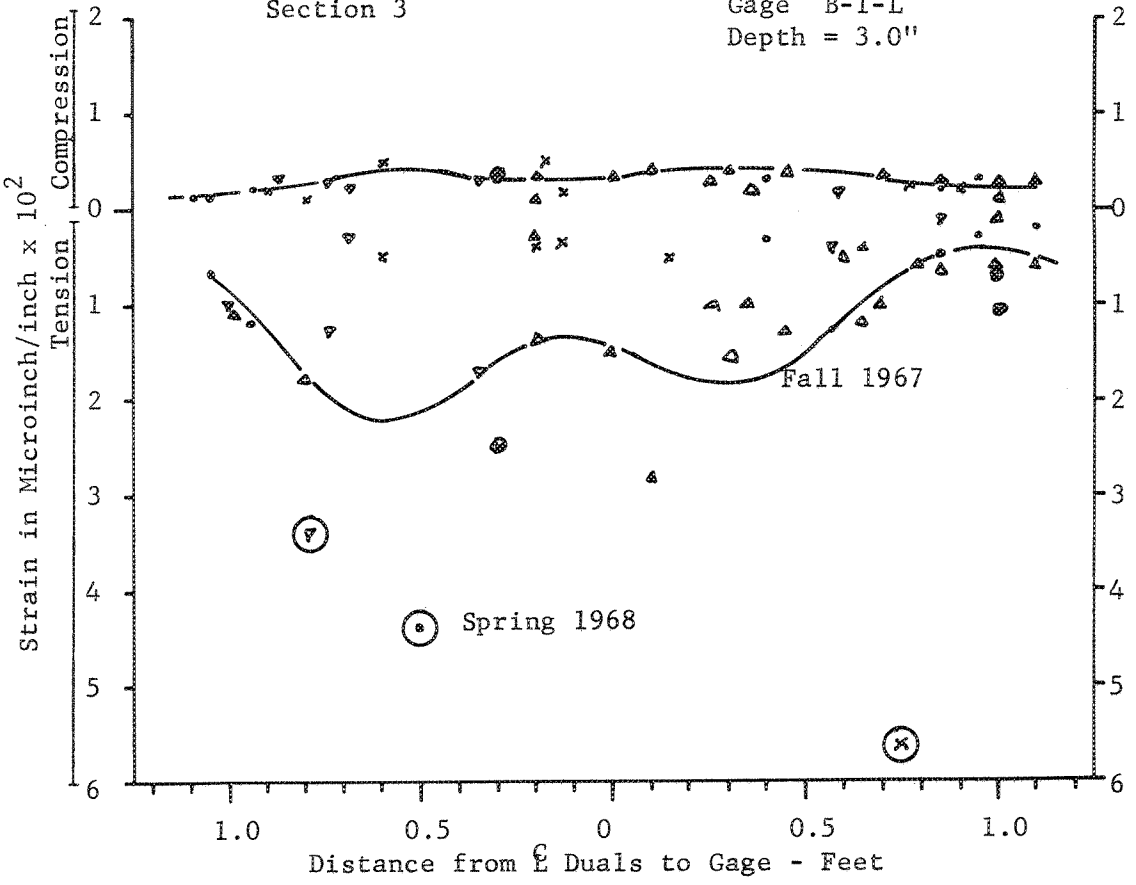

FIGURE 78: TRANSVERSE STRAIN MEASUREMENTS VS. LATERAL DISTANCE
Section 3 3.5" A.T.B. Depth = 3.0"
Gage D-2-T

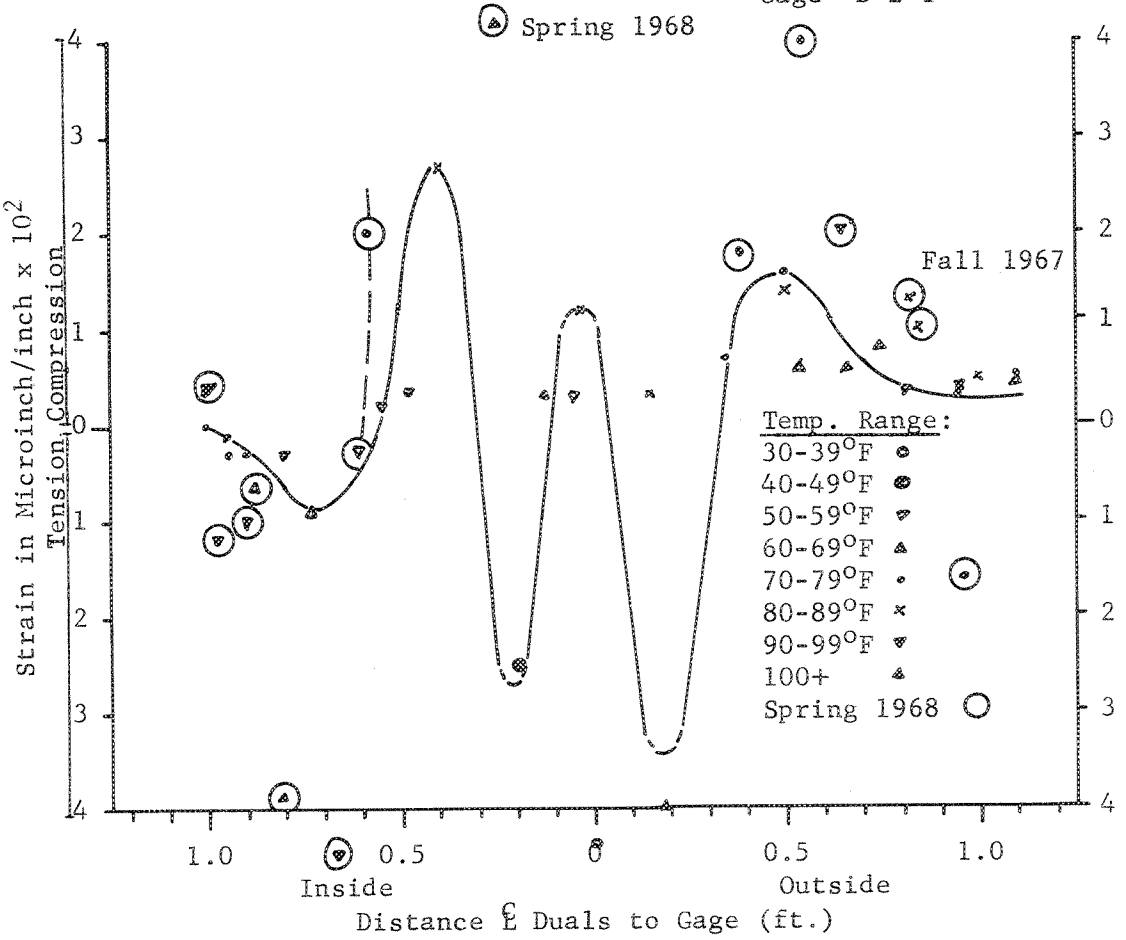

FIGURE 79: TRANSVERSE STRAIN MEASUREMENTS VS. LATERAL DISTANCE
Section 3 Gage *B-2-T
Depth = 3.0"

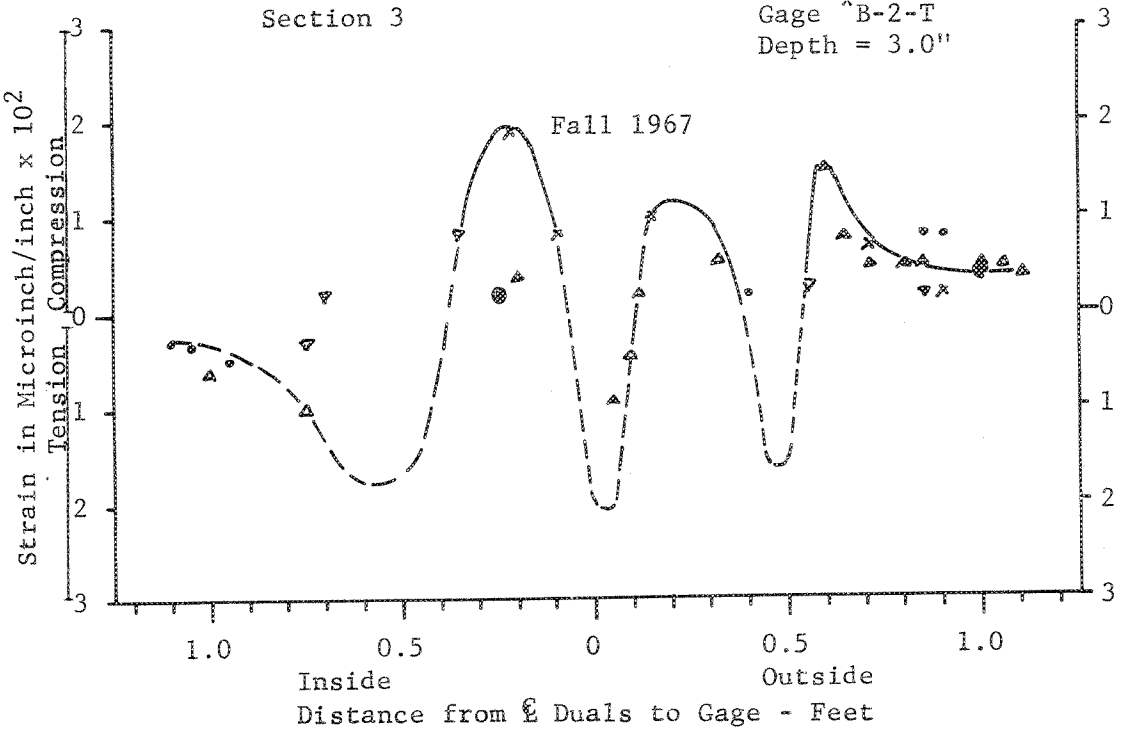

FIGURE 80: LONGITUDINAL STRAIN MEASUREMENTS VS. LATERAL DISTANCE
Section 3 3.5" A.T.B. Depth = 6.5"
Bottom of Base
Gage E-1-L

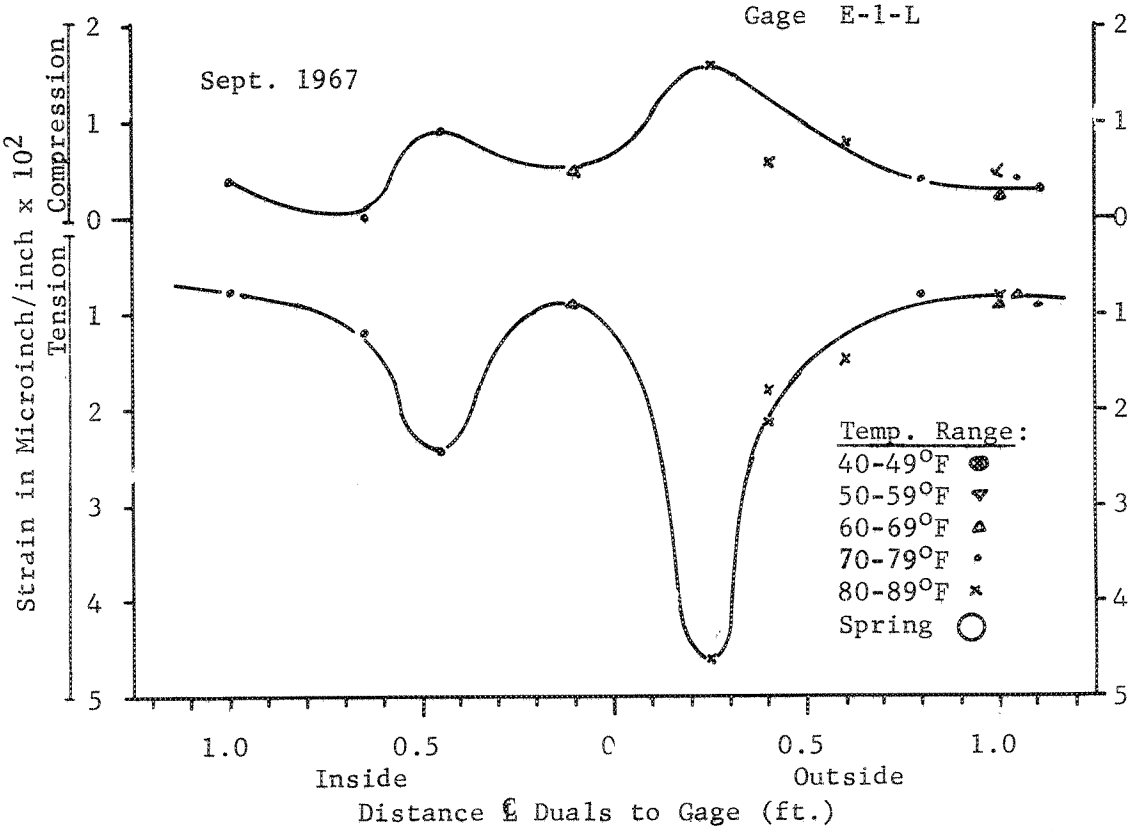

FIGURE 81: TRANSVERSE STRAIN MEASUREMENTS VS. LATERAL DISTANCE
Section 3
Bottom of Base
Gage E-2-T

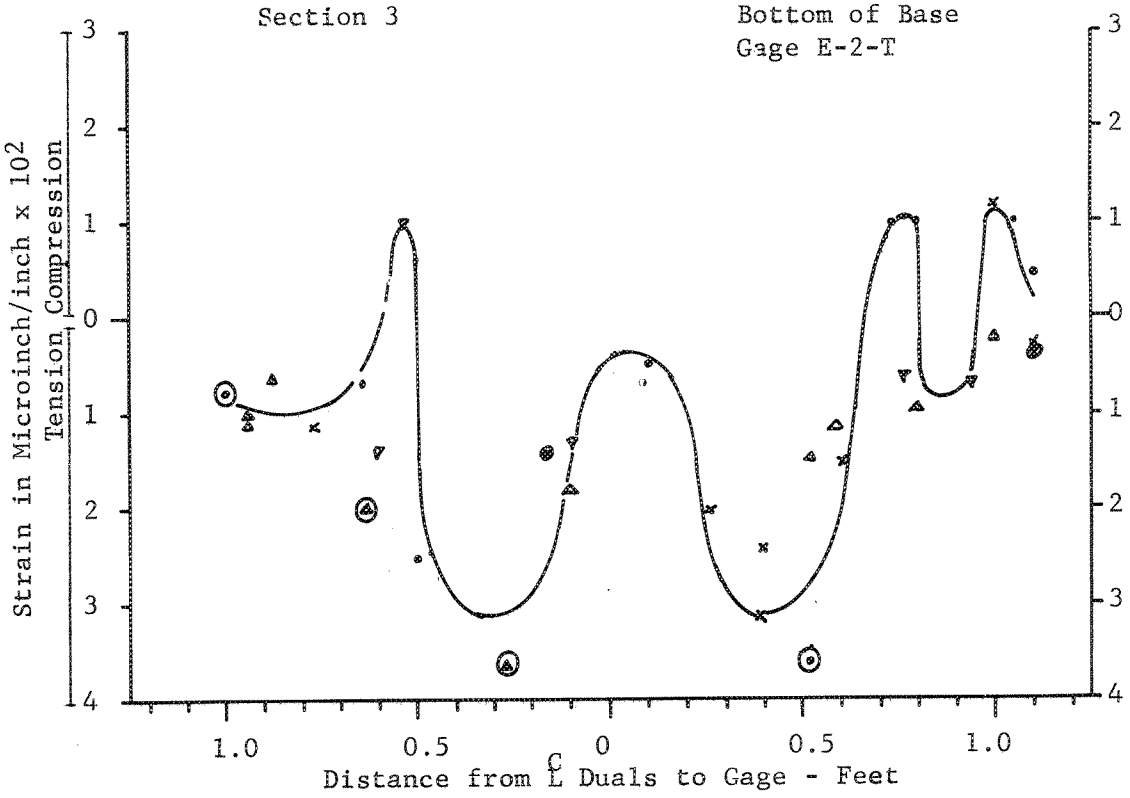

FIGURE 82. STRAIN VS. LATERAL DISTANCE
Section #5 - 4.5" U.T.B.
Surface Transverse Strain Gage B-6
20 mph Oct. 7, 1967 300,819 Wheel Loads

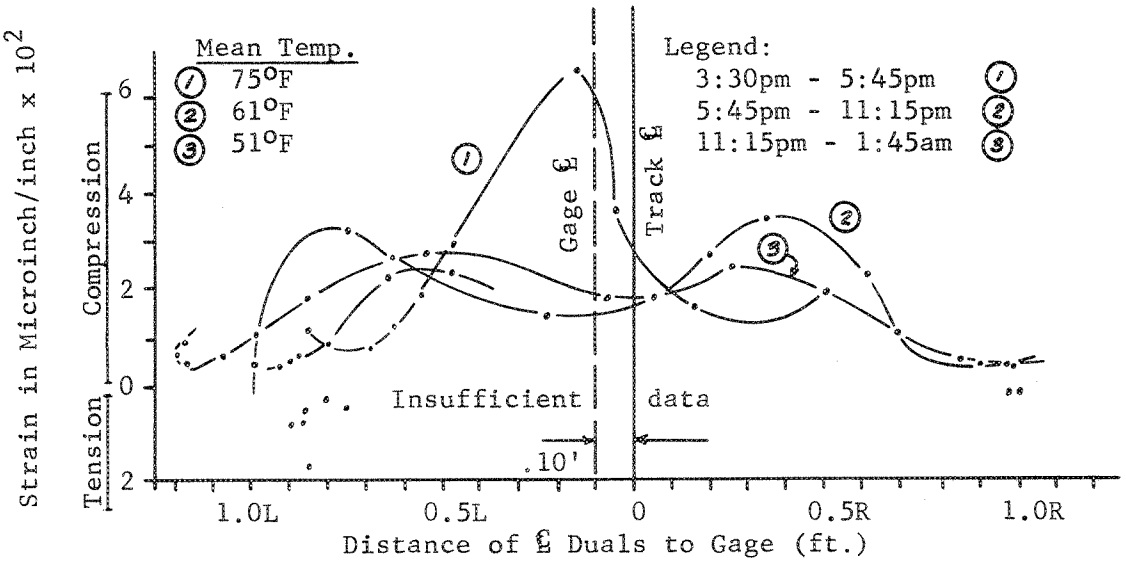

FIGURE 83. STRAIN VS. LATERAL DISTANCE
Section #5 - 4.5" U.T.B.
Surface Longitudinal Strain Gage B-5
20 mph Oct. 7, 1967

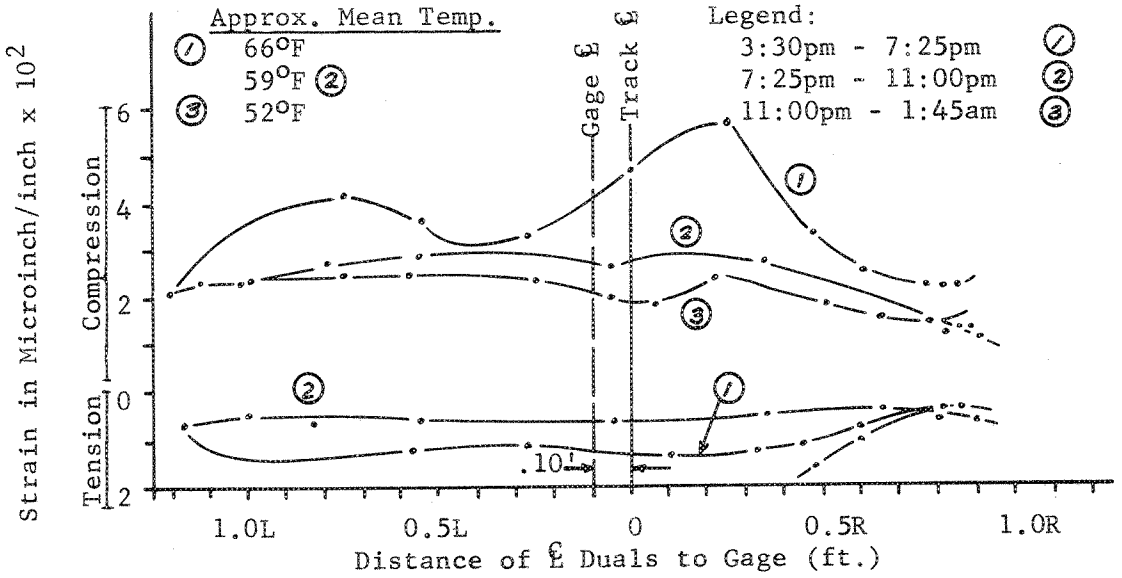

FIGURE 84. STRAIN VS. LATERAL DISTANCE
Section #6 - Ring #3 - 7.0" U.T.B.
Surface Longitudinal Strain Gage B-7*

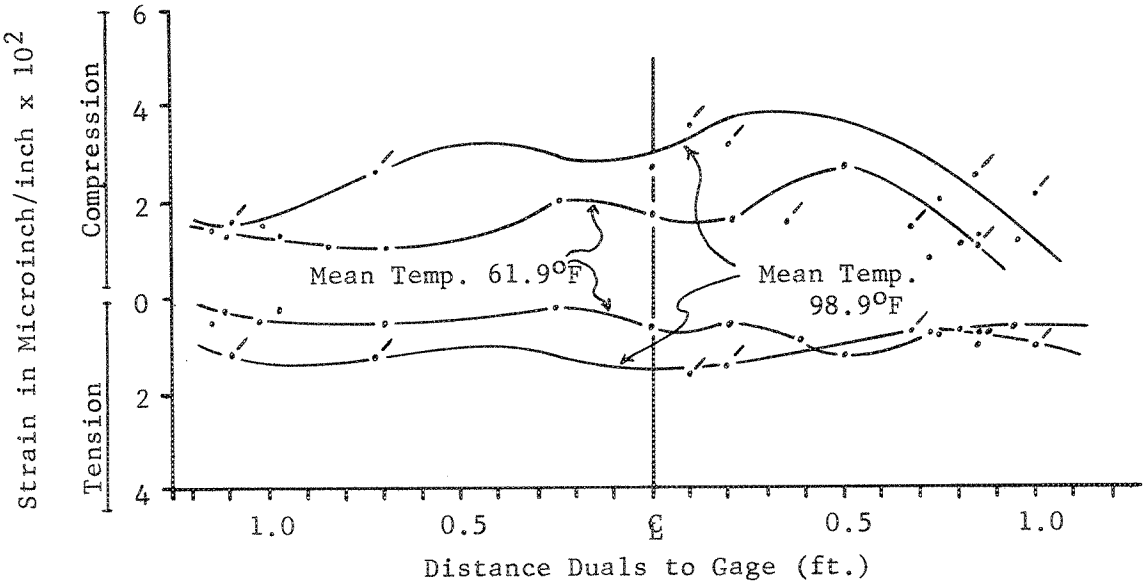

FIGURE 85. STRAIN VS. LATERAL DISTANCE
Section #6 - Ring #3 - 7.0" U.T.B.
Surface Transverse Strain Gage B-8*

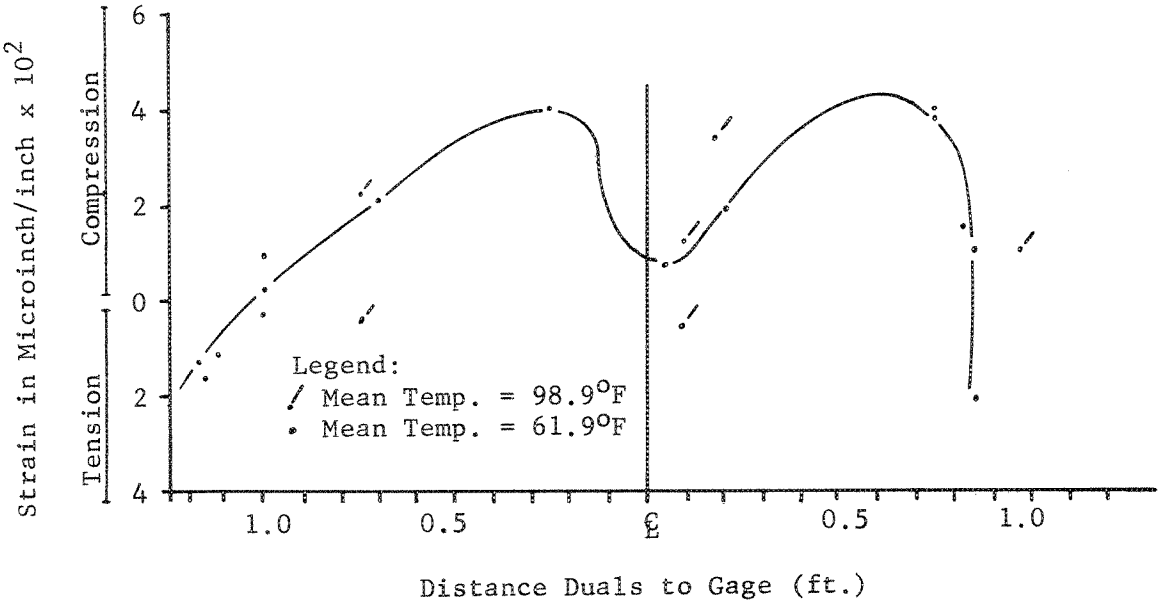

* Data taken from runs, hence wheel load effect is ignored.

FIGURE 86. STRAIN VS. LATERAL DISTANCE
Section #7 - Ring #3 - 9.5" U.T.B.
Surface Transverse Strain Gage B-10-T
Nov. 1, 1967

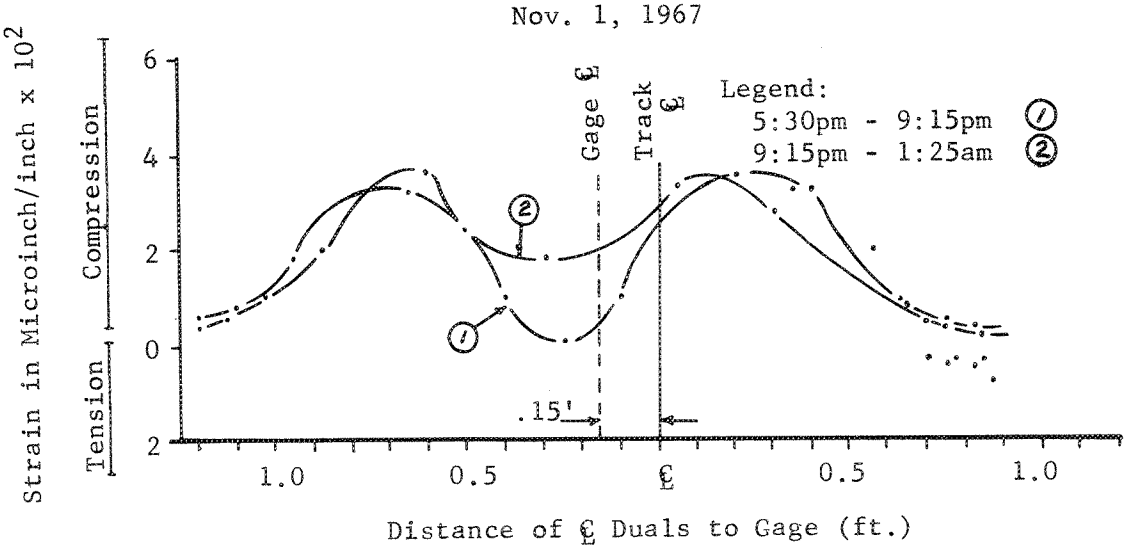

FIGURE 87. STRAIN VS. LATERAL DISTANCE
Section #7 - Ring #3 - 9.5" U.T.B.
Surface Longitudinal Strain Gage B-9-L
Nov. 1, 1967

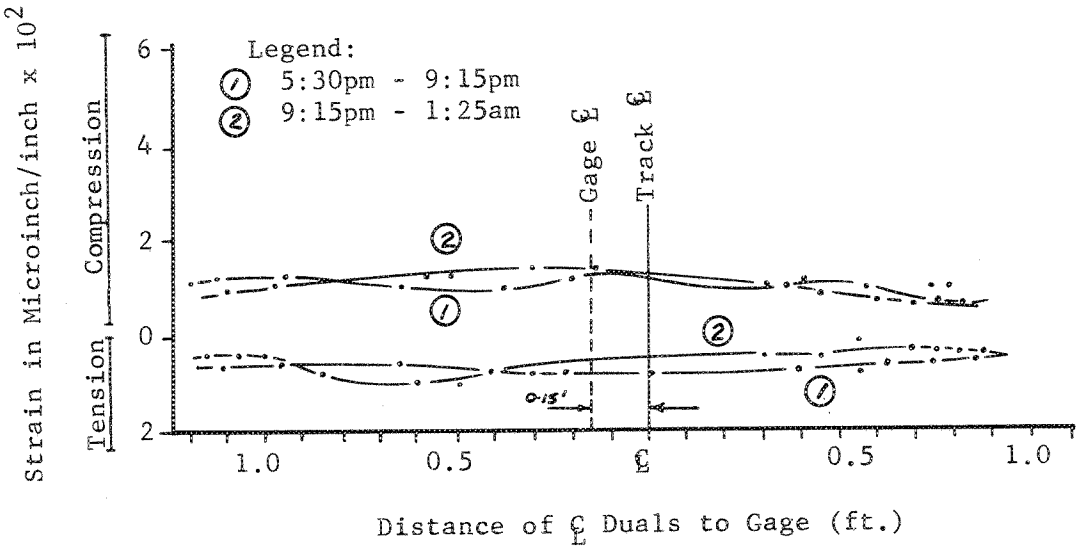

FIGURE 88. STRAIN VS. LATERAL DISTANCE
Section #8 - Ring #3 - 3" U.T.B.
Surface Longitudinal Strain Gage C-1*

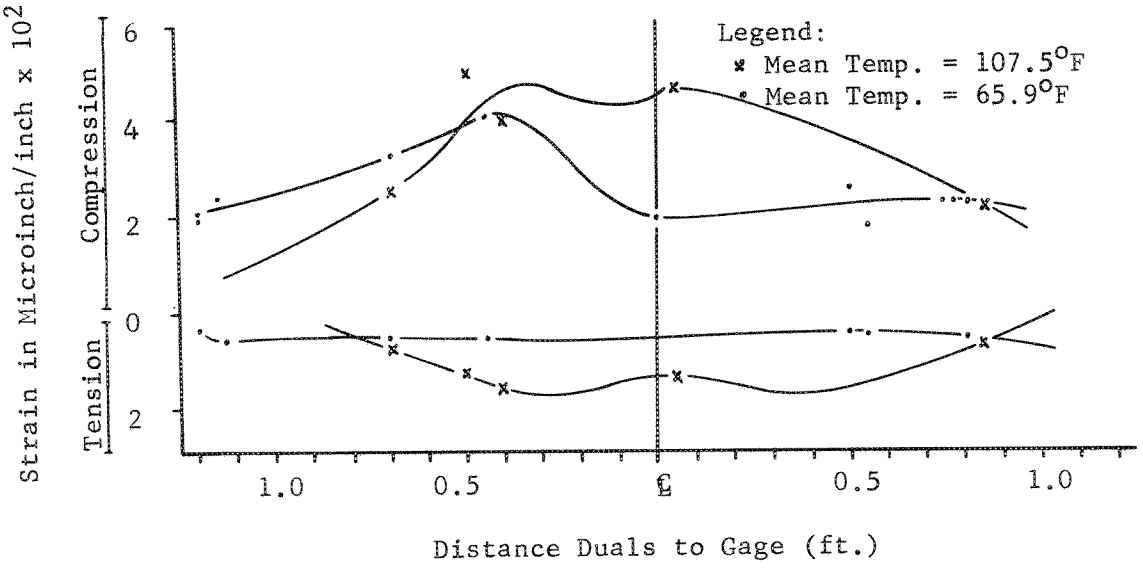

FIGURE 89. STRAIN VS. LATERAL DISTANCE
Section #8 - Ring #3 - 3" U.T.B.
Surface Transverse Strain Gage C-2*

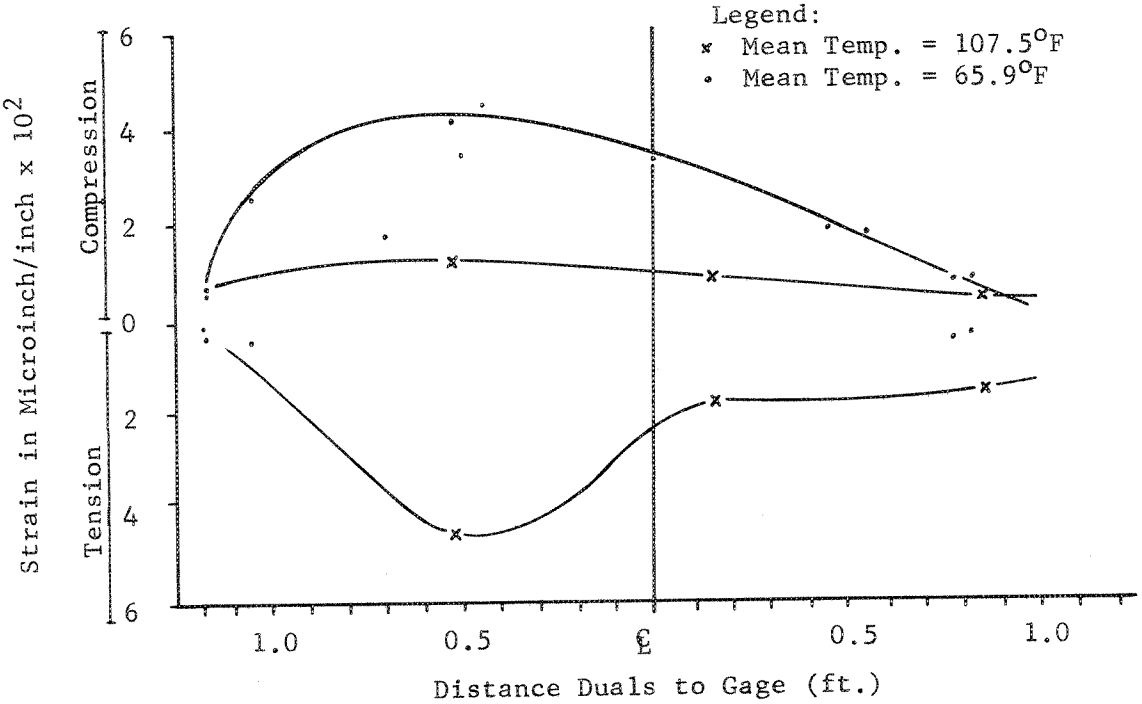

* Data taken from runs, hence wheel load effect is ignored.

FIGURE 90. STRAIN VS. LATERAL DISTANCE
Section #9 - Ring #3 - 3" E.T.B.
Surface Transverse Strain Gage C-4

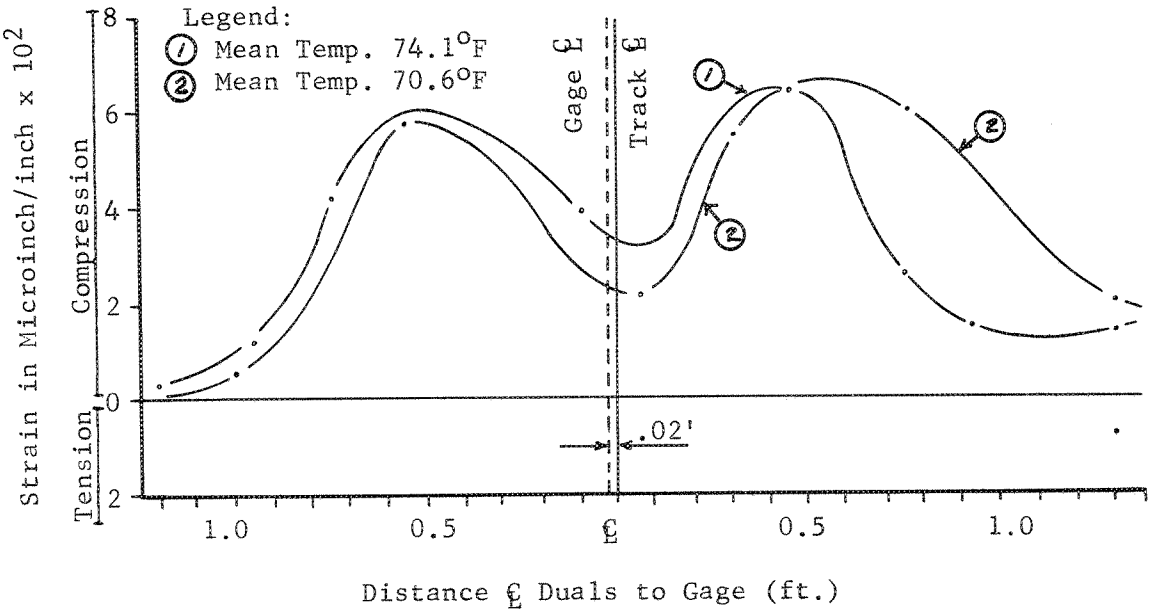

FIGURE 91. STRAIN VS. LATERAL DISTANCE
Section #9 - Ring #3 - 3" E.T.B.
Surface Longitudinal Strain Gage C-3

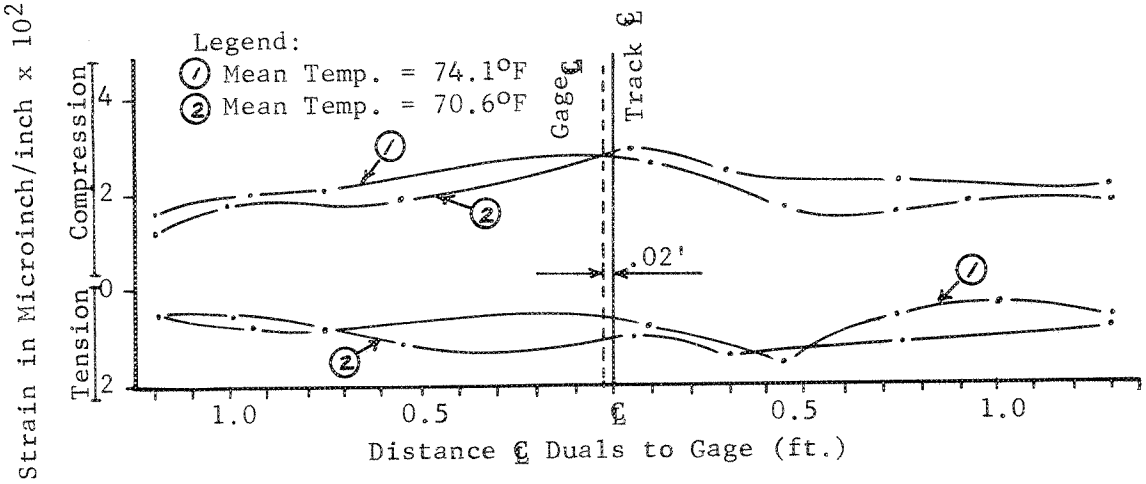

FIGURE 92. STRAIN VS. LATERAL DISTANCE
Section #10 - Ring #3 - 10" E.T.B.
Surface Transverse Strain Gage C-6*

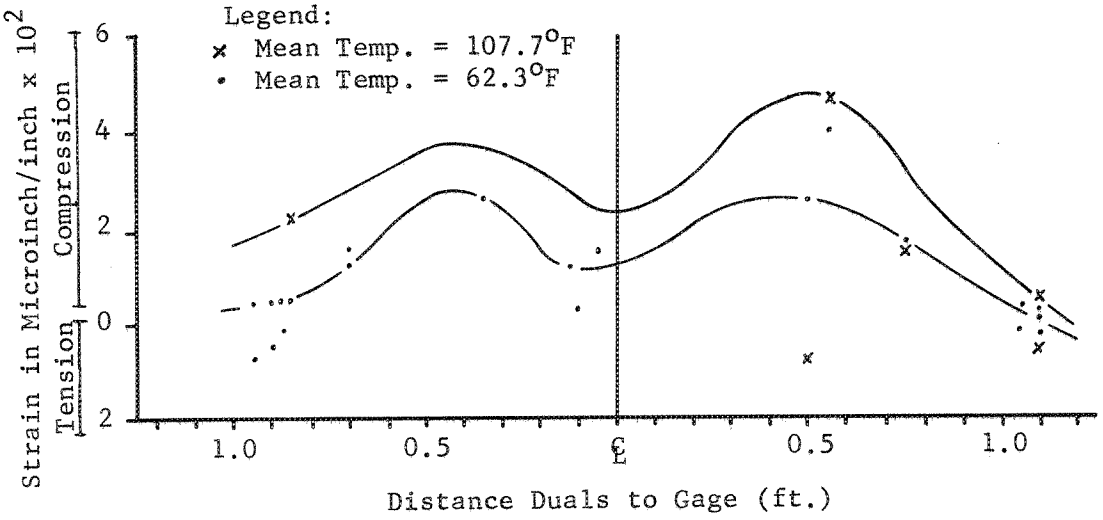

FIGURE 93. STRAIN VS. LATERAL DISTANCE
Section #10 - Ring #3 - 10" E.T.B.
Surface Longitudinal Strain Gage C-5*

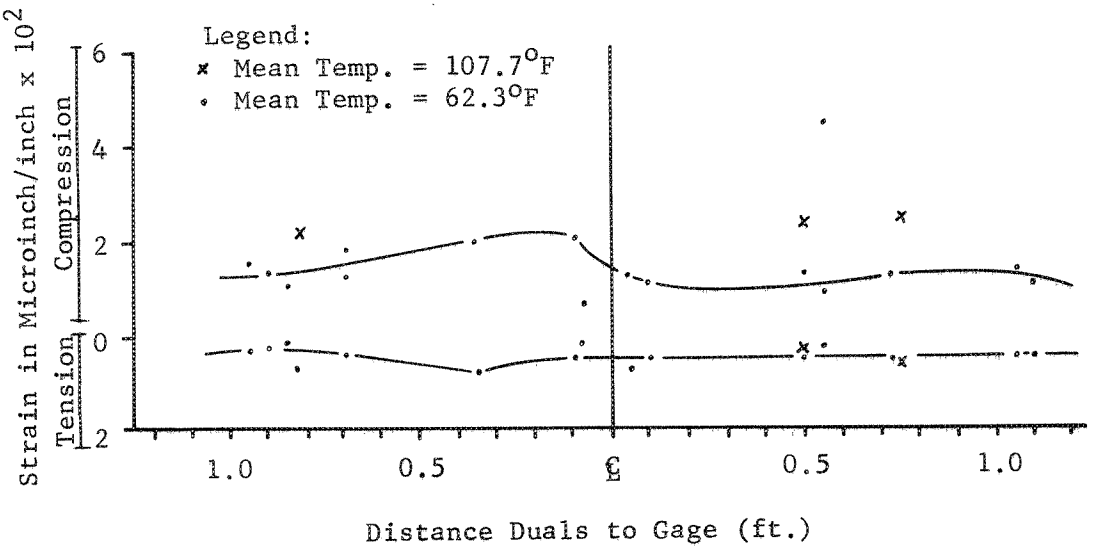

* Data taken from runs, hence wheel load effect is ignored.

FIGURE 94. STRAIN VS. LATERAL DISTANCE
Section #11 - Ring #3 - 8" E.T.B.
Surface Transverse Strain Gage C-8*

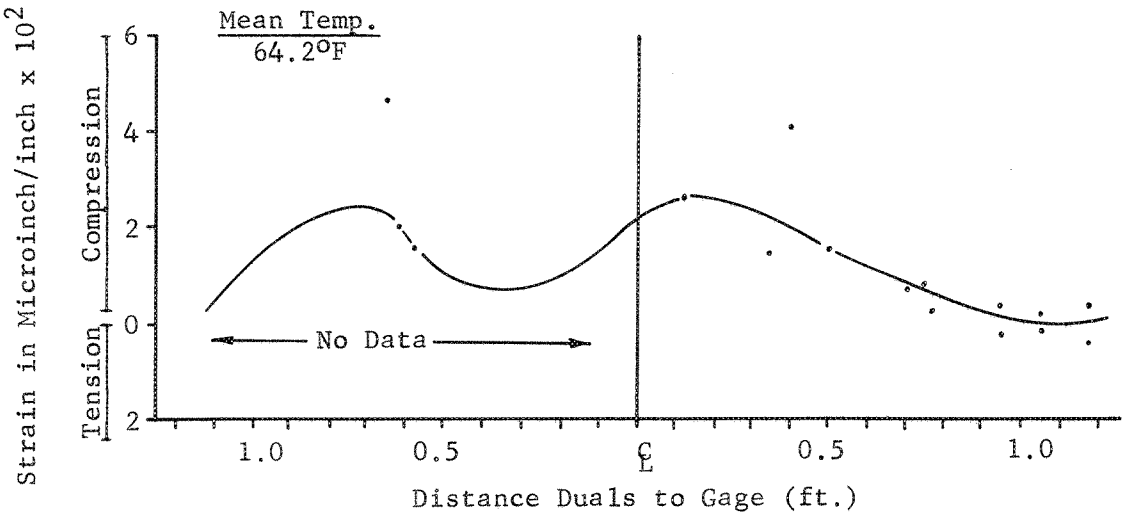

FIGURE 95. STRAIN VS. LATERAL DISTANCE
Section #11 - Ring #3 - 8" E.T.B.
Surface Longitudinal Strain Gage C-7*

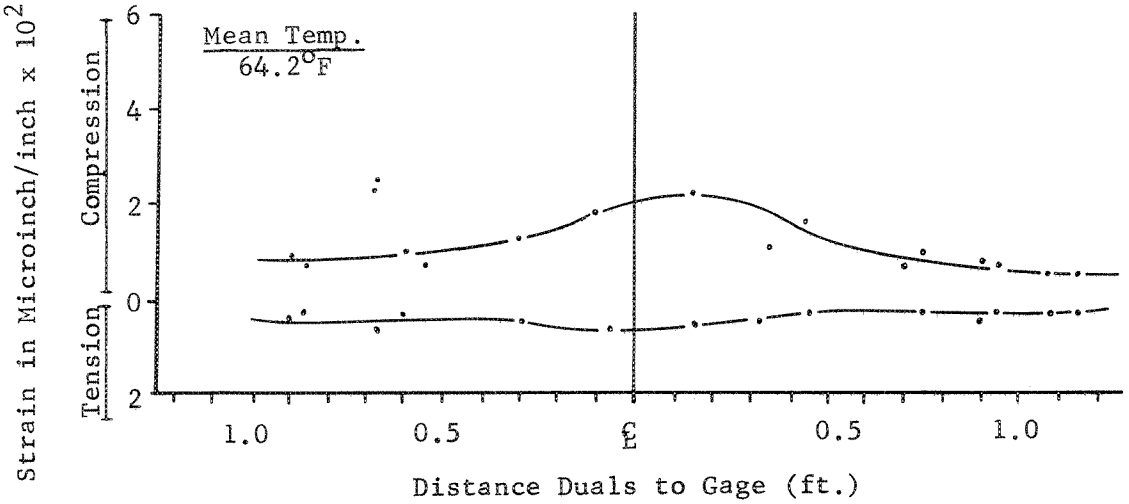

* Data taken from runs, hence wheel load effect is ignored.

FIGURE 96. STRAIN VS. LATERAL DISTANCE
Section #12 - Ring #3 - 9" E.T.B.
Surface Transverse Strain Gage C-10

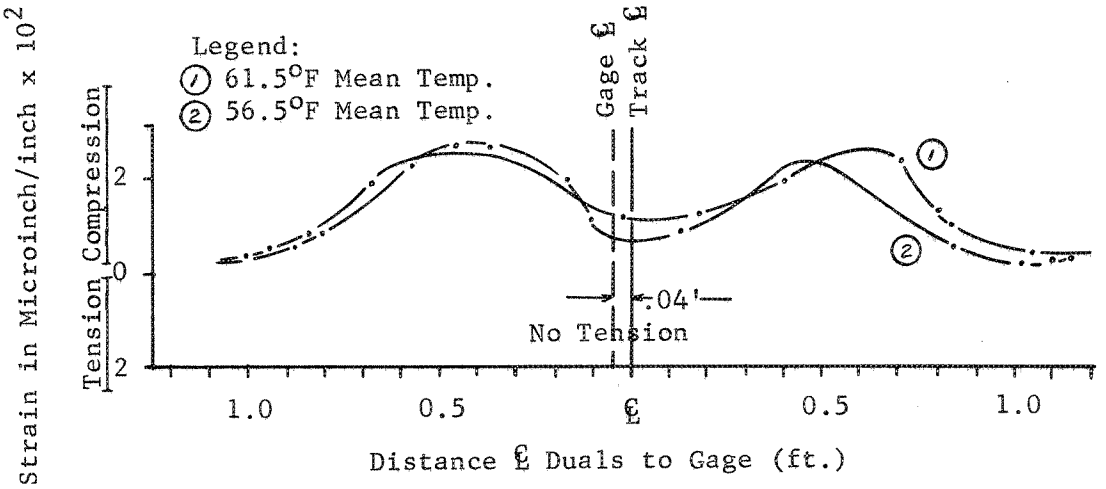

FIGURE 97. STRAIN VS. LATERAL DISTANCE
Section #12 - Ring #3 - 9" E.T.B.
Surface Longitudinal Strain Gage C-9

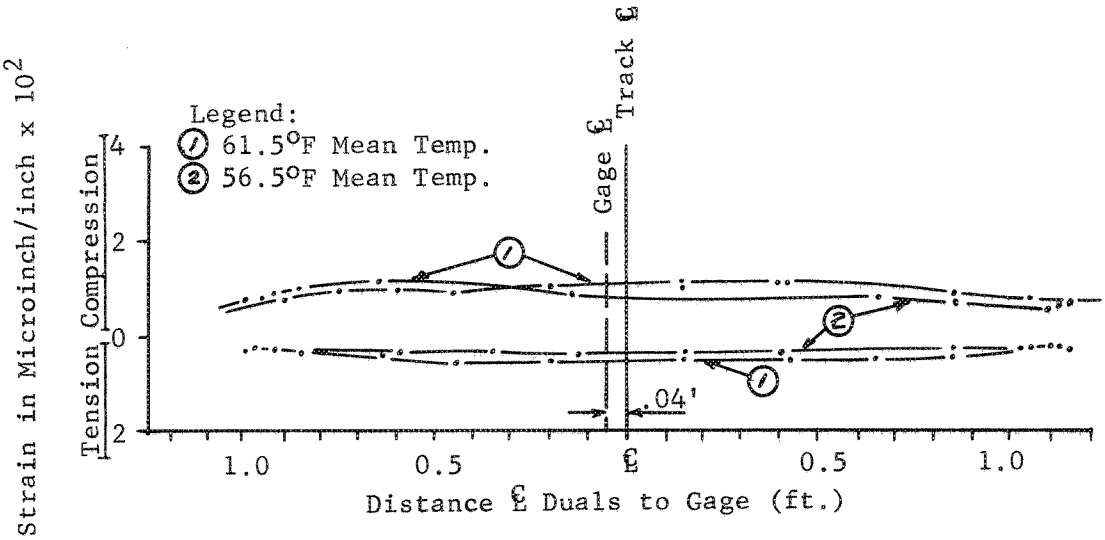

FIGURE 98. STRAIN VS. DEPTH
Section #3 - Ring #3 - 3½" A.T.B.

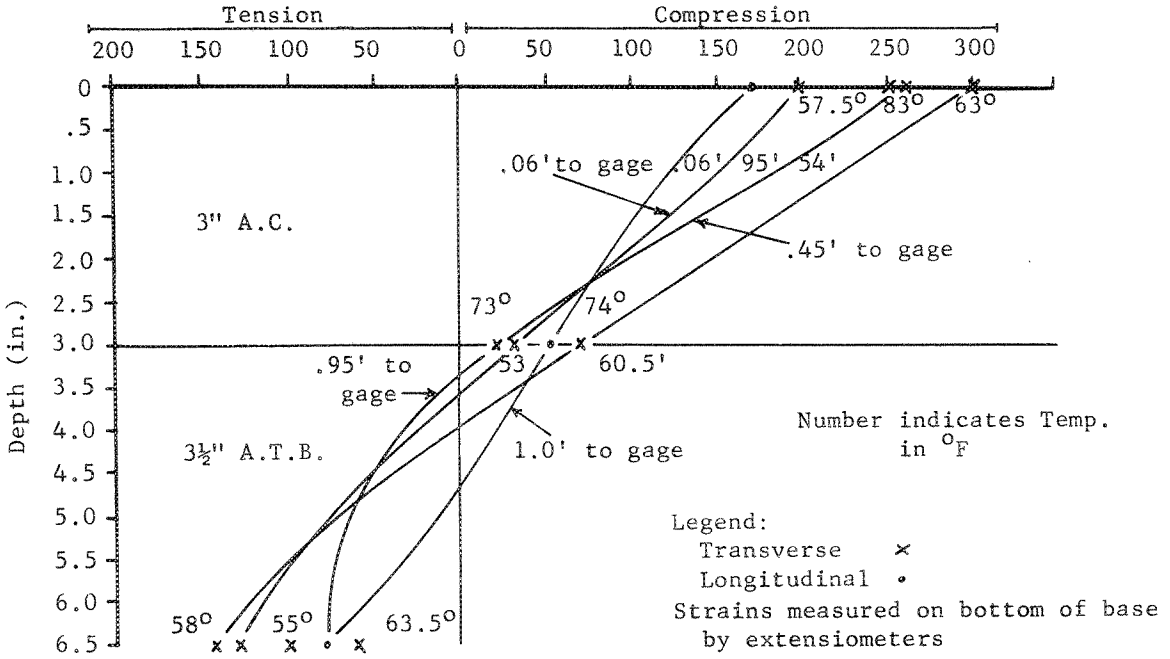

FIGURE 99. STRAIN VS. DEPTH
Section #12 - Ring #3 - 9" E.T.B.

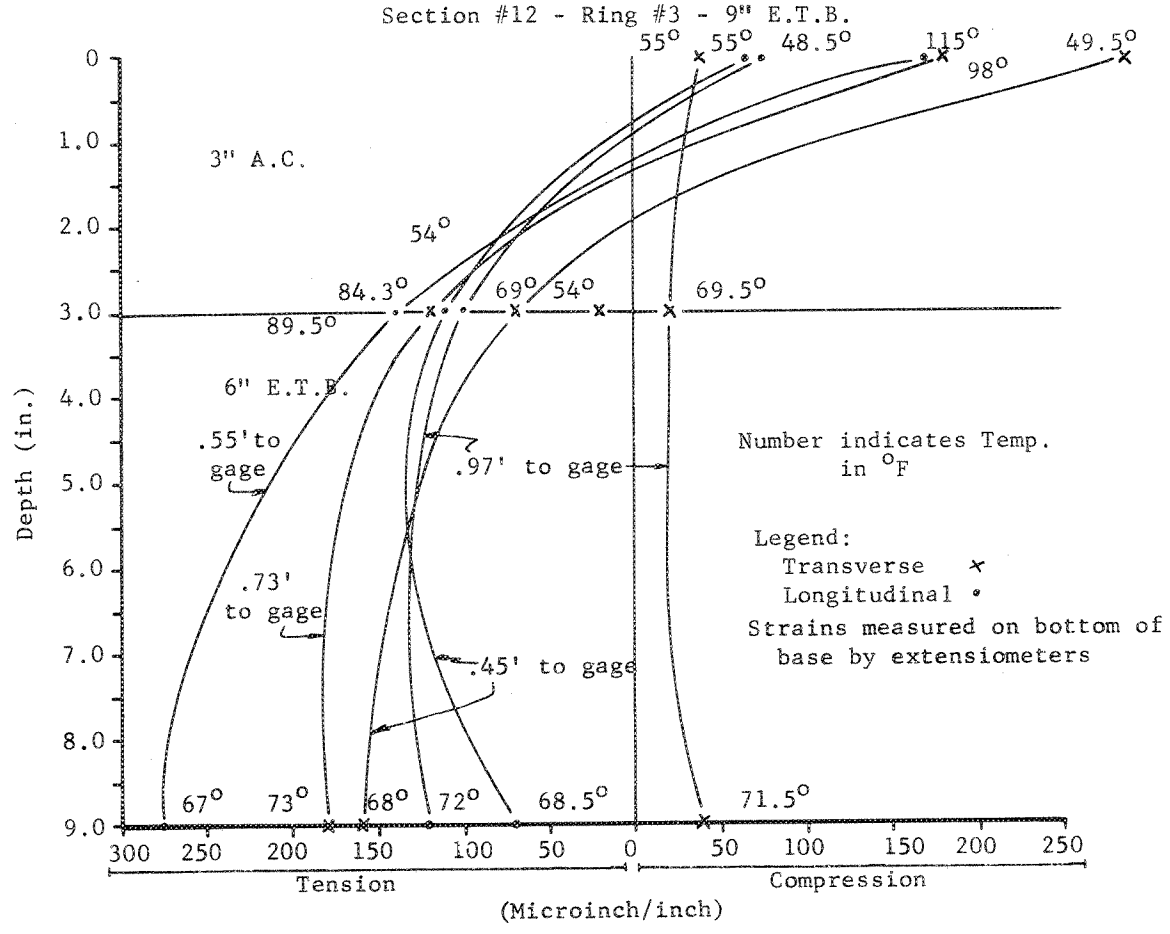

FIGURE 100. STRAIN VS. DEPTH
Section #6 - Ring #3 - 7" U.T.B.

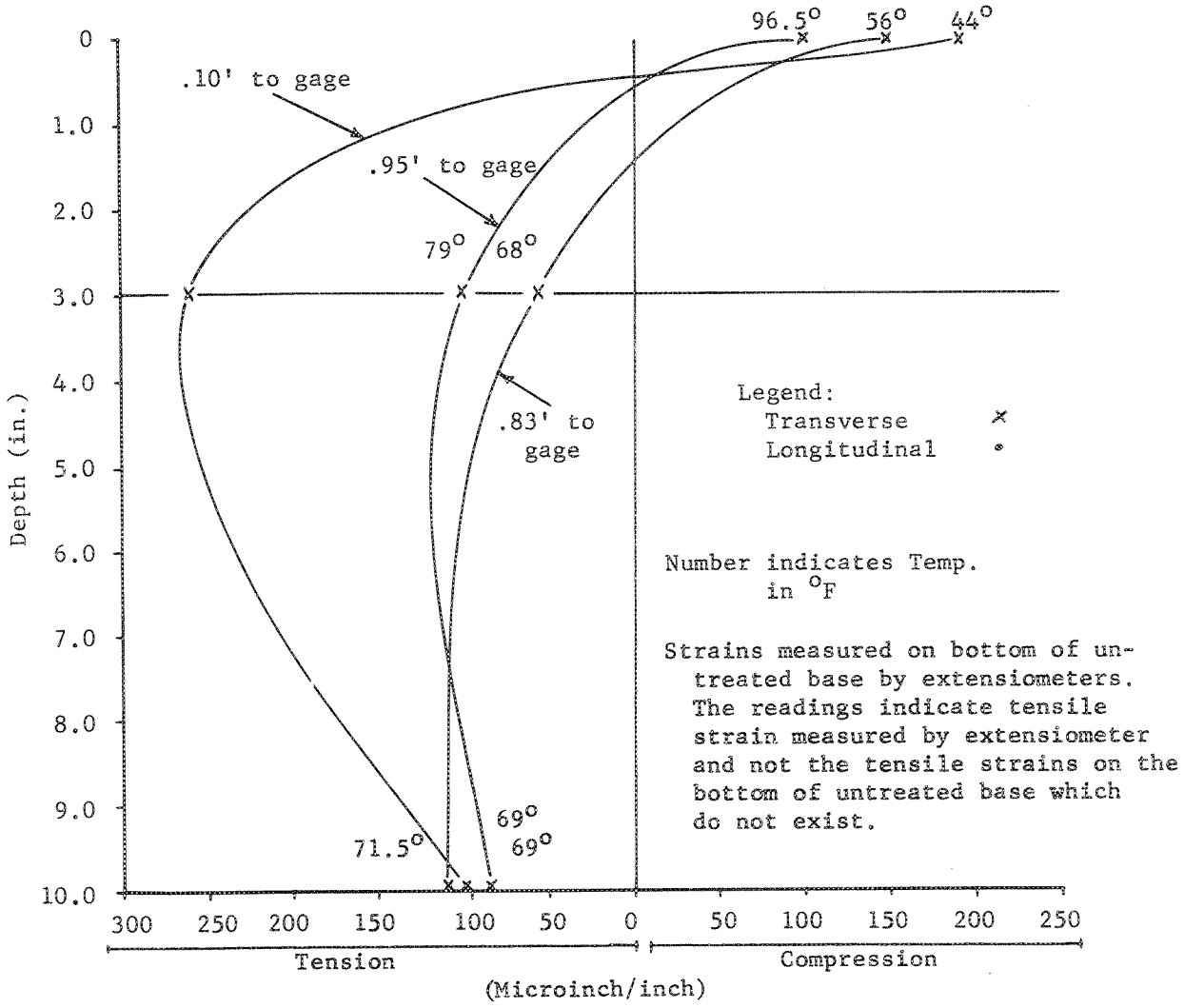

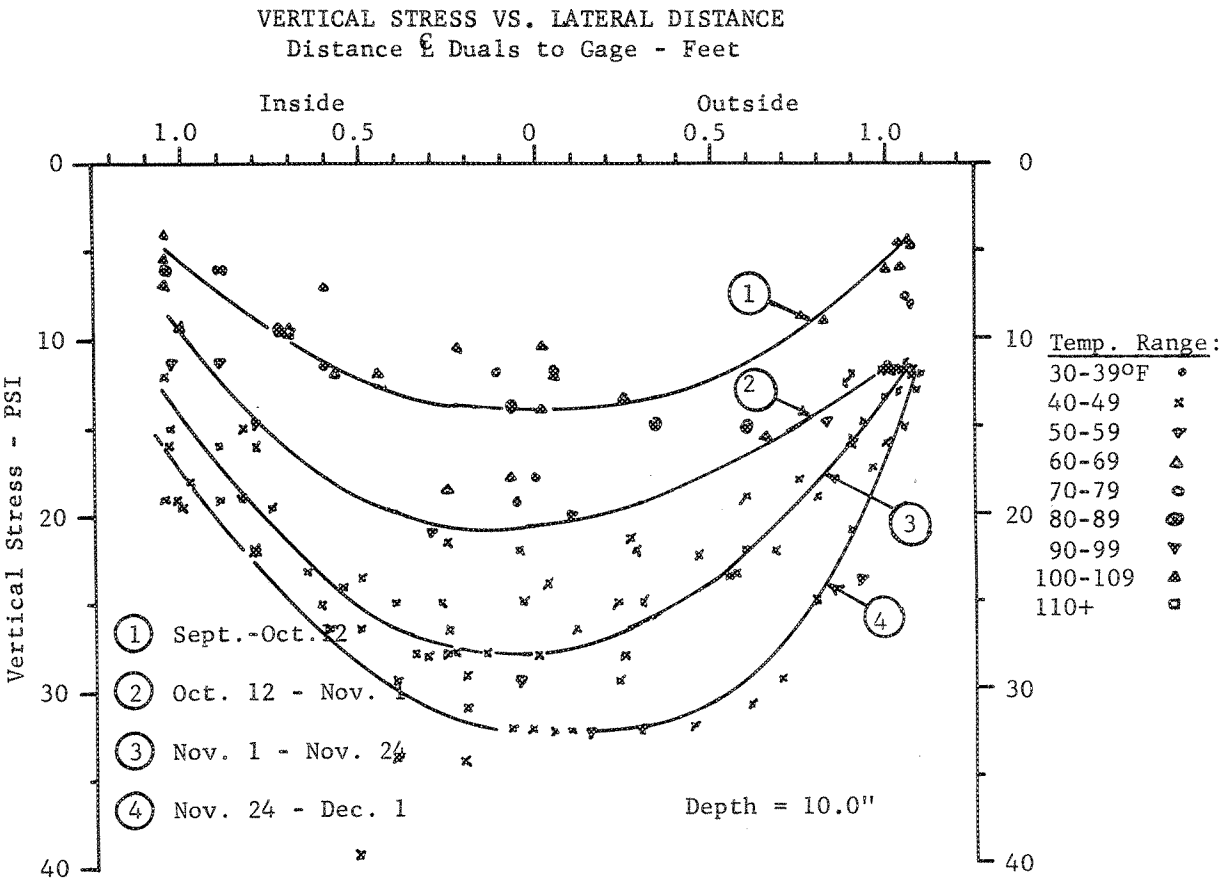

FIGURE 101: SECTION 6 - 7.0" U.T.B. P.C. A-1

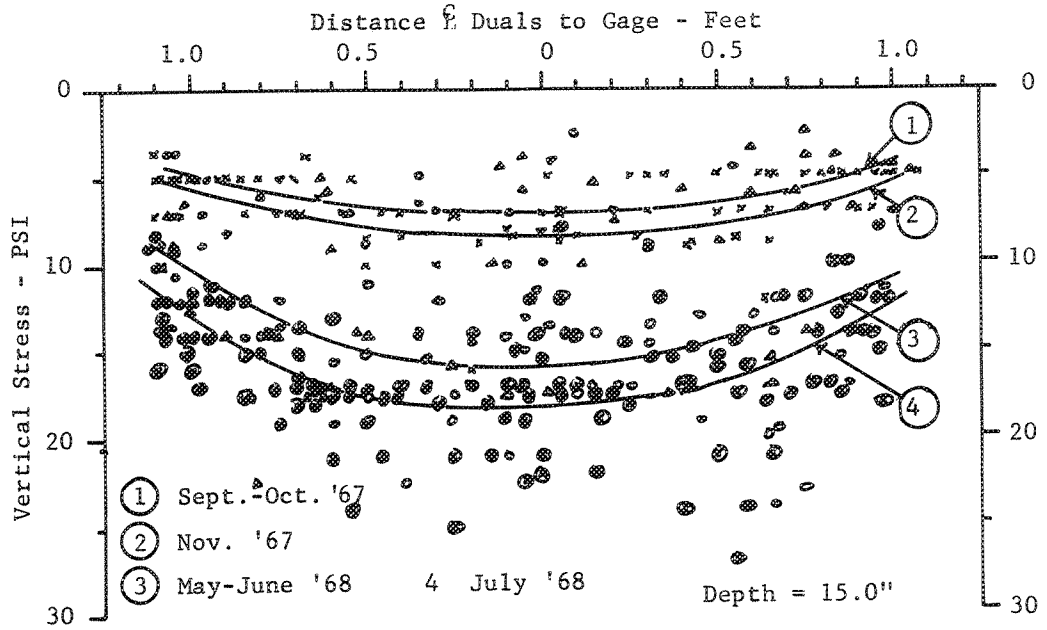

FIGURE 102: SECTION 8 - 12.0" U.T.B. P.C. A-4

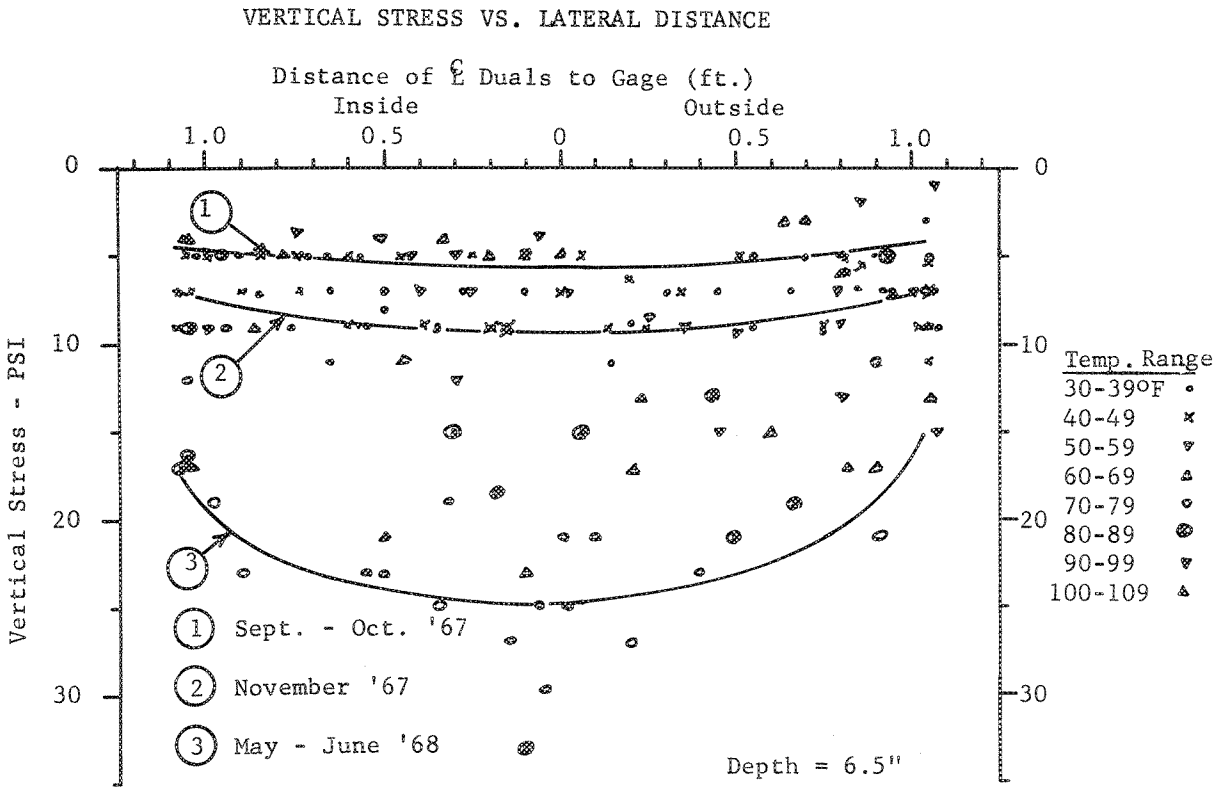

FIGURE 103. Section 3 - 3.5" A.T.B. PC A-1

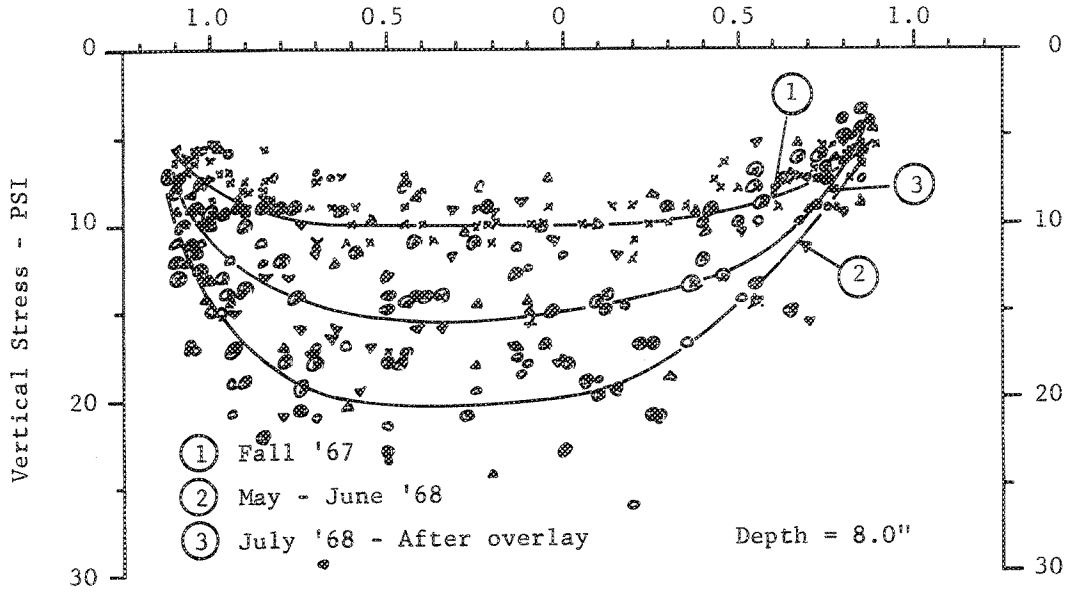

FIGURE 104. Section 10 - 5.0" E.T.B. PC A-5

FIGURE 105: VERTICAL STRESS VS. LATERAL DISTANCE
Ring 3 Section 12 9.0" E.T.B.
Pressure Cell (A-2) Depth = 3.0"

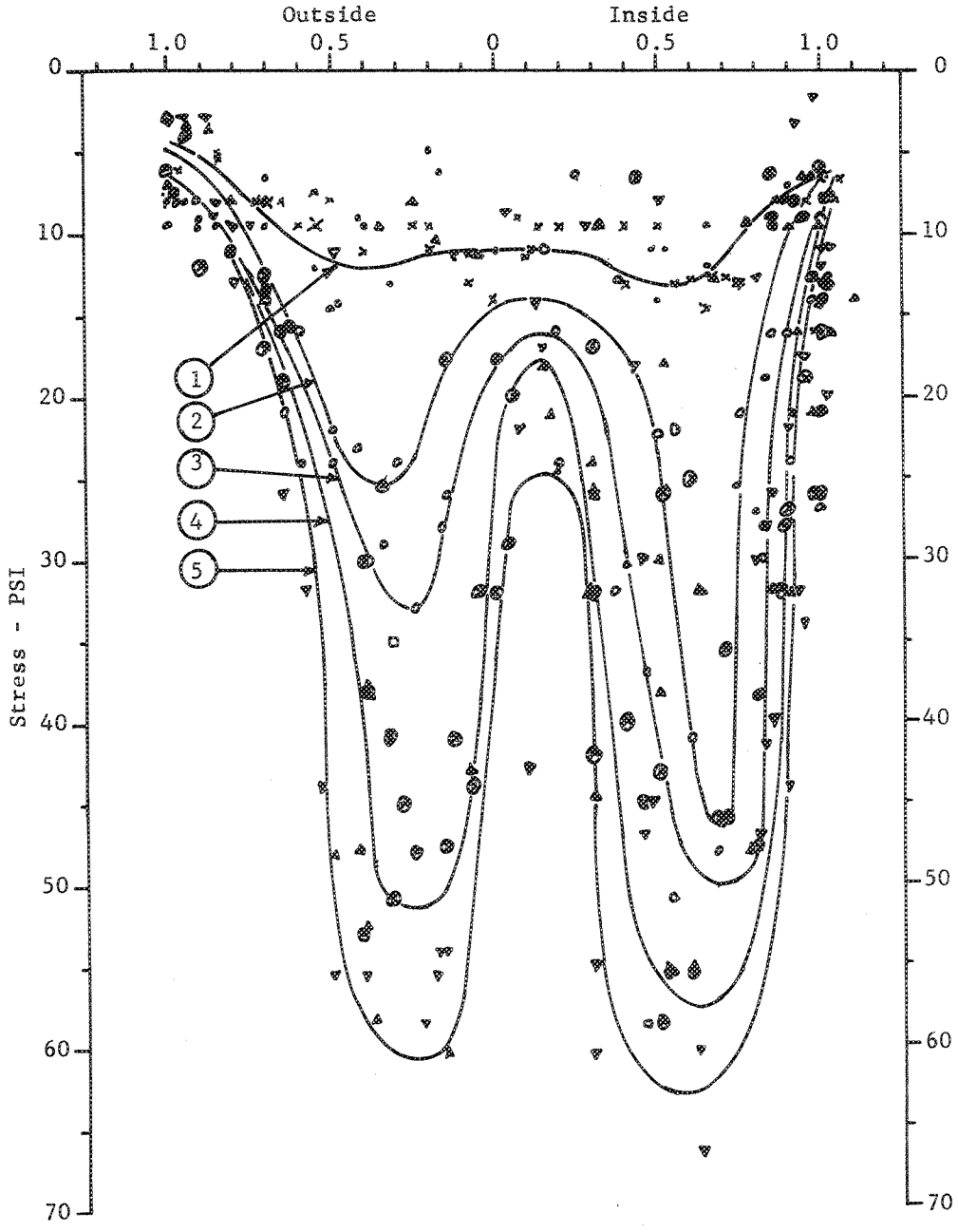

Distance ℄ Duals to Gage - Feet

Temp. Range:
30-39°F
40-49°F
50-59°F
60-69°F
70-79°F
80-89°F
90-99°F
100-109°F
110+

Curve
(1) Fall '67: 40-49°F
(2) Fall '67: 80-89°F
(3) Spring '68: 70-79°F
(4) Spring '68: 80-89°F
(5) Spring '68: 90-109°F

Discussion of Results

Two modes of failure were recognized as occurring in the sections of Ring #3. The failures in the fall were different from those in the spring.

The fall failures may have been due to a combination of thermal and mechanical distress. Thermal distress may have occurred when the combination of temperature and environmental change caused differential stresses in the pavement structure. It is no coincidence that transverse cracks occurred in the thin section just after almost a week of cooling weather along with heavy rainfall. Transverse cracking due to thermal conditions has not been recognized as major factor in local and Washington State pavement failures. Transverse cracking has been observed to be common in the colder states and in Canada (16). It has been observed that transverse cracks can occur under decreasing temperatures (17) and with increases in temperatures (18). This has been noted in the test track as the cracks usually appeared in the morning and afternoon rather than in the evening (19). It is possible that under slowly decreasing temperatures, the pavement builds up enough strength to restrain cracking. It is therefore in a pre-tensioned condition with different stresses on the bottom and the top. Then when a warming spell occurs, the surface loses its strength because it is warmer than the sub-surface elements, which are still pre-tensioned, and suddenly, a crack occurs at the bottom and works upward. This will be accelerated by mechanical loading. Large daily variations in temperature, coupled with heavy wheel loading, could act as a loading device hence increasing the possibility of cracking occurring sooner than expected (20). The combined loading conditions due to thermal and mechanical loads probably caused distress in the thin sections of Ring #3 (19). Environmental changes would probably accelerate this effect.

Failures occurring during the spring testing period were spectacular and catastrophic. Deflections were very high--in excess of 0.080 inches. During this period the speed of the apparatus was 10 mph and because of the eccentric mechanism, which is dependent upon the apparatus speed, the wheels took a long time to cross the wheel path width. Hence, there was a concentration of wheel load on one part of the pavement. Winter conditions may have also elevated the pavement track (10). The first few heavy wheel loads probably caused considerable pavement deformation. This phenomena has been reported by the Canadian Good Roads Association (21). At this point longitudinal surface tension cracks occur. The edge location of the observed failures may have been a factor as suggested by the WASHO Test Road Report (22) and reported by Meyerhoff (23). Examination of the subgrade after test completion showed that the subgrade was completely saturated. The degree of saturation of the subgrade affects the bearing capacity of flexible pavements as indicated by Broms (24). A reduction in relative density and an increase in degree of saturation which occurs during the spring thawing period reduces the subgrade bearing capacity greatly. The resilient modulus of the clay subgrade can be reduced by a factor of two due to the accumulation of moisture (25). This probably occurred in the sections that failed spectacularly in the spring. Rutting also occurred. Excavations revealed that it extended into the subgrade thus verifying the theories of Vesic and Domaschuk (15) which show that certain maximum vertical stress levels exist and remain constant, thus remaining within the pavement structure. When stress levels are exceeded, and they were as measured by the pressure cells during the spring, rutting is extended into the subgrade. Another indication of a different mode of failure occurring during the spring was that LVDT and

Benkelman beam deflections and strains were two to four times greater than in the fall. Since a relatively weak, compressible subgrade and a strong, well-compacted but thin pavement structure existed, structural failure occurred through punching shear. Therefore, one can say that different subgrade conditions occurred during the fall and spring testing periods causing different structural effects and different modes of failure.

Studies of the data obtained by instrumentation reveal definite trends. Lateral wheel placement did affect the measured values of stress, strain and deflection. This has been borne out by other studies (13, 14). Deflections occurring in the untreated bases show that about 40-60% of the movement occurred within the pavement and base structure and that this increased with wheel loads perhaps indicating a decrease in resilient modulus (25). Deflections increased from fall to spring indicating possible variations in the resilient characteristics of the subgrade due to environmental changes during the life of the pavement. This may be especially true during the spring when deflections increase two to fourfold.

Strain readings below the pavement show that maximum strain occurred directly under the tire. Strains were higher in the spring than during the fall. Temperature also affects strain values. Tensile strain increased with depth while compression decreased. Gusfeldt and Dempwold (26), Klomp and Niesman (27) obtained strain results under controlled centered loading and with uniform top to bottom temperatures which were almost similar to that obtained at the test track. Some deviations were observed due to temperature differences between layers and different loading. Correlation of tensile strains with deflection data was not tried, but will be tried in the evaluation report. An effort to try to establish a criterion for measurement of

fatigue failure as mentioned by Hong (28) will be tried. It is hoped that this may be possible as data from the last ring becomes available, along with this and the previous ring.

Work done by Sowers and Vesic (29) and Nijober (30) shows that vertical stress decreases with depth and is affected by the lateral positions of wheels. The different bases had a marked effect on the stress level. During the spring periods, stresses measured increased two to three times. The significance of this has been previously discussed. After distress occurred, high vertical stresses were measured indicating that perhaps pressure points may have been established as the pavement section began to act as separate entities.

Equivalencies based on fall and spring testing periods are shown in Tables 28 and 29. These equivalencies were based on the thinnest sections which survived during the fall period and the thickest sections which failed in the spring. At the AASHO Road Test, one inch of bituminous surface was equivalent to 3 inches of crushed stone base or to 4 inches of sand-gravel subbase (14). Experience in Canada indicates that ratio of the relative supporting capacity of bituminous concrete surface to granular base may be as low as 2 to 1 (31). Shook and Finn (32), using AASHO Road Test data showed that larger equivalencies of asphalt-concrete surfacing in terms of crushed rock base ranged from 2 to 6.7 depending upon the criteria used. Equivalency values can be established using deflection data, strain gage and stress data (33). The values shown in Table 29 seem to be reasonable; these values were based on field tests. However, it should be noted that these equivalencies apply only to the materials used in this test and within the range and degree of this experiment and is subject to modification as results from the other rings become available.

TABLE 28: COMPARISON OF EQUIVALENCIES

RINGS #2 AND #3

Type of Base	Ring No. 2		Ring No. 3	
	Fall '66 Inches[1]	Spring '67 Inches[2]	Fall '67 Inches[1]	Spring '68 Inches[2]
Crushed Stone Base (UTB)	9.5	12.0	9.5	12.0
Emulsion Treated Crushed Stone (ETB)	7.0	9.0	3.0	9.0
Special Aggregate Asphalt Treated (ATB)[3]	2.0	5.0	2.0	5.0

1 The thinnest sections which survived this period.
2 Thickest sections which failed during this period.
3 Hot mix.

TABLE 29: EQUIVALENCIES IN TERMS OF ATB

(3.0" of Cl. "B" A.C. Wearing Course)

Base Type	Ring No. 2		Ring No. 3	
	Fall '66 Inches	Spring '67 Inches	Fall '67 Inches	Spring '68 Inches
UTB	4.75	2.40	4.75	2.40
ETB	3.50	1.80	1.50	1.80
ATB	1.00	1.00	1.00	1.00

Comparison With Ring #2

Tables 28 and 29 show the comparison of equivalencies obtained from Rings #2 and #3. The results are very similar with the exception of the emulsion treated base in Ring #2. The premature failure of the emulsion treated bases in Ring #2 have been discussed by Krukar and Cook (1), Coyne (34), Terrel (35) and Terrel and Krukar (36). The spring equivalencies obtained from both rings were similar. The fact that the equivalencies are similar shows that the test track is capable of reproducing experimental results, and hence is a successful experimental tool.

The fact that the emulsion treated bases in Ring #3 performed so well shows that if conditions are right for curing and the proper mixing procedure is followed, the result is a good base which can give a long life.

Both rings revealed that the thin sections will not survive the combination of thermal and mechanical loads past the fall period. In both rings the untreated bases failed first, and that the thin treated bases had a similar lack of long life. The fact that the modes of failure for the fall and spring were similar for both rings is another indication that the test track is capable of reproducing experimental results.

Instrument measurements showed that the magnitude and modes of the measurements were similar. Some improvements in the instrumentation of Ring #3 may have given better results. Analysis by Terrel (35) and reported by Terrel and Krukar (36) show that the values obtained in the field from Ring #2 could be duplicated by laboratory and theoretical means. Similar analysis awaits the data from Ring #3. Rough comparisons with field data from rings reveal the results are similar within certain boundary conditions.

The Ring #3 experiment ran about twice as long and had four times the wheel loads than the experiment with Ring #2, although the results were similar at the end. Two possible reasons are subgrade preparation and environmental conditions at time of construction. The subgrade was prepared to a greater depth in Ring #3 than in Ring #2. Construction conditions were ideal for Ring #3, with testing operations also starting sooner under excellent environmental conditions as compared to Ring #2. The longevity of Ring #3 indicates that environment during construction is a very important factor in pavement performance, even with construction carefully controlled under rigorous specifications.

CONCLUSIONS

Major Conclusions

1. The Washington State University Test Track is a research tool capable of duplicating results. This is shown by comparison of results from Rings #2 and #3.

2. Equivalencies developed from Ring #3 are summarized in Table 28. The fall equivalencies are based on the thinnest sections that survived, while the spring equivalencies are based on the thickest sections that failed in "ultimate" failure. Comparison with equivalencies obtained from Ring #2 indicate that these equivalencies can be used with confidence, but it should be mentioned that these findings are valid only to the test and under test conditions.

3. The modes of failure were different during the two testing periods. The fall failures were due to thermal and mechanical loads which the thinnest

sections were unable to survive. The spring failures were caused by saturated subgrade conditions which resulted in a reduction in resilient modulus and thus a lack of bearing capacity.

4. On the basis of this test, the special aggregate asphalt treated base seems to have superior load carrying performance ability compared to the emulsion treated and untreated crushed rock bases. The emulsion treated bases performed very well in Ring #3. The untreated crushed rock bases, although developing cracks early, continued to stay in the test for long periods of time indicating resiliency.

5. The thickest sections had no surface cracks, but failed due to rutting. Examination revealed that fatigue failure cracks had started to develop on the bottom of the bases. It may be that for thick sections rutting may be a more valid criteria of failure than cracks.

6. A series of tables summarizing maximum values of static deflections, dynamic deflections, strains and stresses were developed. These could be used for the development of critical values needed for better rational pavement design.

7. The longevity of the testing of Ring #3 points out that environmental conditions may be one of the most important factors, if not the most important factor, in pavement structure life.

Minor Conclusions

1. The lateral position of the dual tires greatly affects the strain gage values and hence this is quite critical for obtaining accurate values of strain with respect to load location. Lateral position of tires also affects the stress and deflection values.

2. Temperature effects were noted on static and dynamic deflections, strains and stresses. Temperature effects did not seem to be as critical in the fall as compared to the spring.

3. Continuous readings on the different gages were better able to establish the behavior patterns than readings taken over different periods of time. Temperature effects became quite noticeable during these tests. There is still need of an automatic system to obtain continuous data.

4. Problems developed with evaluation of data. Even with a manual system of obtaining data, a huge amount was generated which entailed much tabulation and evaluation. This created bottlenecks which caused delays in the evaluation of results.

PRACTICAL IMPLICATIONS FROM THE TEST RINGS TO DATE

The comparison of results obtained from both rings show that the test track is capable of duplicating experimental results. The conclusion from this is that results can be used with some degree of confidence. In the future it may not be necessary to duplicate tests.

The equivalencies developed can now be used with some confidence. This should be of some value to the pavement designer as he now has some values on the equivalent strength of the different materials tested.

Emulsion treated bases, if properly designed, mixed and cured, have a proper place where asphalt plants are not feasible. Economies may be obtained in areas where these types of base treatments can be used. It should be emphasized that moisture is critical and that good curing conditions are necessary otherwise problems may develop similar to those in Ring #2.

The results from Rings #1, #2 and #3 indicate that the use of non-fractured screened aggregate is feasible. This type of base is apparently equal to many types and is probably superior to many others. The highway departments and contractors may be able to realize considerable savings by using these aggregates, especially where glacial and river deposits abound.

The longevity of Ring #3 again points out the importance of environmental factors on pavement structure life. These should be considered in any kind of pavement design. Thermal loads should be considered, especially on thin pavements.

Rutting may be a better criterion of failure for thick sections than initial cracking and other cracking criteria. Hence, the pavement serviceability index developed by AASHO (14) is probably a good index for evaluating pavement conditions.

Benkelman beam measurements can be used to predict where and to some extent when distress may occur. This was done in Ring #3. This would mean correlating deflections with pavement distress. This has practical implications for maintenance. As soon as one knows that a pavement has reached a critical stage, an overlay can be planned. This would require studying deflections for all thicknesses and types of roads, and setting up deflection limits. When these limits are reached, the maintenance department would plan on laying an overlay. This would be economical in that overlays would not have to be applied before necessary. Maximum life of existing pavements could then be achieved. Results from Rings #2, #3 and #4 should help in the development of critical deflection values for pavements of different materials.

Deflections, strains and stresses obtained from LVDT's, strain gages and pressure cells will be useful in helping to evaluate strength parameters in pavements. Data from Rings #2 and #3 showed some interesting trends, which may be further clarified as data from Ring #4 becomes evaluated and available. More analysis is needed on the data from Rings #3 and #4. This may lead to the development of critical values for pavement deflections, strains and stresses so that failure and design pavement theories can be formulated or substantiated. In the long run, this may lead to better and more economical pavements.

REFERENCES

1. Milan Krukar and John C. Cook. Experimental Ring #2: A Study of Untreated, Emulsion Treated, and Asphaltic-Cement Treated Bases, Pavement Research of the Washington State University Test Track, Vol. 2, Highway Research Publication H-29, Research Project Y-651, July, 1968.

2. Theodore W. Horner. Experimental Design and Analysis of Experiments for Comparison of Paving Materials, Engineering Analysis Section, The Asphalt Institute, Booz Allen Applied Research, Inc., August, 1965.

3. John C. Cook, G. A. Riedesel, and Milan Krukar. Experimental Ring #1: A Study of Cement Treated and Asphaltic Treated Bases, Pavement Research at the Washington State University Test Track, Vol. 1, Highway Research Section Publication H-28, Research Project Y-651, 1967.

4. B. F. Kallas. "Summary of Asphalt Institute Laboratory Test Results," Interim Report, The Washington State University Test Track, Internal Asphalt Institute Report (Unpublished), May, 1968.

5. Standard Specifications for Road and Bridge Construction--1963, Washington State Highway Commission, Department of Highways, Olympia, Washington.

6. Specifications--Paving and Surfacing of Pavement Test Track Rings Nos. 3 and 4, Washington State University, Research Project Y-993, April 28, 1967.

7. Pavement Instrumentation Studies for San Diego County Experimental Base Project, The Asphalt Institute, Materials and Research Development (a division of Woodward, Clyde, Sherard and Associates), Oakland, California, February, 1966.

8. D. Croney and J. D. Coleman. "Pore Pressure and Suction in Soil," Proceedings, Pore Pressure and Suctions in Soils Conference, 1960, Butterworth, 1961.

9. Milan Krukar. Highway Test Track Research Project Y-993, Quarterly Reports 2-6, 1967-1968.

10. Milan Krukar. Highway Test Track Research Project Y-993, Quarterly Report No. 9, June 30, 1969.

11. "Pavement Evaluation Studies in Canada," Technical Publication No. 19, Canadian Good Roads Association, Ottawa, Canada, September, 1963.

12. R. Ian Kingham. "A New Temperature-Correction Procedure for Benkelman-Beam Rebound Deflections," Research Report 69-1, The Asphalt Institute, College Park, Maryland, February, 1969.

13. "Three-Year Evaluation of Shell Avenue Test Road," Highway Research Record No. 117, Shell Avenue Test Road Committee, Highway Research Board, Washington, D.C., 1965.

14. "The AASHO Road Test, Report 5, Pavement Research," Special Report 61E, Highway Research Board, Washington, D.C., 1962.

15. A. S. Vesic and L. Domaschuk. "Theoretical Analysis of Structural Behavior of Road Test Flexible Pavements," National Cooperative Highway Research Program Report 10, Highway Research Board, Washington, D.C., 1964.

16. R. Ian Kingham. Prepared Discussion--Symposium on Non-Traffic Associated Cracking of Asphalt Pavements, Proceedings, The Association of Asphalt Paving Technologists, Vol. 35., Minneapolis, Minnesota, February, 1966.

17. F. D. Young, I. Deme and Others. "Ste-Anne Test Road: A Field Study of Transverse Crack Development in Asphalt Pavements--Construction Summary and Performance After Two Years Service," Proceedings, Canadian Technical Asphalt Association, Edmonton, Alberta, Canada, November, 1969.

18. B. P. Shields. Discussion--Symposium on Non-Traffic Associated Cracking of Asphalt Pavements, Proceedings, The Association of Asphalt Paving Technologists, Vol. 35, Minneapolis, Minnesota, February, 1966.

19. Milan Krukar and John C. Cook. "Cracking of Asphaltic Pavements as a Function of Base Thickness and Environment under Controlled Loading Conditions at the WSU Test Track," Paper presented before the Western meeting of the Highway Research Board, Denver, Colorado on August 12-13, 1968.

20. Douglas Bynum, Jr. and R. N. Traxler. "Performance Requirements of High Quality Flexible Pavements," Research Report No. 127-1, Research Study No. 2-8-69-127, Texas Transportation Institute, Texas A & M University, College Station, Texas, August, 1969.

21. "Pavement Evaluation Studies in Canada," Technical Publication No. 19, Canadian Good Roads Association, Ottawa, Canada, September, 1963.

22. "The WASHO Road Test, Part 2 Test Data Analyses Findings," Special Report No. 22, Highway Research Board, Washington, D.C., 1955.

23. G. G. Meyerhoff. "Influence of Shoulders on Flexible Pavement Strength," Proceedings, Canadian Good Roads Association Meeting, 1960.

24. Bengt. B. Broms. "Effects of Degree of Saturation on Bearing Capacity of Flexible Pavements," Highway Research Record No. 71, Washington, D.C., 1965.

25. H. B. Seed, F. G. Mitry, C. L. Monismith, and C. K. Chan. "Prediction of Flexible Deflections from Laboratory-Repeated Load-Tests," National Cooperative Highway Research Program Report 35, Highway Research Board, Washington, D.C., 1967

26. K. H. Gusfeldt and K. R. Dempwolff. "Stress and Strain Measurements in Experimental Road Sections Under Controlled Loading Conditions," Proceedings, Second International Conference on the Structural Design of Asphalt Pavements, University of Michigan, Ann Arbor, August, 1967.

27. A. J. G. Klomp and Th. W. Niesman. "Observed and Calculated Strains at Various Depths in Asphalt Pavements," Proceedings, Second International Conference on the Structural Design of Asphalt Pavements, University of Michigan, Ann Arbor, August, 1967.

28. Hyoungkey Hong. "Fatigue Characteristics of Flexible Pavement," Proceedings of the American Society of Civil Engineers, Journal of the Highway Division, April, 1967.

29. G. F. Sowers and A. B. Vesic. "Vertical Stresses in Subgrade Beneath Statically Loaded Flexible Pavements," Highway Research Board Bulletin 342, Washington, D.C., 1962.

30. L. W. Nijober. "Testing Flexible Pavements under Normal Traffic Loadings by Means of Measuring Some Physical Quantities Related to Design Theories," Proceedings, Second International Conference on the Structural Design of Asphalt Pavements, University of Michigan, Ann Arbor, August, 1967.

31. Report on AASHO Road Test, Canadian Good Roads Association, Ottawa, Canada, 1962.

32. J. F. Shook and F. N. Finn. "Thickness Design Relationships for Asphalt Pavements," Proceedings, First International Conference on the Structural Design of Asphalt Pavements, University of Michigan, Ann Arbor, August, 1962.

33. Bonner S. Coffman, George Ilves, and William Edwards. "Theoretical Asphaltic Concrete Equivalencies," Highway Research Record 239, Highway Research Board, Washington, D.C., 1968.

34. L. D. Coyne. "Washington State University Test Track--Ring 3--Test Data Summary," Internal Report for Chevron Asphalt Company (Unpublished), Western Laboratory, Emeryville, California, May, 1969.

35. Ronald L. Terrel. Analysis of Ring No. 2 Washington State University Test Track, for The Asphalt Institute, University of Washington, Seattle, Washington, December, 1968.

36. Ronald L. Terrel and Milan Krukar. "Evaluation of Test Track Pavements," Proceedings, The Association of Asphalt Paving Technologists, Vol. 38, Kansas City, Missouri, February, 1969.

APPENDIX

Modified CGRA Benkelman Beam Rebound Procedure

Scope

This method of test covers a procedure for the determination of the static Benkelman beam rebound at a point on a flexible pavement under a standardized axle load, tire size, tire spacing and tire pressure for the Washington State University Test Track.

Equipment

The equipment shall include the following:

1. A Benkelman beam having the following dimensions:

	ft.	in.
a. Length of probe arm from pivot to probe point	8	0
b. Length of measurement arm from pivot to dial	4	0
c. Distance from pivot to front legs	0	10
d. Distance from pivot to rear legs	5	5½

2. A 5-ton truck is recommended as the reaction. The vehicle shall have an 18,000 pound rear axle load equally distributed on two wheels, each equipped with dual tires. WSU loading is fixed at a minimum of 10,800 pounds on each set of duals. This is directly equivalent to a 21,600 pound single rear axle load. The tires shall be 10.00 x 20, 12-ply, inflated to a pressure of 80 psi. WSU tire size is 11.00 x 22, 12-ply, tire pressure 80 psi. The use of tires with tubes and rig treads is recommended.

3. Tire pressure measuring gauge.

4. Thermometer (0-120°F.) with 1°divisions.

5. A mandrel for making a 1.75-inch-deep hole in the pavement for temperature measurement. The diameter of the hole at the surface shall be ½ inch. This equipment not used at WSU. Thermocouples are installed at time of construction as part of instrumentation.

Procedure

1. The point on the pavement to be tested is selected and marked. For highways, the points are located at specified distances from the edge of the pavement according to the width of the lane, as follows:

Land Width (feet)	Distance from Pavement Edge (feet)
9 or less	1.5
10	2.0
11	2.5
12 or more	3.0

2. The dual wheels of the truck are centered above the selected point. WSU readings are taken between the duals. The duals move laterally across the track; locations can be chosen or random.

3. The probe of the Benkelman beam is inserted between the duals and placed on the selected point.

4. The locking pin is removed from the beam and the legs adjusted so that the plunger of the beam is in contact with the stem of the dial gauge.

5. The dial gauge is set at approximately 0.4 inches. The initial reading is recorded when the rate of deformation of the pavement is equal to or less than 0.001 inches per minute (i.e., measurement dial rate is less than 0.005 inches per minute). The initial reading should be taken 3 minutes after positioning the beam if the rate of movement criteria is not satisfied.

6. The truck is slowly driven forward a distance of 8 feet 10 inches and stopped. WSU wheels are pulled to the desired distance through use of a pick-up truck.

7. An intermediate reading is recorded when the rate of recovery of the pavement is equal to or less than 0.001 inches per minute. The intermediate reading should be taken 3 minutes after positioning the wheels if the rate of movement criteria is not satisfied.

8. WSU wheels are pulled forward a further 30 feet.

9. The final reading is recorded when the rate of recovery of the pavement is equal to or less than 0.001 inches per minute. The final reading should be taken 3 minutes after positioning the wheels if the rate of movement criteria is not satisfied.

10. Pavement temperature is recorded at least once every hour, inserting the thermometer in the standard hole filled with water. At the same time the air temperature is recorded. WSU instrumentation eliminates this particular procedure.

11. The tire pressure is checked at 2- to 3-hour intervals during the day and adjusted to the standard if necessary.

Calculations

1. Subtract the final dial reading from the initial dial reading. Subtract the intermediate dial reading from the initial dial reading.

2. If the differential reading obtained compare within 0.001 inches the actual pavement rebound is the final differential reading for a direct-reading Benkelman beam.

3. If the differential readings obtained do not compare to 0.001 inches, the final differential dial reading represents the apparent pavement rebound.

4. Apparent rebounds for direct reading Benkelman beam are corrected by means of the following formula:

$$X_T = X_A + 0.9863Y$$

where X_T = true pavement rebound

X_A = apparent pavement rebound

Y = vertical movement of the front legs (i.e., the difference between the final and intermediate dial readings).